Vol. 105 Nº2 ISSN 2545-8655

ANALES DE LA ASOCIACIÓN QUÍMICA ARGENTINA

Octubre 2018

Volumen Especial DJPQ-AQA

Anales de la Asociación Química Argentina

Volumen Especial: Materia Blanda

Editada desde 1913

Registro de Propiedad Intelectual Nº 164.756

Asociación Química Argentina
Sánchez de Bustamante 1749, 1425 Buenos Aires, Argentina
TE/FAX: 54-11-4822-4886 http://www.aqa.org.ar

División de Jóvenes Profesionales
FB @djpq.aqa – TW @jovenes_AQA

Contenido

Vol. 105 Nº2, Octubre de 2018 – Materia Blanda

Mini-Reviews

NOTA DEL EDITOR

Estimados Lectores de Anales de la Asociación Química Argentina:

En este nuevo número de nuestra revista les presentamos el primer número temático editado por la División de Jóvenes Profesionales en Química, de la Asociación Química Argentina (DJPQ-AQA). Esta nueva División de la AQA tiene como objetivo central conectar a los jóvenes profesionales de la química que se encuentran ejerciendo su profesión en las distintas regiones de nuestro país, catalizando el intercambio de ideas y la cooperación entre sus miembros.

De ese intenso intercambio y cooperación surge el contenido de este primer volumen dedicado a *Materia Blanda (Soft Matter)* cuyo Editor Invitado es el Dr. Matías Rafti, Investigador del Instituto de Investigaciones Fisicoquímicas Teóricas y Aplicadas (INIFTA).

Aprovechamos para invitar a los jóvenes profesionales de la química a conectarse con la DJPQ-AQA a través del email djpq.aqa@gmail.com.

Dra. Susana Larrondo

Editora en Jefe

NOTE FROM THE EDITOR

Dear Readers of Anales de la Asociación Química Argentina:

In this new issue of our journal we present the first issue edited by the Division of Young Professionals in Chemistry of the Argentine Chemical Association (DJPQ-AQA). The main objective of this new AQA Division is to connect Young Chemists from the different regions of our country, catalysing the exchange of ideas and cooperation among them.

From this intense exchange and cooperation emerge the content of this first volume dedicated to *Soft Matter*, whose Guest Editor is Dr. Matías Rafti, researcher of the Institute of Theoretical and Applied Physicochemical Research (INIFTA).

We take this opportunity to invite Young Chemists to connect with the DJPQ-AQA through the email djpq.aqa@gmail.com

Dra. Susana Larrondo

Chief Editor

NOTA DEL EDITOR INVITADO

Pierre-Gilles de Gennes, en la conferencia dictada en ocasión del otorgamiento de su premio Nobel de Física 1991, terminó de popularizar el término Soft Matter acuñado en la década del 70 mientras trabajó en Orsay, Francia (aunque traducible como Materia Blanda al castellano, el original matière molle en francés surgió como una broma por su doble sentido). En los términos usados por el propio de Gennes, pueden englobarse dentro de esta categoría aquellos sistemas físico-químicos capaces de presentar; (i) complejidad (en un sentido análogo al que se observa en la biología moderna cuando se compara el comportamiento de los organismos más simples como las bacterias con los organismos pluricelulares), y (ii) flexibilidad (refiriéndose con esto a sistemas capaces de mostrar cambios drásticos a nivel macroscópico como resultado de la suma de pequeños cambios en su estructura microscópica). Los biomateriales, polímeros, cristales líquidos, sistemas micelares y suspensiones coloidales, son un excelente ejemplo de lo que hoy se denomina Materia Blanda; presentan un interesante fenómeno comúnmente observado en los organismos vivos: la auto-organización y el auto-ensamblado mediante interacciones débiles actuando en conjunto (e.g., interacciones tipo van der Waals, puentes de Hidrógeno, etc.).

Los ejemplos del desarrollo de esta disciplina en la Argentina son numerosos y al igual que en el resto del mundo, el aumento del número de trabajos científicos publicados y hasta de revistas dedicadas específicamente ha sido notorio. Es el objetivo de este número temático retratar dicho desarrollo; en su contribución J. Giussi y col. nos detallan sobre el surgimiento surfactantes poliméricos no convencionales, S. Moya y col. discuten el uso de recubrimientos con polielectrolitos en la mejora de la adhesión celular. C.E. Hoppe y col. describen el efecto fototérmico en el marco de aplicaciones de gran importancia como el auto-curado y los tratamientos por hipertermia magnética; mientras que N.M. Correa y col. repasan el impacto de los surfactantes cataniónicos para aplicaciones a sistemas en Materia Blanda.

Finalmente, W. Marmisollé y col. discuten el uso de polímeros conductores en plataformas electroquímicas para el biosensado y el almacenamiento de energía, y A.M. Fracaroli y col. introducen una familia relativamente nueva de materiales poliméricos porosos con clústeres metálicos y linkers orgánicos denominados MOFs (Metal Organic Frameworks) y sus posibles aplicaciones en catálisis y adsorción selectiva.

Dr. Matías Rafti

Editor Invitado

NOTE FROM THE GUEST EDITOR

Pierre-Gilles de Gennes, in his conference in the occasion of its Nobel prize in 1991, popularized the term *Soft Matter*, coined in the 70´s while he worked in Orsay, France (although originally, *matière molle* in French refers to a double-meaning). In the terms used by de Gennes, this category can be used when referring to physical systems capable of featuring *(i) complexity* (in the sense of the complexity observed when comparing simple unicellular organisms such as bacteria against mammals or plants), and *ii) flexibility* (referring to systems capable of drastic macroscopic changes as a result of a multitude of small microscopic modifications on its structure). Biomaterials, polymers, liquid crystals, micelles and colloids constitute an excellent example of what is considered today *Soft Matter*; these systems feature an interesting phenomenon common in living organisms: self-organization and self-assembly through multiple weak interactions acting together (e.g., van der Waals, Hidrogen bonds, etc.).

Many examples of the *Soft Matter* development in Argentina can be mentioned, and (as in the rest of the world) there has been a drastic increment on the number of scientific publications and journals devoted to its diffusion. Our primary objective with the edition of this thematic issue of minireviews on *Soft Matter* is to portrait such development and to encourage novel researchers to engage in topics related.

In this contribution, J. Giussi et al. present a detailed review on the emergence of new polymeric surfactants, S. Moya et al. discuss on the application of polyelectrolyte layers as cellular adhesion enhancers. C.E. Hoppe et al. describe the photothermal effect in relation to interesting applications in materials featuring self-healing and magnetic hyperthermia treatments; while N.M. Correa et al. survey on the impact of catanionic surfactants on *Soft Matter* world.

Finally, W. Marmisollé et al. discuss on the use of conducting polymers as electrochemical platforms for biosensing applications and energy storage, and A.M. Fracaroli et. Al. introduce a relatively new family of porous polymeric materials with metallic clusters linked by organic linkers known as Metal Organic Frameworks (MOFs), and review some examples on possible applications in catalysis and selective adsorption.

Dr. Matías Rafti

Guest Editor

Anales de la Asociación Química Argentina

División Jóvenes Profesionales

Mini-Review

METAL-ORGANIC FRAMEWORKS (MOFS): STRUCTURAL MULTIFUNCTIONALITY AND INTEGRATION INTO DIVERSE PLATFORMS

Jimena S. Tuninetti,[1] Matías Rafti,[1,*] and Alejandro M. Fracaroli[2,*]

1. *Instituto de Investigaciones Fisicoquímicas Teóricas y Aplicadas, INIFTA-CONICET, Softmatter Laboratory, La Plata, Argentina (mrafti@quimica.unlp.edu.ar)*
2. *Instituto de Investigaciones en Fisicoquímica de Córdoba, INFIQC – CONICET, Facultad de Ciencias Químicas, Departamento de Química Orgánica, Universidad Nacional de Córdoba, Ciudad Universitaria, X5000HUA Córdoba, Argentina (a.fracaroli@unc.edu.ar)*

Resumen Gráfico - Graphical Abstract

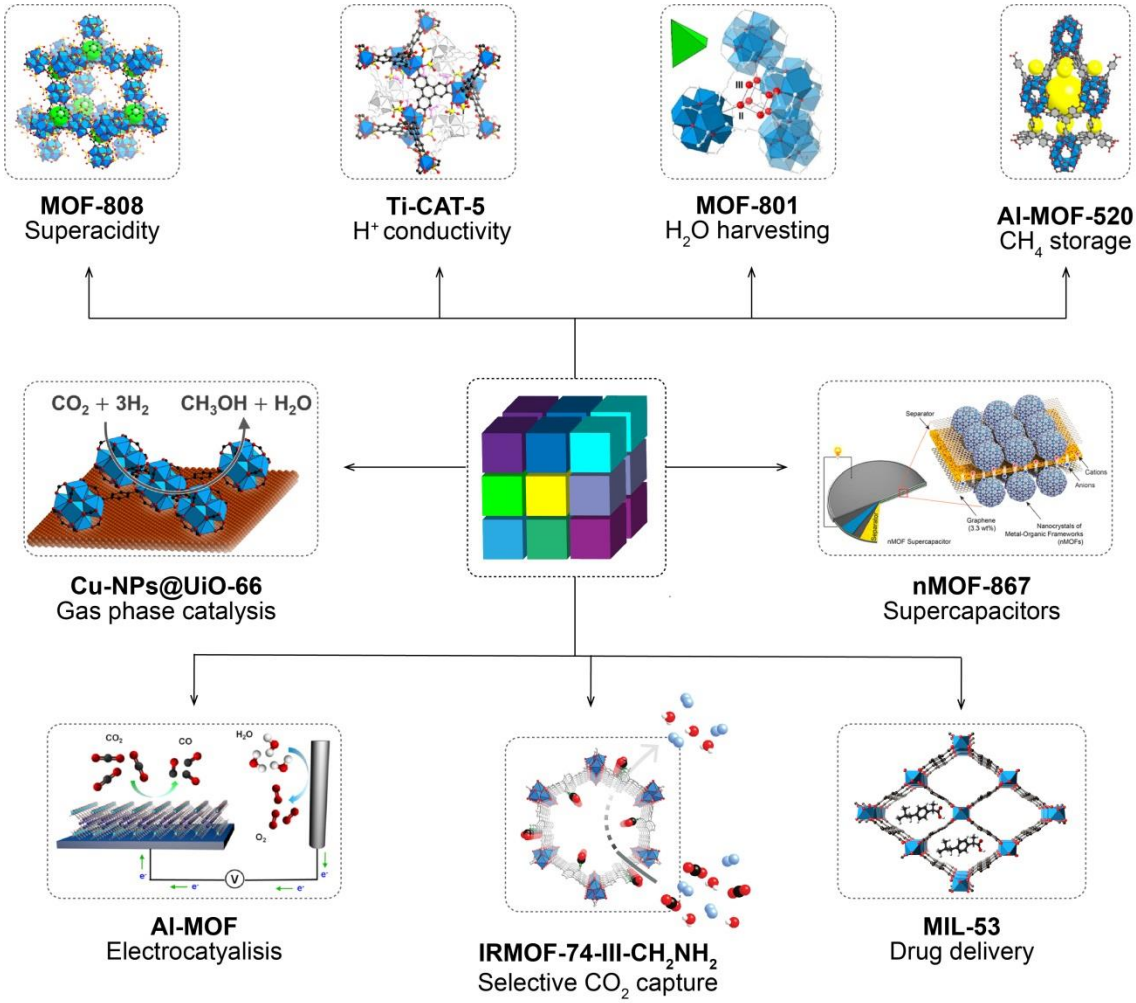

Resumen

Los Entramados Metal-Orgánicos o MOFs (Metal-Organic Frameworks), son una clase relativamente nueva de materiales cristalinos porosos constituidos por la coordinación de nodos metálicos (o clústeres) y conectores orgánicos de variada naturaleza química. Debido a su gran versatilidad estructural y a la posibilidad de incorporar pre- o post-sintéticamente múltiples funcionalidades, los MOFs resultan prometedores en diversas aplicaciones tales como la adsorción y almacenamiento selectivo de gases y toxinas, la construcción de sensores, y el almacenamiento y conversión de energía, entre otras. Este artículo constituye una revisión breve de avances recientes en métodos novedosos de síntesis y modificación post-sintética de MOFs y otros materiales integrando MOFs en su estructura. Los materiales revisados presentan propiedades interesantes tales como súper-acidez, quimioselectividad en catálisis heterogénea, pre-concentración en interfaces electroquímicas, y adsorción selectiva de gases de interés industrial o ambiental.

Abstract

Metal-Organic Frameworks (MOFs) are a relatively new class of porous materials constituted by strong bonds between inorganic clusters (or secondary building units - SBUs) and organic struts forming open crystalline networks. Due to the large variety of inorganic and organic building units possible to be connected, there are more than 10000 MOFs crystallographic structures reported so far in the Cambridge Structural Database (CSD). This structural versatility together with the possibility for their pre- and post-synthetic functionalization, provide with a great number of opportunities in terms of surface chemistry and functionalization for their application in diverse fields such as selective gas adsorption and storage, sensors and actuators, energy storage and conversion, among others. In this article, we briefly survey significant contributions related to synthesis and post-synthetic modification of MOFs and composite materials integrating MOFs. These materials feature interesting properties such as superacidity, high chemoselectivity in heterogeneous catalysis, pre-concentration at electrochemical interfaces, or selective adsorption of industrial and environmentally relevant gases.

Palabras Clave: *Entramados Metal-Orgánicos, Materiales Nanoestructurados, Films Microporosos, Adsorción de Gases, Multifuncionalidad Estructural.*

Keywords: *Metal-Organic Frameworks, Nanostructured Materials, Microporous Films, Gas Adsorption, Structural Multifunctionality.*

1. Introduction

Metal Organic Frameworks (MOFs), also known as Porous Coordination Polymers (PCPs), constitute a relatively new class of microporous materials built from organic struts and metal clusters or secondary building units (SBUs) stitched together by strong covalent bonds (Figure

1). Their construction flexibility allow to access great diversity of materials, in terms of pore structure, environment and chemical functionalization.[1–5]

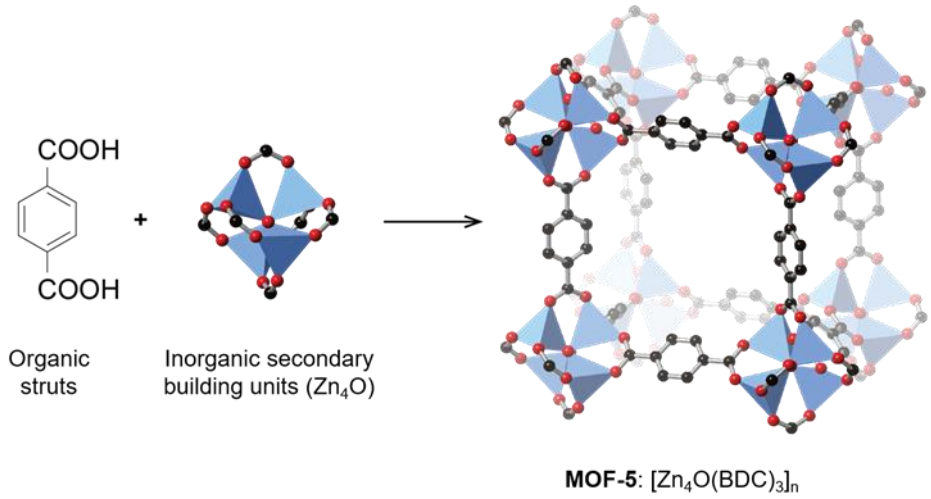

Figure 1. Schematic representation for the construction of MOF-5, in which terephtalic acid organic strut is covalently bound to zinc oxide clusters to form a highly porous 3D structure.

Although several synthetic strategies have been used to prepare MOFs and MOF-containing materials (e.g., compact and defect-free MOF thin films,[6] solvent-free MOF microcrystals,[7] or layer-by-layer surface growth of MOF-membranes[8]), the most utilized synthetic method has been the solvothermal reaction of the precursors to yield the crystalline materials. These structures can be separated from the unreacted materials by simple filtration. After the synthesis, the material internal surface (pores) become available through a process known as "*activation"*, in which the crystals obtained are thoroughly washed with solvent to remove unreacted starting materials and byproducts, and the remaining solvent inside the structure is removed by heat, vacuum, supercritical carbon dioxide, or a combinations of the previous.[9] Recent years have witnessed an expansion in the number of journal publications and patents featuring specifically designed MOFs constructed to offer alternative solutions to a wide variety of challenges; e.g. capture of greenhouse gases, drug-delivery, biomedicine,[10–12] gas and liquid phase separation technologies,[13–19] and catalysis among others (Figure 2).[20–22]

One of the main reasons for the exponential growth in the number of MOFs reported structures, is the great variety of building units that can be combined to create different pore architectures by design, and the ease with which these porous structures can be functionalized by post-synthetic modifications, organic struts mixing (multivariate strategy), and integration with other nanomaterials and polymers. Specifically, designed pores can endow MOFs with "superacidity", selective carbon dioxide capture in the presence of water, enzyme-like selectivity in catalysis, selective permeation, unique sensing capabilities, etc.[23]

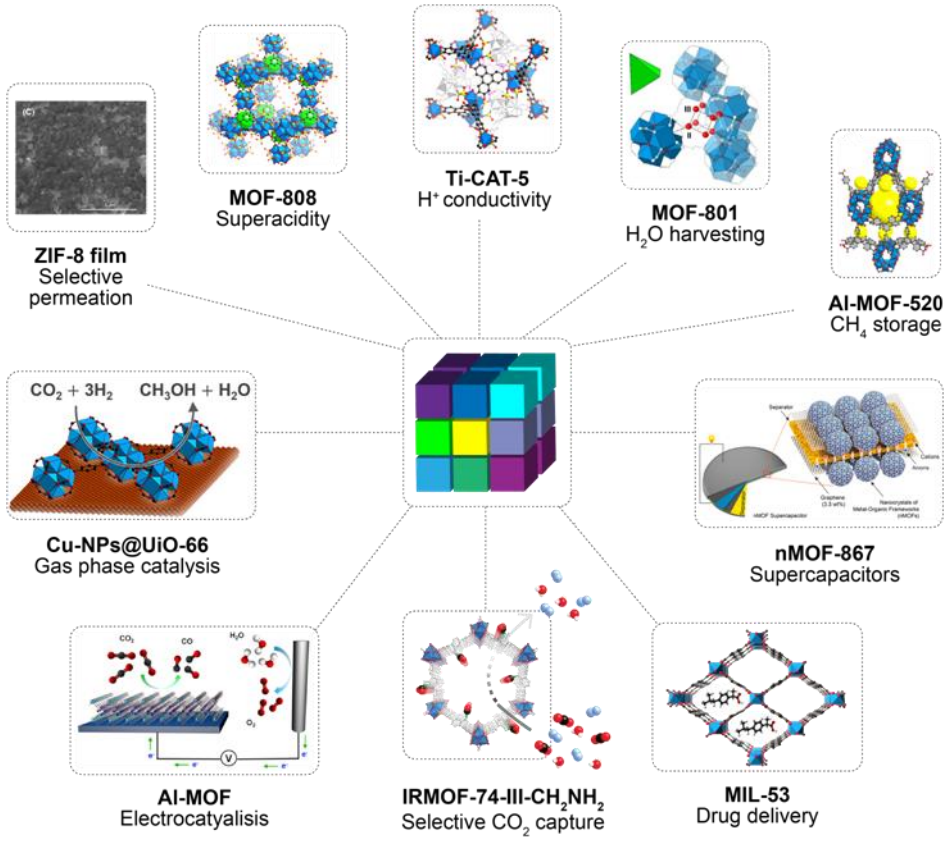

Figure 2. MOFs structural versatility and ease of functionalization which lead to materials suitable for a number of potential applications.

Recent reviews cover suitable strategies for the synthesis of MOFs with specific properties typically found in other classes of materials (e.g., to introduce macro and mesoporosity into otherwise homogeneous microporous MOF without losing crystalline order).[24] However, the above mentioned strategies include the use of metal nanoparticles, functional surfaces, or inorganic nanocrystals among others in the construction of MOF-containing hybrid materials.[25]

The possibility of manufacturing a porous network nearly at will, with surface areas beyond 7000 $m^2.g^{-1}$,[26] is an appealing opportunity to develop highly active heterogeneous catalysts in which the crystallinity of these materials also provide the unique advantage of placing catalytically active centres (e.g.; metal nanoparticles) within this high inner surface.[27,28]

Chemical and structural flexibility of MOFs find application also as porous supports for the fabrication of microdevices (e.g., through the so-called "nanoarchitectonics" approach, as coined recently by Ariga).[29–32] Since many of these attractive properties are enhanced by the use of films, a great deal of effort has been devoted to study several growth and anchoring strategies, and to explore suitable characterization techniques.[33–39] If MOF films are grown on a electrochemically active substrate, and given that MOF film can selectively adsorb the reactants which will be subject of redox reactions at the surface (e.g., CO_2 or O_2), then an interesting

enhancement effect on the electrode reaction can be observed.[40] In order to achieve this functional composite material, affinity between substrate surface and MOF film must be ensured because this would ultimately provide mechanical stability and thickness control.[41,42]

Throughout this article, we will briefly describe some examples of the above discussed characteristics and applications of MOFs, with emphasis on the latest developments regarding synthesis strategies oriented to enhance functional properties.

2. Pre- and post-synthetic MOF functionalization.

Architectural versatility and functionality can be achieved in MOFs by the infinite variety and combination of building units. Nevertheless, further introduction of reactive chemical functionalization can be achieved by pre- and post-synthetic transformation of the building units.

Different kind of functionalities can be incorporated also by the simple functionalization the organic struts prior to MOF synthesis, strategy named "pre-synthetic functionalization". However the functional groups thus incorporated must be compatible with the MOFs synthetic conditions. Examples of this procedure can be found in literature, since the report of isoreticular MOFs (IRMOFs) derivatives, where halogens, aromatic amines and other functionalities, were introduced to the cubic MOF-5 structure.[43] For instance, the MOF-5 structure is compose of octahedral ZnO clusters linked by terephtalic acid as organic strut, reticulating a primitive cubic structure (see Figure 3a) with exceptional rigidity and surface area. On the other hand, the use of 2-aminoterephtalic acid, instead of terephtalic acid, yield crystals of IRMOF-3 which has the same underlying topology than MOF-5 but features aromatic amine functionalities decorating the MOF surface area (see Figure 3b).

In addition, it was also demonstrated that different functionalities can be incorporated simultaneously to the pores of MOF-5, originating multivariate MOFs (MTV-MOFs, Figure 3c) with different properties compared with their non-functionalized or homogeneously-functionalized versions.[44]

There are, however, some reactive functional groups that cannot be directly introduced to the precursors by pre-synthetic modifications or MTV-approach, as these functionalities might interfere with the formation of the MOFs extended structures. A clear example is

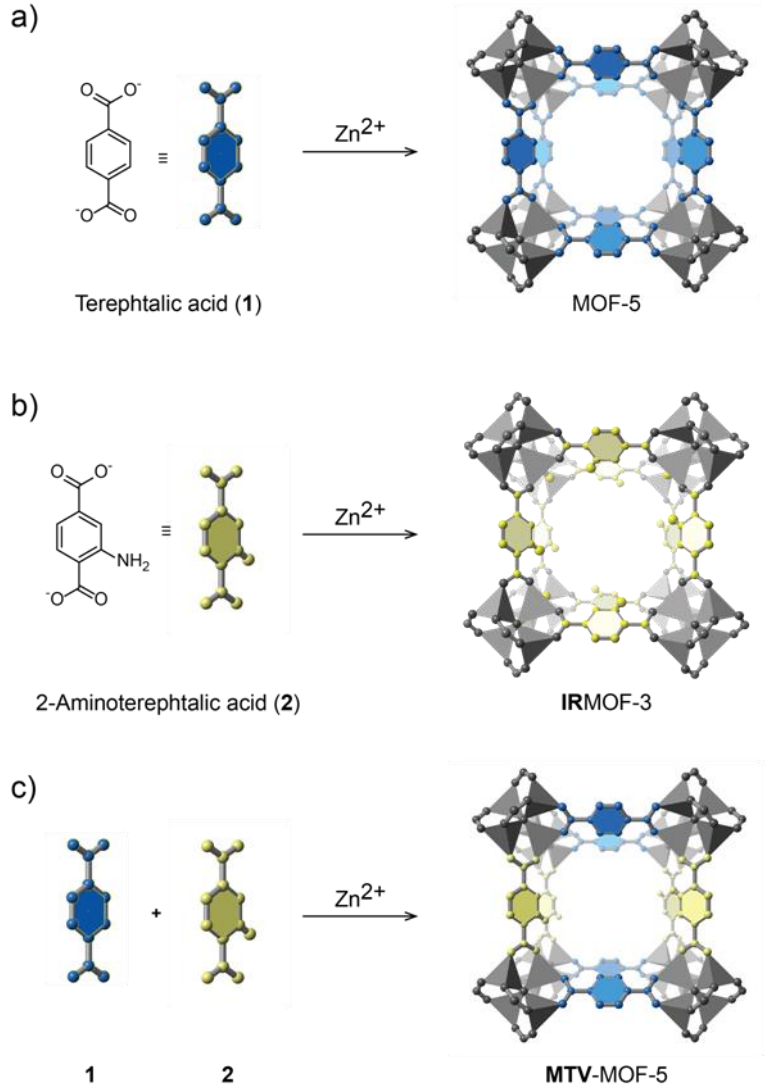

Figure 3. Schematic representation for the pre-synthetic functionalization of MOF-5. a) Synthesis of MOF-5, b) synthesis of IRMOF-3 which features the same underlying topology than MOF-5 but incorporating aromatic amine functionalities in its pores, and c) preparation of MTV-MOF-5, by organic struts mixing.

introduction of primary or secondary amines to the pores, which cannot be achieved by simple functionalization of the organic struts as these groups will affect the metal coordination and the solution pH, preventing the MOF crystalline structure from forming under the above described solvothermal conditions.[45] Thus, a wide variety of strategies were recently developed to incorporate these reactive functionalities to the MOF. One successful strategy consists in performing reactions over the already prepared MOF crystals, approach known as *post-synthetic modifications* (PSM). These PSMs can be achieved on both, the inorganic clusters (known as *dative* PSM) or the organic struts present in the MOFs (i.e. *post-synthetic deprotections* and *covalent modifications*). For instance, in order to incorporate the organocatalyst proline (containing a secondary amine) to IRMOF-10 (an expanded version of MOF-5), *tert*-

butyloxycarbonyl (Boc) protecting group was employed. Thus the protected version of the secondary amine did not interfere with the MOF synthesis, and the protecting group was successfully removed with no deterioration of the MOF crystallinity or porosity. This later bond-breaking reaction to release secondary amine functional groups in the MOF pores, represents a successful example of the *post-synthetic deprotection*, mentioned above.[45]

Covalent incorporation of reactive functionalities such as primary and secondary amines have a deep impact in the materials properties and represent an opportunity to fine-tune the pore environments for a particular application.

It was reported that MOF constructed from magnesium oxide rods joined by the linear 2,5-dihydroxyterephthalic acid strut is an exceptional material for taking up carbon dioxide[46] (8.9 wt. % dynamic capacity), however it losses almost 80% of its capacity in the presence of water, an impurity commonly present in the flue gases. On the other hand, primary amine functionalized IRMOF-74-III showed 3.5 wt. % dynamic CO_2 uptake capacity, but this capacity remains unchanged in the presence of water.[16]

Taking advantage of protecting groups and the crystallographic precision with which functional groups can be installed into MOF structures, it is possible to further react functionalized frameworks to achieve high complexity in the pore environment. Recently, it was demonstrated that this primary amino-functionalized IRMOF-74-III can undergo up to seven post-synthetic modifications *in tandem* to install tripeptides in the pore interior. More importantly, these seven reactions performed over the previously synthetized MOF proceed with no loss in the material crystallinity or porosity.[47] This reported example suggest that enzyme-pocket architectures can be achieved in the MOF pore environments, making possible to carry out examples of catalysis previously known only by enzymes (Figure 4).

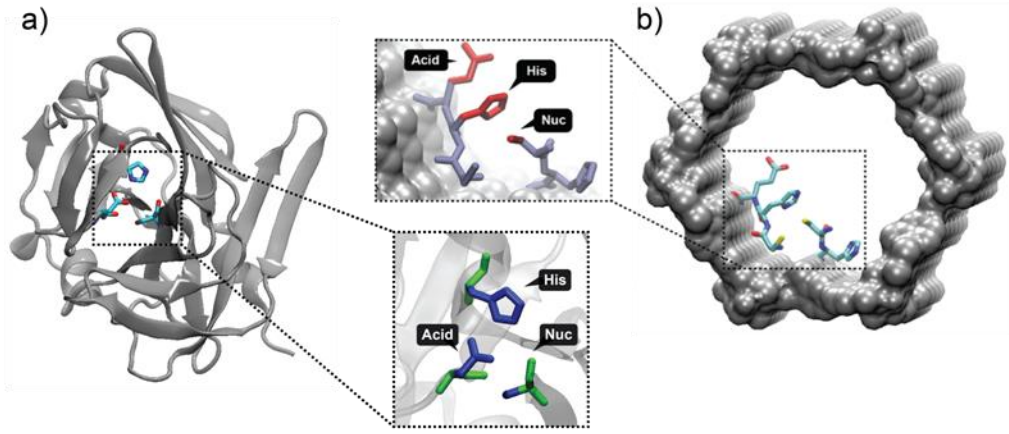

Figure 4. **a)** Comparative representation of 1D pores of IRMOF-74-III covalently modified with the tripeptide -CH_2NH-Asp-His-Cys-NH_2, and **b)** the catalytic triad in the active site of TEV-protease.

Post synthetic modification has proved to be a useful strategy also in the area of MOF film formation, where it can be applied not only to improve film deposition quality, but to modify the properties of the synthesized film. A recent example of this strategy was used in ZIF-8 MOF nanocrystals as recently reported.[48] In this work, an archetypal member of the Zeolite Imidazolate Frameworks (ZIFs) MOF subclass, constituted by tetrahedrally coordinated Zn^{2+} ions with 2-methylimidazolate linkers, was surface modified without crystallinity lost, using a controlled and simple methodology in order to obtain surface confined thiol moieties that can be used to create self-assembled films on gold substrates. This proof of concept constitutes an interesting example for two main reasons; it represents a general way to confer MOF nanocrystals with specific affinity for a given desired surface, and on the other hand, the modified material features chemisorption of tunable size units resembling to their molecular analogues in a typical thiolate Self Assembled Monolayers (SAMs).

Another example of the above described approach, is the recently reported modification of MOF films with highly charged polyelectrolytes as capping agent.[49] In this study, it was demonstrated that the hydrophobic/hydrophilic character of MOF films can be modulated by simple dip-coating of the films in PSS (poly-styrene sulfonate) aqueous solutions. More importantly, it was proved that the capping agent modification was not limited to the film surface but also permeates through the mesocavities present, thus changing the transport properties of the entire film. This modification of hydrophilicity constitutes an interesting alternative to important applications in catalysis as it allowed for the synthesis of d-block metal nanoparticles *via* direct aqueous chemical reduction of the precursors in the polyelectrolyte-modified film.

3. MOF films: influence of surface anchoring sites on growth dynamics and structure.

MOF films and membranes can be produced in a straightforward way following several different procedures. Among them one can mention the *seeded-growth method*,[50] which involves the seeding of solvothermal pre-synthesized units forming a layer (e.g., *via* spin-coating), followed by secondary heterogeneous growth under different conditions aimed to favor certain desired morphology.[51] As in general for nucleation of crystalline solids in presence of interfaces, both homogeneous and heterogeneous nucleation processes are present when synthesizing a MOF film. Depending on supersaturation and temperature conditions used, a critical size nuclei leading to solid formation need an induction time to occur.[52]

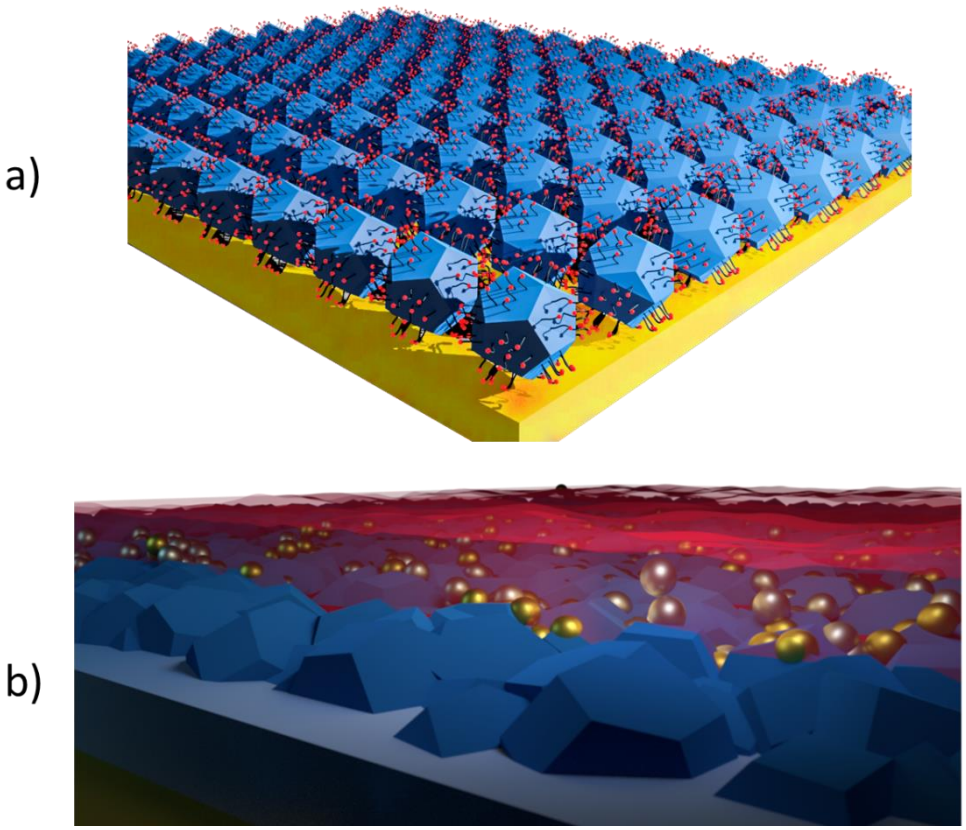

Figure 5. Schematic representation of **a)** film formation of chemical assembled Cys-modified ZIF-8 crystallites, **b)** ZIF-8 film modification with PSS as capping agent and reaction-diffusion synthetized d-block metal nanoparticles throughout film z-direction.

Different from the above discussed examples, *one-pot* MOF film synthesis strategies, offer simpler procedures and extra degree of control on the obtained material. The need of seeded surfaces can be circumvented by using suitable surface modifications of the substrates employed, in this way, the induction time can be drastically reduced. This effect was reported for the synthesis of several MOF films, were surface chemistry compatible with building blocks showed both a strong effect decreasing the induction time, and also promoting preferential growth in a certain crystalline direction.[42,52,53] Figure 6 shows an example of time evolution and growth extent observed for Zn-based ZIF-8 MOF films synthesized over different chemically-modified Au substrates followed by Quartz Crystal Microbalance (QCM) technique.

Aside from the interesting different induction times observed in Figure 5, self-assembled monolayers (SAMs) featuring $-SO_3^-$ moieties (MPSA) present an important enhancement of film growth. This was hypothesized to occur due to strong coordinative interactions between sulfonate groups and Zn^{2+} ions, as already reported.[42] A further example of this enhancement effect was obtained using grafting of tridimensional primers, rather than 2D SAMs, constituted by polymeric brushes of 3-sulfopropylmethacrylate monomers.[41] In this way, preconcentration of metal ions within the macromolecular 3D primer triggers a rapid increase of nucleation sites in

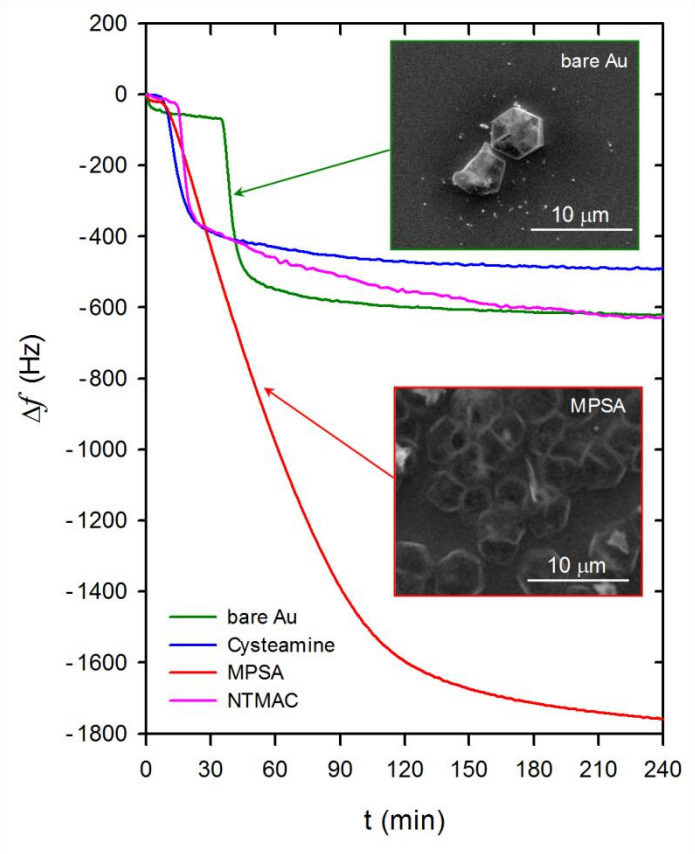

Figure 6. Time evolution of ZIF-8 film growth over Au and three different chemically modified Au substrates. Bare Au, and Self-Assembled Monolayers (SAMs) of the following thiol-baring molecules: cysteamine exposing primary amine moieties, MPSA (3-mercapto-1-propanesulfonic acid) exposing sulfonate moieties, and NTMAC (N,N,N-trimethyl(3-mercaptopropyl)-ammonium chloride) exposing quaternary amine terminal groups.

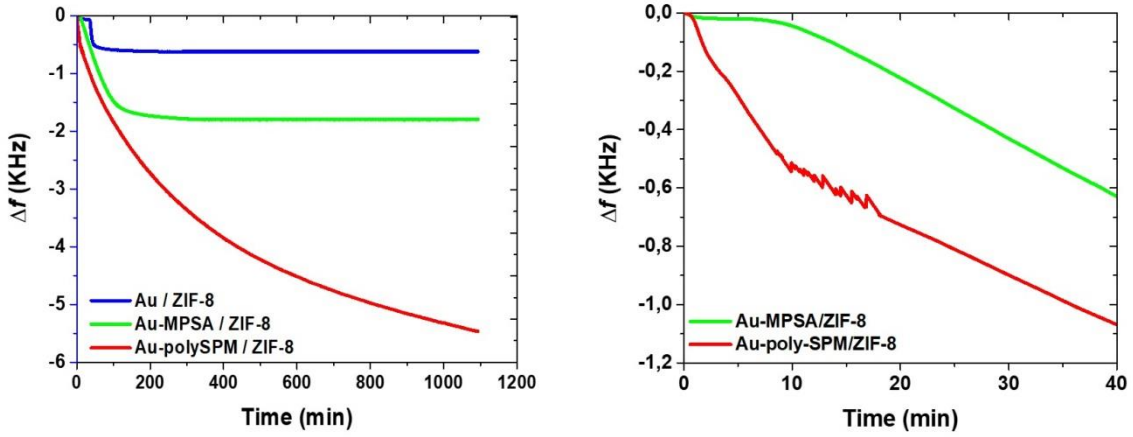

Figure 7. *Left*, deposition of ZIF-8 films on different surfaces, as detected by QCM: (blue) bare gold, (green) MPSA modified-gold, and (red) polymer brush. MOF film growth is directly proportional to the frequency change. *Right*, early stages of time in the film growth evolution.

the primer. Figure 7 shows the obtained increase in both growth speed and extent when polymeric brushes with sulfonate pendant groups are present. Figure 8 shows the 3D primer surface as observed *via* Atomic Force Microcopy, together with schematics of synthesis procedure.

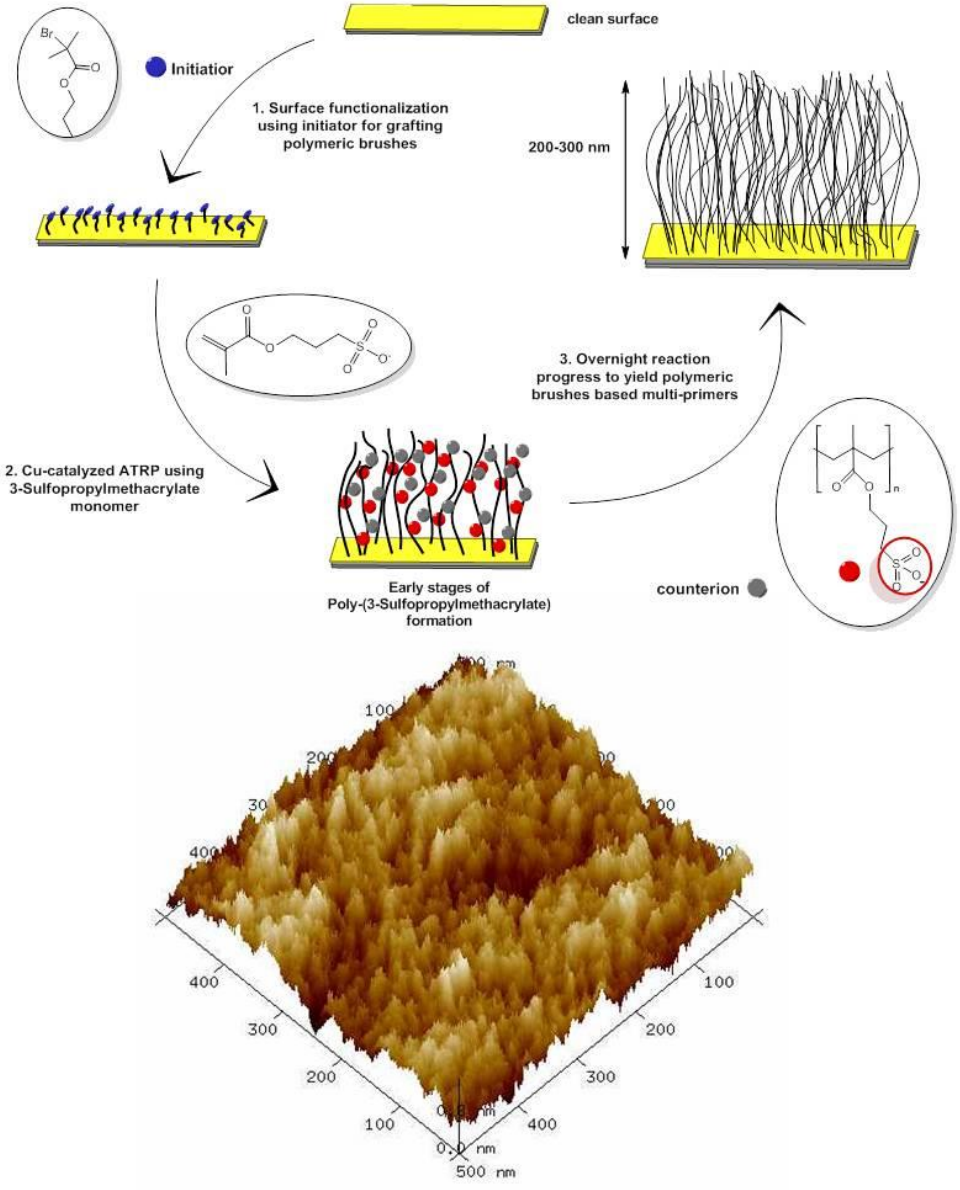

Figure 8. *Top*, schematic representation of the fabrication of polymeric brushes. *Bottom*, surface of modified Au substrate as obtained *via* AFM

.

4. Applications.

4.1 Enhancement of the Oxygen Reduction Reaction (ORR).

As discussed above, high porosity and the versatility of the pore identity are crucial characteristics allowing MOF to be applicable in wide range of fields. Integrating MOFs to *functional composites*, it was proved that ZIF-8 can be assembled on electroactive conductive polymers based on aniline and *p*-amino benzoic acid (PANI-PABA), and synergically by an easy, mild and low cost process, to obtain stable composites, that can improve electrocatalytic oxygen reduction reaction (ORR) via selective oxygen adsorption from neutral pH aqueous solutions, as shown in Figure 9.[40]

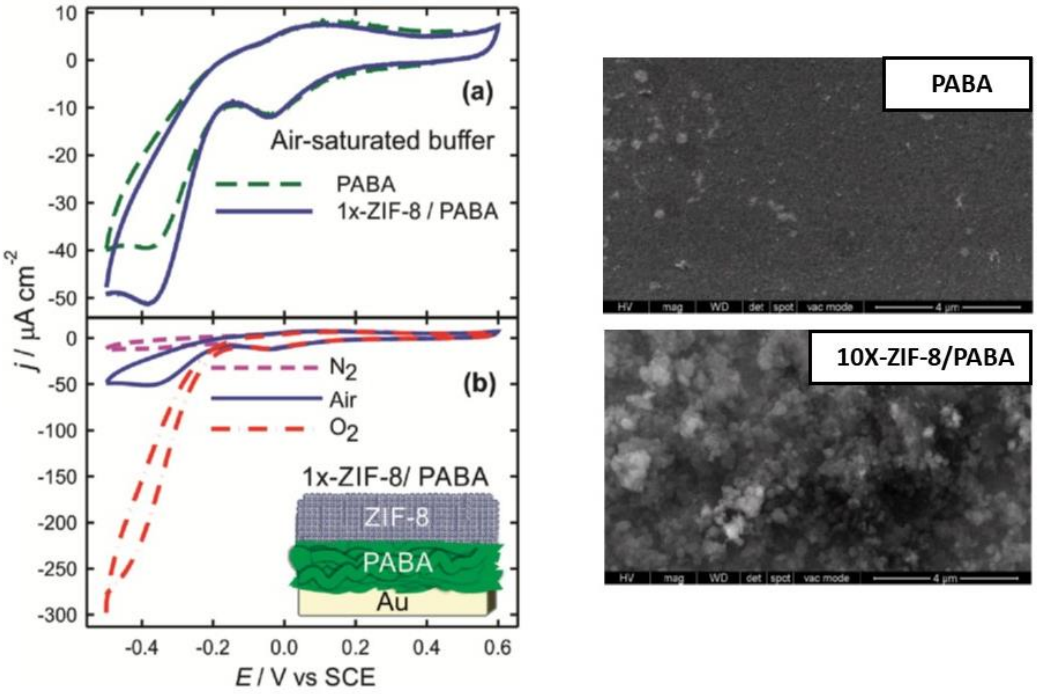

Figure 9. *Left*, **a)** Voltammetric response of PABA and 1x-ZIF-8/PABA modified electrodes in air saturated buffer. **b)** Comparison of the CV response of a 1x-ZIF-8/PABA-modified electrode at different concentrations of dissolved O_2. *Right*, SEM images of PABA top surface and 10x-ZIF-8/PABA modified electrodes top surface.

The incorporation of ZIF-8 to the composite material helps preventing contamination of the electroactive film (antifouling), whilst the intergrain mesoporosity gained by MOF inclusion helps to enhance diffusion properties of the conductive polymer.

4.2 Carbon capture and storage.

Anthropogenic carbon dioxide (CO_2) emissions have been identified as a significant cause of global warming and climate change. In order to improve this situation, carbon capture and

storage (CCS), has been developed and is becoming increasingly commercially viable. Currently employed technologies such as monoethanolamine scrubbing present important drawbacks in terms of energy consumption, adsorbent regeneration, and pipeline corrosion.[54] These challenges motivated the development of porous solids as CO_2 sorbents including mesoporous carbons, mesoporous silica, porous polymers, zeolites and recently, metal-organic frameworks (MOFs). Porous solid are attractive due to their high surface areas, improved gas-solid mass transfer, and lower regeneration energies due to smaller heat capacities in comparison with aqueous amine solutions.[55] However, very often the capacity of these porous adsorbents drop when they are exposed to common flue gas contaminants from which carbon dioxide must be separated, especially water. The possibility of carefully and covalently bind functionalities to MOFs in precise positions throughout the material surface area, has given to these porous materials an advantage compare to the other listed above. In this sense, several successful examples of post-synthetically modified MOFs have been reported for the selective capture of CO_2. Among the chosen strategies to enhance MOF selectivity and uptake capacity for CO_2, perhaps the most explored one is the incorporation of amine functionalities to the pores of MOFs. In order to bind active amines to the MOF surface we can clearly distinguish two different approaches: **a**) dative post/synthetic binding of alkylamines to the MOF SBUs[56,57], and **b**) pre-synthetic incorporation of alkylamines followed by post-synthetic deprotection (Figure 9).[16,17,58] In the first approach developed by the Long group (**a**), already prepared by immersion of the already prepared MOF into an alkyldiamine solution. Due to its affinity for the coordinatively unsaturated metal at the MOF SBUs, one of the amines anchors to the metal, leaving the second hanging in the MOF pore. The product of the dative post-synthetic modification on Mg_2(dobpdc), where H_4dobpdc = 4,4′-dihydroxy-(1,1′-biphenyl)-3,3′-dicarboxylic acid] with N,N′-dimethylethylenediamine, showed high affinity for CO_2 at low partial pressures (8.1 wt % at 0.39 mbar) demonstrating the efficiency of this approach to enhance the material as CO_2 sorbent. The second approach developed by Yaghi group (**b**), reactive alkyl amines are incorporated through pre-synthetic functionalization of the organic struts with protected derivatives of these amines. Those amines, are later thermally deprotected in a complete post-synthetic step leaving the free amines in the pores of MOF. The compound prepared by this strategy (IRMOF-74-III-CH_2NH_2), showed a CO_2 uptake capacity of 3.5 wt % under humid and *dynamic conditions.*[a] Although the **b** approach involves a larger number of synthetic steps, the amines are covalently bound to the MOF pores, providing the material with an enhanced stability of this active sites against the conditions under which very often this CO_2 capture takes place.

[a] Uptake capacity determined by break-through experiments in which a column is packing with the adsorbent material and the time that takes a gas in a mixture of gases to break through this column is measured.

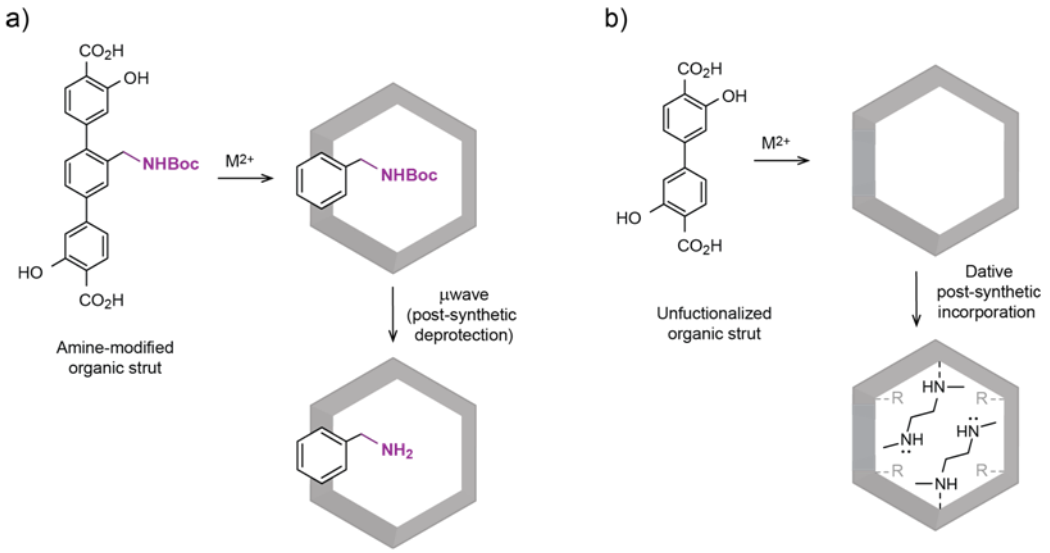

Figure 10. Schematic representation of two different strategies for the amine-functionalization of a MOF featuring hexagonal 1D pores.

Other interesting strategies were employed in order to modify MOFs to enhance CO_2 selectivity in the capture process. Hydrophobic pores, adjustment of pore size, covalent incorporation of other functionalities like OH groups,[59–63] are some of them, however we do not describe those strategies in deep in this article.

4.3 Enzyme-inspired catalysis.

The efficiency and selectivity with which enzymes perform in catalytic processes is rarely achieved by artificial systems. Therefore, preparing synthetic materials that can function in a similar way than enzymes but in a wider range of conditions has been a long standing goal. The crystallinity, pore-geometry control and ease of functionalization achieved in MOFs allowed several examples of careful tuning of pore properties to enhance the materials catalytic activity.[64,65] Recently, and taking advantage of sequential post-synthetic modifications without losing crystallinity or pore access, it was demonstrated that MOF pores can function in a way that was previously only known for enzyme pockets (see ref. 47 and Figure 4). The crystalline precision with which atoms are located in the pores of MOFs, the opportunity of tuning the pore geometry and size, and the ease of functionalization by either pre- or post-synthetic modifications allow to design catalytic nanocavities that resemble enzyme pockets.[66–68]

3. Conclusions

In this minireview, we have introduced fundamental aspects of the *state of the art* in MOF and MOFs membranes focusing on their synthesis, functionalization and applications. Being a relatively new class of porous material and due to their remarkable versatility (both chemical and

structural), the number of reported possible applications are continuously increasing, and thus difficult to cover in detail. This is why in terms of the materials applications, we have restricted our description to some key aspects that will have the stronger impact in the next few decades, namely: *i)* CO_2 *capture* related applications (both carbon capture and sequestration, and conversion technologies); *ii)* MOF composite film synthesis and its application to *sensor and energy conversion/storage technologies*; *iii)* different aspects of applications in *heterogeneous catalysis*. Although the seminal work included here constitute starting points for future research directions, they also represent a clear evidence of the impact of recently developed MOFs in the field of material science, both in fundamental and applied research.

Acknowledgments

Matías Rafti and Jimena Tuninetti are thankful for the valuable contribution of the Soft Matter Laboratory group to the multidisciplinary work and results discussions. Matías Rafti and Jimena Tuninetti are CONICET fellows. A. M. Fracaroli acknowledge SuNaLab and Berkeley Global Science Institute for the valuable discussions and support, and he is thankful to CONICET and the Office of Naval Research Global (ONRG) for funding.

References

(1) Hoskins, B.; Robson, R. Infinite Polymeric Frameworks Consisting of Three Dimensionally Linked Rod-like Segments. *J. Am. Chem. Soc.* **1989**, *111* (15), 5962–5964.

(2) Furukawa, H.; Cordova, K. E.; O'Keeffe, M.; Yaghi, O. M. The Chemistry and Applications of Metal-Organic Frameworks. *Science.* **2013**, *341* (6149), 1230444–1230444.

(3) Zhou, H. C.; Long, J. R.; Yaghi, O. M. Introduction to Metal-Organic Frameworks. *Chemical Reviews*. 2012, 112(2), 673-674.

(4) Meek, S. T.; Greathouse, J.; Allendorf, M. D. Metal-Organic Frameworks: A Rapidly Growing Class of Versatile Nanoporous Materials. *Adv. Mater.* **2011**, *23* (2), 249–267.

(5) Čejka, J. Metal-Organic Frameworks. Applications from Catalysis to Gas Storage. Edited by David Farrusseng. *Angew. Chemie Int. Ed.* **2012**, *51* (20), 4782–4783.

(6) Shekhah, O.; Eddaoudi, M. The Liquid Phase Epitaxy Method for the Construction of Oriented ZIF-8 Thin Films with Controlled Growth on Functionalized Surfaces. *Chem. Commun. (Camb).* **2013**, *49* (86), 10079–10081.

(7) Klimakow, M.; Klobes, P.; Rademann, K.; Emmerling, F. Characterization of Mechanochemically Synthesized MOFs. *Microporous Mesoporous Mater.* **2012**, *154*, 113–118.

(8) Diestel, L.; Bux, H.; Wachsmuth, D.; Caro, J. Pervaporation Studies of N-Hexane, Benzene, Mesitylene and Their Mixtures on Zeolitic Imidazolate Framework-8 Membranes. *Microporous Mesoporous Mater.* **2012**, *164*, 288–293.

(9) Li, J. R.; Sculley, J.; Zhou, H. C. Metal-Organic Frameworks for Separations. *Chemical Reviews*. 2012, 112(2), 869–932.

(10) Férey, G.; Mellot-Draznieks, C.; Serre, C.; Millange, F.; Dutour, J.; Surblé, S.; Margiolaki, I. A Chromium Terephthalate-Based Solid with Unusually Large Pore Volumes and Surface Area. *Science* **2005**, *309* (5743), 2040–2042.

(11) Faust, T. MOFs Move to Market. *Nat. Chem.* **2016**, *8* (11), 990–991.

(12) Millward, A. R.; Yaghi, O. M. Metal-Organic Frameworks with Exceptionally High Capacity for Storage of Carbon Dioxide at Room Temperature. *J. Am. Chem. Soc.* **2005**, *127* (51), 17998–17999.

(13) Wang, B.; Côté, A. P.; Furukawa, H.; O'Keeffe, M.; Yaghi, O. M. Colossal Cages in Zeolitic Imidazolate Frameworks as Selective Carbon Dioxide Reservoirs. *Nature* **2008**, *453* (7192), 207–211.

(14) Sumida, K.; Rogow, D. L.; Mason, J. A.; McDonald, T. M.; Bloch, E. D.; Herm, Z. R.; Bae, T. H.; Long, J. R. Carbon Dioxide Capture in Metal-Organic Frameworks. *Chem. Rev.* **2012**, *112* (2), 724–781.

(15) Férey, G.; Serre, C.; Devic, T.; Maurin, G.; Jobic, H.; Llewellyn, P. L.; De Weireld, G.; Vimont, A.; Daturi, M.; Chang, J.-S. Why Hybrid Porous Solids Capture Greenhouse Gases? *Chem. Soc. Rev.* **2011**, *40* (2), 550–562.

(16) Fracaroli, A. M.; Furukawa, H.; Suzuki, M.; Dodd, M.; Okajima, S.; Gándara, F.; Reimer, J. A.; Yaghi, O. M. Metal-Organic Frameworks with Precisely Designed Interior for Carbon Dioxide Capture in the Presence of Water. *J. Am. Chem. Soc.* **2014**, *136* (25), 8863–8866.

(17) Flaig, R. W.; Osborn Popp, T. M.; Fracaroli, A. M.; Kapustin, E. A.; Kalmutzki, M. J.; Altamimi, R. M.; Fathieh, F.; Reimer, J. A.; Yaghi, O. M. The Chemistry of CO_2 Capture in an Amine-Functionalized Metal-Organic Framework under Dry and Humid Conditions. *J. Am. Chem. Soc.* **2017**, *139* (35), 12125

(18) Horcajada, P.; Gref, R.; Baati, T.; Allan, P. K.; Maurin, G.; Couvreur, P.; Férey, G.; Morris, R. E.; Serre, C. Metal-Organic Frameworks in Biomedicine. *Chem. Rev.* **2012**, *112* (2), 1232–1268.

(19) Horcajada, P.; Chalati, T.; Serre, C.; Gillet, B.; Sebrie, C.; Baati, T.; Eubank, J. F.; Heurtaux, D.; Clayette, P.; Kreuz, C.; et al. Porous Metal–organic-Framework Nanoscale Carriers as a Potential Platform for Drug Delivery and Imaging. *Nat. Mater.* **2010**, *9* (2),

172–178.

(20) Keskin, S.; Kizilel, S. Biomedical Applications of Metal Organic Frameworks. *Ind. Eng. Chem. Res.* **2011**, *50* (4), 1799–1812.

(21) Cook, T. R.; Zheng, Y. R.; Stang, P. J. Metal-Organic Frameworks and Self-Assembled Supramolecular Coordination Complexes: Comparing and Contrasting the Design, Synthesis, and Functionality of Metal-Organic Materials. *Chem. Rev.* **2013**, *113* (1), 734–777.

(22) Lu, G.; Li, S.; Guo, Z.; Farha, O. K.; Hauser, B. G.; Qi, X.; Wang, Y.; Wang, X.; Han, S.; Liu, X.; et al. Imparting Functionality to a Metal–organic Framework Material by Controlled Nanoparticle Encapsulation. *Nat. Chem.* **2012**, *4* (4), 310–316.

(23) Santos, V. P.; Wezendonk, T. A.; Jaén, J. J. D.; Dugulan, A. I.; Nasalevich, M. A.; Islam, H. U.; Chojecki, A.; Sartipi, S.; Sun, X.; Hakeem, A. A.; et al. Metal Organic Framework-Mediated Synthesis of Highly Active and Stable Fischer-Tropsch Catalysts. *Nat. Commun.* **2015**, *6*.

(24) Furukawa, H.; Müller, U.; Yaghi, O. M. "Heterogeneity within Order" in Metal-Organic Frameworks. *Angew. Chemie - Int. Ed.* **2015**, *54* (11), 3417–3430.

(25) Esken, D.; Turner, S.; Lebedev, O. I.; Van Tendeloo, G.; Fischer, R. A. Au@ZIFs: Stabilization and Encapsulation of Cavity-Size Matching Gold Clusters inside Functionalized Zeolite Imidazolate Frameworks, ZIFs. *Chem. Mater.* **2010**, *22* (23), 6393–6401.

(26) Farha, O. K.; Eryazici, I.; Jeong, N. C.; Hauser, B. G.; Wilmer, C. E.; Sarjeant, A. A.; Snurr, R. Q.; Nguyen, S. T.; Yazaydin, A. Ö.; Hupp, J. T. Metal-Organic Framework Materials with Ultrahigh Surface Areas: Is the Sky the Limit? *J. Am. Chem. Soc.* **2012**, *134* (36), 15016–15021.

(27) Choi, K. M.; Na, K.; Somorjai, G. A.; Yaghi, O. M. Chemical Environment Control and Enhanced Catalytic Performance of Platinum Nanoparticles Embedded in Nanocrystalline Metal-Organic Frameworks. *J. Am. Chem. Soc.* **2015**, *137* (24), 7810–7816.

(28) Rafti, M.; Brunsen, A.; Fuertes, M. C.; Azzaroni, O.; Soler-Illia, G. J. A. A. Heterogeneous Catalytic Activity of Platinum Nanoparticles Hosted in Mesoporous Silica Thin Films Modified with Polyelectrolyte Brushes. *ACS Appl. Mater. Interfaces* **2013**, *5* (18), 8833–8840.

(29) Ariga, K.; Ji, Q.; Mori, T.; Naito, M.; Yamauchi, Y.; Abe, H.; Hill, J. P. Enzyme Nanoarchitectonics: Organization and Device Application. *Chem. Soc. Rev.* **2013**, *42* (15), 6322–6345.

(30) Angew, R. *Manipulation of Nanoscale Materials: An Introduction to Nanoarchitectonics*;

2012.

(31) Li, P.; Modica, J. A.; Howarth, A. J.; Vargas L., E.; Moghadam, P. Z.; Snurr, R. Q.; Mrksich, M.; Hupp, J. T.; Farha, O. K. Toward Design Rules for Enzyme Immobilization in Hierarchical Mesoporous Metal-Organic Frameworks. *Chem* **2016**, *1* (1), 154–169.

(32) Liu, W. L.; Wu, C. Y.; Chen, C. Y.; Singco, B.; Lin, C. H.; Huang, H. Y. Fast Multipoint Immobilized MOF Bioreactor. *Chem. - A Eur. J.* **2014**, *20* (29), 8923–8928.

(33) Bétard, A.; Fischer, R. A. Metal-Organic Framework Thin Films: From Fundamentals to Applications. *Chem. Rev.* **2012**, *112* (2), 1055–1083.

(34) Liu, B.; Ma, M.; Zacher, D.; Bétard, A.; Yusenko, K.; Metzler-Nolte, N.; Wöll, C.; Fischer, R. A. Chemistry of SURMOFs: Layer-Selective Installation of Functional Groups and Post-Synthetic Covalent Modification Probed by Fluorescence Microscopy. *J. Am. Chem. Soc.* **2011**, *133* (6), 1734–1737.

(35) Tu, M.; Wannapaiboon, S.; Khaletskaya, K.; Fischer, R. A. Engineering Zeolitic-Imidazolate Framework (ZIF) Thin Film Devices for Selective Detection of Volatile Organic Compounds. *Adv. Funct. Mater.* **2015**, *25* (28), 4470–4479.

(36) Zacher, D.; Shekhah, O.; Wöll, C.; Fischer, R. A. Thin Films of Metal–organic Frameworks. *Chem. Soc. Rev.* **2009**, *38* (5), 1418–1429.

(37) Yao, J.; Wang, H. Zeolitic Imidazolate Framework Composite Membranes and Thin Films: Synthesis and Applications. *Chem. Soc. Rev.* **2014**, *43* (13), 4470–4493.

(38) Mcguire, C. V; Forgan, R. S. The Surface Chemistry of Metal – Organic Frameworks. *Chem. Commun.* **2015**, *51*, 5199–5217.

(39) Horcajada, P.; Serre, C.; Grosso, D.; Boissière, C.; Perruchas, S.; Sanchez, C.; Férey, G. Colloidal Route for Preparing Optical Thin Films of Nanoporous Metal-Organic Frameworks. *Adv. Mater.* **2009**, *21* (19), 1931–1935.

(40) Rafti, M.; Marmisollé, W. A.; Azzaroni, O. Metal-Organic Frameworks Help Conducting Polymers Optimize the Efficiency of the Oxygen Reduction Reaction in Neutral Solutions. *Adv. Mater. Interfaces* **2016**, *3* (16), 3–7.

(41) Rafti, M.; Allegretto, J. A.; Segovia, G. M.; Tuninetti, J. S.; Giussi, J. M.; Bindini, E.; Azzaroni, O. Metal–organic Frameworks Meet Polymer Brushes: Enhanced Crystalline Film Growth Induced by Macromolecular Primers. *Mater. Chem. Front.* **2017**, *1* (11).

(42) Tuninetti, J. S.; Rafti, M.; Azzaroni, O. Early Stages of ZIF-8 Film Growth: The Enhancement Effect of Primers Exposing Sulfonate Groups as Surface-Confined Nucleation Agents. *RSC Adv.* **2015**, *5* (90), 73958–73962.

(43) Eddaoudi, M.; Kim, J.; Rosi, N.; Vodak, D.; Wachter, J.; Keeffe, M. O.; Yaghi, O. M.; Eddaoudi, M.; Kimrn, J.; Rosi, N.; et al. Systematic Design of Pore Size and Functionality

in Isoreticular MOFs and Their Application in Methane Storage Published by : American Association for the Advancement of Science Linked References Are Available on JSTOR for This Article : Systematic Design. **2002**, *295* (5554), 469–472.

(44) Deng, H.; Doonan, C. J.; Furukawa, H.; Ferreira, R. B.; Towne, J.; Knobler, C. B.; Wang, B.; Yaghi, O. M. Multiple Functional Groups of Varying Ratios in Metal-Organic Frameworks. *Science.* **2010**, *327* "(5967), 846-850.

(45) Lun, D. J.; Waterhouse, G. I. N.; Telfer, S. G. A General Thermolabile Protecting Group Strategy for Organocatalytic Metal-Organic Frameworks. *J. Am. Chem. Soc.* **2011**, *133* (15), 5806–5809.

(46) Britt, D.; Furukawa, H.; Wang, B.; Glover, T. G.; Yaghi, O. M. Highly Efficient Separation of Carbon Dioxide by a Metal-Organic Framework Replete with Open Metal Sites. *Proc. Natl. Acad. Sci. U. S. A.* **2009**, *106* (49), 20637–20640.

(47) Fracaroli, A. M.; Siman, P.; Nagib, D. A.; Suzuki, M.; Furukawa, H.; Toste, F. D.; Yaghi, O. M. Seven Post-Synthetic Covalent Reactions in Tandem Leading to Enzyme-like Complexity within Metal-Organic Framework Crystals. *J. Am. Chem. Soc.* **2016**, *138* (27), 8352–8355.

(48) Segovia, G. M.; Tuninetti, J. S.; Moya, S.; Picco, A. S.; Ceolín, M. R.; Azzaroni, O.; Rafti, M. Cysteamine-Modified ZIF-8 Colloidal Building Blocks: Direct Assembly of Nanoparticulate MOF Films on Gold Surfaces via Thiol Chemistry. *Mater. Today Chem.* (2018), 29-35

(49) Allegretto, J. A.; Tuninetti, J. S.; Lorenzo, A.; Ceolín, M.; Azzaroni, O.; Rafti, M. Polyelectrolyte Capping As Straightforward Approach toward Manipulation of Diffusive Transport in MOF Films. *Langmuir* **2018**, *34* (1), 425–431.

(50) Ranjan, R.; Tsapatsis, M. Microporous Metal Organic Framework Membrane on Porous Support Using the Seeded Growth Method. *Chem. Mater.* **2009**, *21* (20), 4920–4924.

(51) Lee, J. S.; Jae, H. K.; Young, J. L.; Nak, C. J.; Kyung, B. Y. Manual Assembly of Microcrystal Monolayers on Substrates. *Angew. Chemie Int. Ed.* **2007**, *46* (17), 3087–3090.

(52) Van Vleet, M. J.; Weng, T.; Li, X.; Schmidt, J. R. In Situ, Time-Resolved, and Mechanistic Studies of Metal-Organic Framework Nucleation and Growth. *Chem. Rev.* **2018**, *118* (7), 3681–3721.

(53) McCarthy, M. C.; Varela-Guerrero, V.; Barnett, G. V; Jeong, H. K. Synthesis of Zeolitic Imidazolate Framework Films and Membranes with Controlled Microstructures. *Langmuir* **2010**, *26* (11), 14636–14641.

(54) Gouedard, C.; Picq, D.; Launay, F.; Carrette, P. L. Amine Degradation in CO2 capture. A

Review. *Int. J. Greenh. Gas Control* **2012**, *10*, 244–270.

(55) Choi, S.; Drese, J. H.; Jones, C. W. Adsorbent Materials for Carbon Dioxide Capture from Large Anthropogenic Point Sources. *ChemSusChem* **2009**, *2* (9), 796–854.

(56) McDonald, T. M.; Lee, W. R.; Mason, J. A.; Wiers, B. M.; Hong, C. S.; Long, J. R. Capture of Carbon Dioxide from Air and Flue Gas in the Alkylamine-Appended Metal-Organic Framework Mmen-Mg 2(Dobpdc). *J. Am. Chem. Soc.* **2012**, *134* (16), 7056–7065.

(57) McDonald, T. M.; Mason, J. A.; Kong, X.; Bloch, E. D.; Gygi, D.; Dani, A.; Crocellà, V.; Giordanino, F.; Odoh, S. O.; Drisdell, W. S.; et al. Cooperative Insertion of CO2 in Diamine-Appended Metal-Organic Frameworks. *Nature* **2015**, *519* (7543), 303–308.

(58) Trickett, C. A.; Helal, A.; Al-Maythalony, B. A.; Yamani, Z. H.; Cordova, K. E.; Yaghi, O. M. The Chemistry of Metal–organic Frameworks for CO2 Capture, Regeneration and Conversion. *Nat. Rev. Mater.* **2017**, *2* (8), 17045.

(59) Nguyen, N. T. T.; Furukawa, H.; Gándara, F.; Nguyen, H. T.; Cordova, K. E.; Yaghi, O. M. Selective Capture of Carbon Dioxide under Humid Conditions by Hydrophobic Chabazite-Type Zeolitic Imidazolate Frameworks. *Angew. Chemie - Int. Ed.* **2014**, *53* (40), 10645–10648.

(60) Nugent, P.; Giannopoulou, E. G.; Burd, S. D.; Elemento, O.; Giannopoulou, E. G.; Forrest, K.; Pham, T.; Ma, S.; Space, B.; Wojtas, L.; et al. Porous Materials with Optimal Adsorption Thermodynamics and Kinetics for Co2separation. *Nature* **2013**, *495* (7439), 80–84.

(61) Stephen R. Caskey, Antek G. Wong-Foy, A. J. M. Dramatic Tuning of Carbon Dioxide Uptake via Metal Substitution in a Coordination Polymer with Cylindrical Pores. *J. Am. Chem. Soc.* **2008**, *130(33)*, 10870–10871.

(62) Chen, K. J.; Yang, Q. Y.; Sen, S.; Madden, D. G.; Kumar, A.; Pham, T.; Forrest, K. A.; Hosono, N.; Space, B.; Kitagawa, S.; et al. Efficient CO2Removal for Ultra-Pure CO Production by Two Hybrid Ultramicroporous Materials. *Angew. Chemie - Int. Ed.* **2018**, *57* (13), 3332–3336.

(63) Wriedt, M.; Sculley, J. P.; Yakovenko, A. A.; Ma, Y.; Halder, G. J.; Balbuena, P. B.; Zhou, H. C. Low-Energy Selective Capture of Carbon Dioxide by a Pre-Designed Elastic Single-Molecule Trap. *Angew. Chemie - Int. Ed.* **2012**, *51* (39), 9804–9808.

(64) Jiang, J.; Gándara, F.; Zhang, Y. B.; Na, K.; Yaghi, O. M.; Klemperer, W. G. Superacidity in Sulfated Metal-Organic Framework-808. *J. Am. Chem. Soc.* **2014**, *136* (37), 12844–12847.

(65) Corma, A.; García, H.; Llabrés i Xamena, F. X. Engineering Metal Organic Frameworks

for Heterogeneous Catalysis. *Chem. Rev.* **2010**, *110(8)*, 4606–4655.

(66) Hu, Z.; Jiang, J. A Helical Peptide Confined in Metal-Organic Frameworks: Microscopic Insight from Molecular Simulation. *Microporous Mesoporous Mater.* **2016**, *232* (232), 138–142.

(67) Stylianou, K. C.; Gõmez, L.; Imaz, I.; Verdugo-Escamilla, C.; Ribas, X.; Maspoch, D. Engineering Homochiral Metal-Organic Frameworks by Spatially Separating 1D Chiral Metal-Peptide Ladders: Tuning the Pore Size for Enantioselective Adsorption. *Chem. - A Eur. J.* **2015**, *21* (28), 9964–9969.

(68) Bonnefoy, J.; Legrand, A.; Quadrelli, E. A.; Canivet, J.; Farrusseng, D. Enantiopure Peptide-Functionalized Metal-Organic Frameworks. *J. Am. Chem. Soc.* **2015**, *137* (29), 9409–9416.

Alejandro M. Fracaroli received his PhD in Chemistry from Universidad Nacional de Córdoba (UNC), Argentina, in 2009 and working under the supervision of Dr. Rita H. de Rossi. Soon after, he joined the group of Kentaro Tashiro at the Intenational Center for Materials Nanoarchitectonics (MANA-NIMS), in Tsukuba Japan, where he stayed until January 2013. Between February 2013 and April 2016, he was a postdoctoral Fellow with Omar Yaghi at the University of California, Berkeley. From May 2016, he is appointed Assistant Professor and Researcher (INFIQC-CONICET), at the Department of Organic Chemistry, in the College of Chemical Sciences of Universidad Nacional de Córdoba, where he has started his research program on reticular materials such as MOFs and COFs (http://rhr.investigacion.unc.edu.ar/).

Jimena S. Tuninetti has a degree in chemistry (UNRC, 2008). She obtained her PhD in chemistry at the Advanced Materials Investigation and Development Laboratory (LIDMA, UNRC, 2008-2013) under the supervision of Dr. César Barbero, where she worked on the synthesis and modification of Smart hydrogels. She later joined as postdoctoral fellow at the Softmatter Laboratory (INIFTA, 2013-2017) during which she specialized under Dr. Omar Azzaroni supervision in polymeric films with many potential applications, particularly in porous coordination polymers or Metal Organic Frameworks. Jimena is currently a CONICET assistant researcher at Softmatter Laboratory under the supervision of Dr. Matías Rafti where she is currently working on a project that combines the synthesis of microporous materials (MOFs) along with its assembly and final application as delivery systems, specific adsorption systems and smart sensors.

Matías Rafti received his PhD in Chemistry from Universidad Nacional de La Plata in 2007, under joint supervision of Prof. Vicente (UNLP) and Prof. Imbihl (Leibniz Universitat Hannover). Financed by DAAD and DFG scholarships and grants, he joined Prof. Imbihl group at the Institute for Electrochemistry and Physical Chemistry in Hannover as post-doc between 2008 and 2011. From 2012 throughout 2014, with funding from Fulbright and ICAM, he joined Prof. Migone (Carbondale, IL, US) and Prof. Matzger (Ann Arbor, MI, US) labs were he pursued research focused on Metal Organic Frameworks. From 2011 he was appointed as Staff Researcher from CONICET at the INIFTA-UNLP (Instituto de Investigaciones Fisicoquimicas Teoricas y Aplicadas), at the Softmatter Lab (http://softmatter.quimica.unlp.edu.ar), with main focus on the integration of MOFs into composites relevant for energy conversion and storage technologies. He also performs teaching duties at the UNLP.

Anales de la Asociación Química Argentina

División Jóvenes Profesionales

Mini-Review

AMPHIPHILIC COPOLYMERS WITH DIFFERENT ARCHITECTURES AS AN ALTERNATIVE TO CONVENTIONAL SURFACTANTS

Agustín Iborra[1], Gabriel Ríos Valer[1] and Juan M. Giussi[1,*]

[1] *Instituto de Investigaciones Fisicoquímicas Teóricas y Aplicadas (INIFTA) – Softmatter Laboratory, La Plata, Argentina.*

** Autor Corresponsal: jmgiussi@inifta.unlp.edu.ar*

Resumen Gráfico - Graphical Abstract

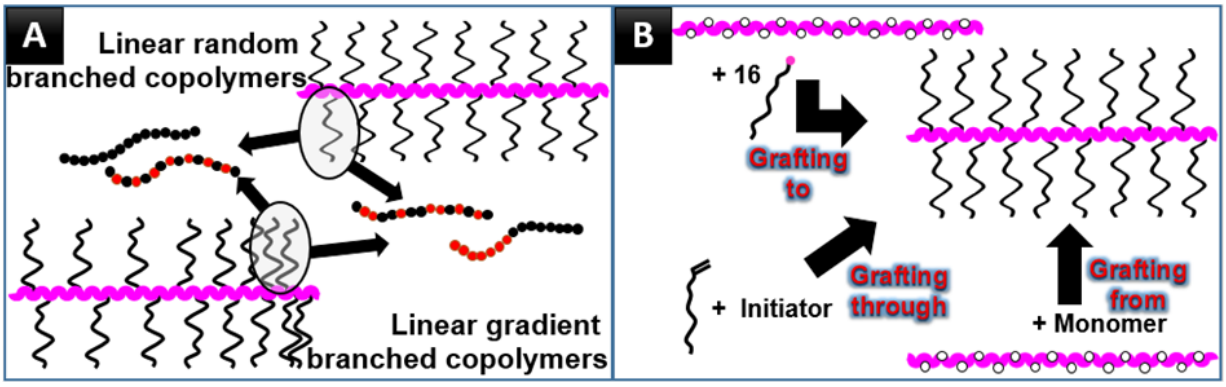

Resumen

El uso de macrosurfactantes anfifílicos como agentes emulsificantes a demostrado tener mayor eficiencia que los surfactantes de bajo peso molecular usualmente empleados. Tradicionalmente, los copolímeros en bloque han sido los primeros sistemas macromoleculares en ser probados como surfactantes. Debido a la introducción de técnicas de polimerización controlada en la década del 90, recientemente se han reportado una serie de avances en cuanto a la preparación de macromoléculas de arquitectura compleja para este tipo de aplicaciones. En este mini-review, vamos a reportar el estado del arte y los avances más recientes en la preparación de macromoléculas anfifílicas con especial énfasis en copolímeros con arquitecturas complejas (tipo estrella y cilindricas). También presentaremos un resumen de las posibles rutas de síntesis y monómeros que ofrecen una alternativa para obtener surfactantes novedosos.

Abstract

The use of amphiphilic macrosurfactants as emulsifying agents has shown to have higher efficiency with respect to low molecular weight surfactants. Traditionally, block copolymers have been the first macromolecular systems used for this purpose. Due to the introduction of controlled polymerization techniques in the late nineties, the last decade showed an increase in the number of papers that report the

preparation of macromolecules with complex architectures. In this mini-review, we report some advances in the preparation of amphiphilic macromolecules, with special emphasis in copolymers with complex architectures, star and cylindrical. We present a summary list about the synthetic methods and monomers employed to obtain amphiphilic systems as possible alternatives to traditional surfactant.

Palabras Clave: *surfactantes macromoleculares, copolímeros anfifílicos, polimerización controlada.*

Keywords: *macromolecular surfactants, amphiphilic copolymers, controlled polymerization.*

1. Introduction

Surfactants are amphiphilic organic compounds that present two regions with very different polarity, these amphiphilic molecules have the ability to self-assemble in aqueous environment producing micelles. One region of surfactants are hydrophilic/lipophobic and the other is lipophilic/hydrophobic. This context gives to these chemical entities, formidable characteristics and applications. Many products that we use in our daily life are based or contain amphiphilic molecules.[1] Figure 1 shows a simple representation of a general surfactant. Commonly, these molecules have as lipophilic group large hydrocarbon moieties, such as octyl (C_8), lauryl (C_{12}), stearyl (C_{18})s hydrophilic part can contain ionic or non-ionic (polar) groups. The most common ionic groups are sulfonates, phosphates, quaternary ammonium salts; as non-ionic groups, generally, oligo ethylene glycols are used. In order to decrease the free energy, surfactants can be adsorbed at the interface water-oil or can incorporate small oil phases in the formed micelles (figure 1).

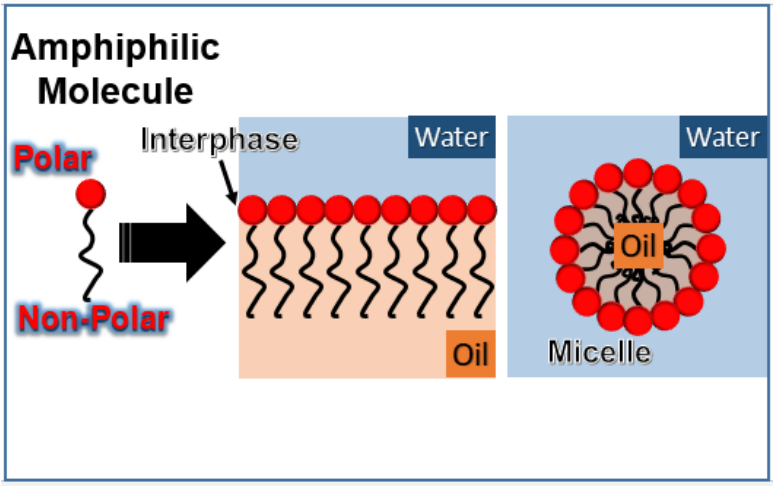

Figure 1. Schematic representation of a surfactant and its behaviour at the interface water-oil or micelle formation.

Recently, amphiphilic copolymers have been employed as macrosurfactants with good results in many areas.[2] Polymeric systems have some advantages compared to small molecule surfactants.

Due to their size, amphiphilic polymers produce a better control over lyophilic/lyophobic balance. This generates more thermodynamically stable structures, producing a lower critical micelle concentration (CMC) than small molecule analogues.[3] Some commercially available polymeric surfactants, such as block copolymers of poly(ethylene oxide) and poly(propylene oxide), have already found a widespread use as wetting agents, emulsifiers, foam stabilizers, and detergents. These copolymers are called Poloxamers and Pluronics.

More recently, polymeric structures with complex architectures have attracted attention because these structures provide unique opportunities to control the molecular packing and the symmetry (figure 2).

In this mini-review, we describe the most recently amphiphilic copolymer systems prepared in the scientific community with a special emphasis in copolymers with complex architectures, star and cylindrical branched copolymers. Firstly, a short description about traditional block copolymers will be presented and then, a deeper description about star and cylindrical branched copolymers will be presented. Figure 2 shows a schematic illustration of cylindrical branched copolymers relative to the conventional amphiphilic block copolymer and small molecule surfactant.

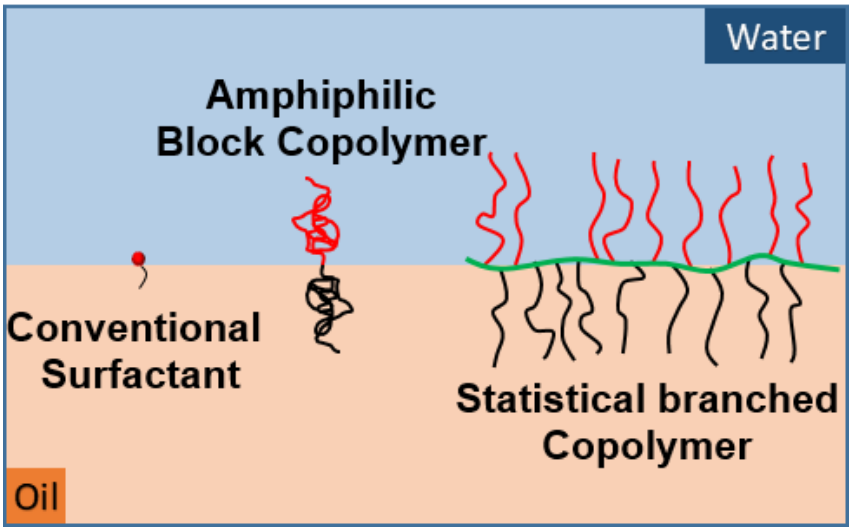

Figure 2. Schematic illustration of cylindrical branched copolymers relative to the conventional amphiphilic block copolymer and small molecule surfactant.

2. Linear copolymers

Linear copolymers can be classified based on how the units are arranged along the chain.[4] Four are the principal and most common arranged forms, alternating copolymers, block copolymers, statistical copolymers and sequential copolymers (Figure 3). For the first case; i.e., alternating copolymers, the monomers present an alternation along the chain (*1* in figure 3). On the other

hand, block copolymers present two blocks of each monomer in the same chain (*2* in figure 3). Statistical copolymers are systems in which the sequence of monomers does not present an ordered pattern (3 in figure 3) and, finally, in sequential copolymers the monomer units are arranged in a repeating sequence (4 in figure 3). All microstructures mentioned can be designed to present two regions with very different polarity. In the following sections, the strategies to provide amphiphilic characteristic to each linear copolymer microstructure will be explained.

2.1 Linear Block Copolymers

Linear block copolymers are the most common copolymers employed as amphiphilic entities. Block copolymers are heterogeneous polymer systems, different blocks from which they are built is independent of each other. As a result, block copolymers often combine the relevant properties of each homopolymer. This feature is the reason why a block copolymer formed by two monomers with very different polarity will present two regions with very different polarity.

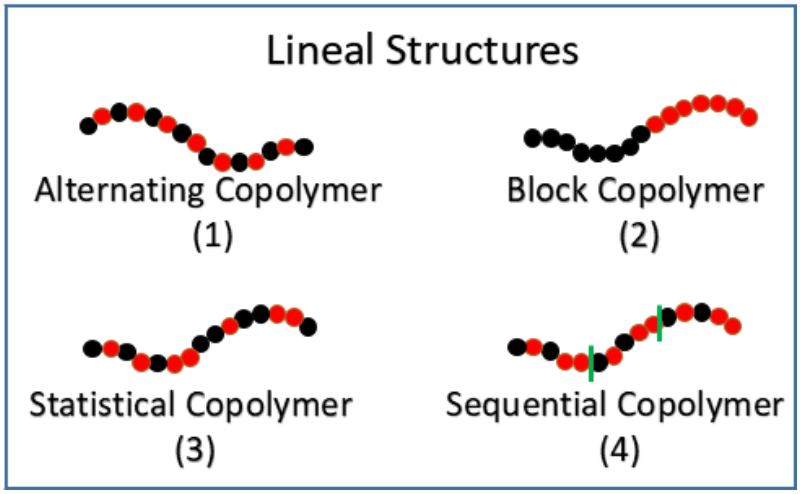

Figure 3. Most common copolymer microstructures: alternating copolymers, block copolymers, statistical copolymers and sequential copolymers.

One of the most used and studied non-ionic hydrophilic monomer is the ethylene oxide (EO). Blocks copolymer based on EO have strong implications in many industrial processes. When propylene oxide (PO) is used as a hydrophobic entity, EO and PO produce a very used block and triblock copolymers. Moreover, triblock copolymers POE-PPO-PEO are commercially available as non-ionic macromolecular surface-active agents.[5] An important characteristic of POE-PPO-PEO solutions is their self-assembling and thermo-gelling behaviour. Concentrated aqueous solutions of POE-PPO-PEO are liquid at low temperature and form a gel at higher temperature in a reversible process. This feature and due of their amphiphilic structures, POE-PPO-PEO copolymers have useful in many industrial applications, such as emulsification, dispersion

stabilization, detergency, lubrication, separation, cosmetics, pharmaceutical applications, bioprocessing, release among others.[6]

Several ionic monomers have been employed as hydrophilic entities to obtain amphiphilic block copolymers. Sternhagen et al.[7] synthesized amphiphilic ionic peptoid block copolymers. These copolymers have been studied in water at pH = 9 and their amphiphilic capability produced small spherical micelles with a hydrodynamic radius of ∼5−10 nm and critical micellar concentration (CMC) in the 0.034−0.094 mg/mL range.

Matsuoka et al,[8–10] obtained a diblock copolymers having sulfonic acid groups in its hydrophilic chain with poly(diethylsilacyclobutane) or polystyrene as a hydrophobic segment. These authors found that the water surface tension depends on copolymer composition and chain lengths. The micelles size were 100-200 Å and were confirmed by dynamic light scattering and small-angle X-ray scattering experiments. Due to strong ionic character of this class of amphiphilic block copolymer, these authors suggest some peculiar behaviour in the surface tension.

2.2 Linear non-block Copolymers

This class of copolymers have been employed as a new alternative to linear block copolymers. The synthetic procedures to obtain non-block copolymers use to be easier than block copolymers. In this class of macromolecules, the amphiphilic behaviour is provided by the pendant group. In the last decades, the papers about these systems have grown significantly. Figure 4 shows a schematic representation of this class of copolymers and the most common monomers used to give the amphiphilic behaviour. This class of macromolecules is also known as branched polymers or cylindrical brunched polymers (in section 3, this class of macromolecules will be explained again).

Some authors described the preparation and use of non-block copolymers with amphiphilic properties. Some of these authors have used free radical copolymerization of monomers with long polar and nonpolar pendant groups.[11–15] This context generates linear backbones with hydrophilic and hydrophobic polymeric pendant group statistically, alternately or sequentially distributed along the backbone. More recently, the literature shows works in which controlled radical copolymerization techniques allowed to obtain this kind of systems with better composition, molecular weight, and polydispersity.

Respect to the aforementioned non-block copolymers, block copolymers have a clear separation between hydrophobic and hydrophilic regions and this situation give good intermolecular self-assemblies and produce dispersions with monodisperse size and morphology. Although hydrophilic/hydrophobic statistical copolymers had less intermolecular self-assemblies to produce micelles, these copolymers have demonstrated potential capabilities as emulsified agents to generate disperse systems similar to the case of Pickering emulsions.

2.3 Star-branched copolymer

Star polymers are branched macromolecules consisting of several linear polymer chains connected to a central point.[16–18] The central point called “the core”, is generally a simple molecule, or macromolecule with low molecular weight. The chains, commonly called "the arms", can be linear homo- or copolymer chains. For copolymer chains, these can present their own structural characteristics previously descript, alternating, block, statistical and sequential. On the other hand, based on chains distribution anchored to the core, star polymers can be classified as homo-arm star polymers[10] or mikto-arm star copolymers (figure 4).[11] The first category consists in a symmetrical structure with all arms containing identical chemical composition and similar chain length. Contrary, mikto-arm star polymers contain different arm species with different chemical compositions and/or chain length. This short review will focus on the first-mentioned category.

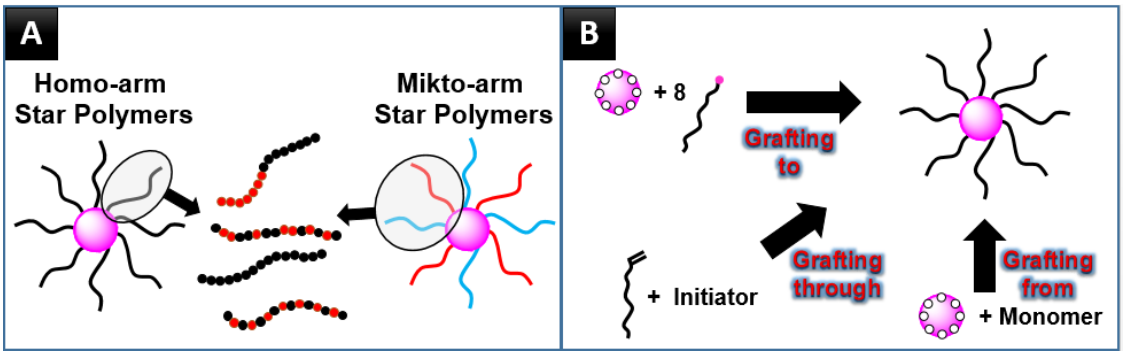

Figure 4. Schematic representation of star copolymers with homo and mikto arms (a) and the most common synthetic approaches (b)

Star polymers can be synthesized in different ways (figure 4b), (a) growing the polymer chains from a preformed core (grafting from),[21–23] (b) coupling preformed polymer chains and preformed core[24–26] or (grafting to) (c) generating the core from preformed polymer chains (grafting through).[27,28]

Several authors have been prepared amphiphilic star copolymers with promising and improved properties with respect to traditional analogous. Below, synthetic strategies and emulsification properties of some amphiphilic star copolymers are mentioned.

2.4 Star Block branched Copolymers

This kind of block copolymers is a new class of water-soluble amphiphilic block copolymers. Several monomers have been combined to prepare these materials, ionic and non-ionic and the final the properties generally improve with respect to non-branches analogous. The most

important contributions of this class of polymers have been in bioscience.[29–32] Below, some relevant examples of synthesis and properties of these copolymers are mentioned.

Kreutzer et al.[33] have synthesized water-soluble, amphiphilic star block copolymers with a large number of arms based on n-butyl methacrylate (BMA) and poly-(ethylene glycol) methyl ether methacrylate (PEGMA). Using fourth-generation hyperbranched polyester (Boltorn H40, core entity) terminated in 2-bromoisobutyric acid as a macroinitiator, sequential atom transfer radical polymerization (ATRP) allowed obtaining star polymers that contained on average 20 diblock copolymer arms. The AFM image in figure 5 clearly shows the individual arms of the star polymers and allows for the determination of the exact number of arms per molecule. These authors obtained after analysis of more than 1000 molecules an average number of arms of 16, a value slightly lower than the number determined by alcoholysis of the H40 precursors.

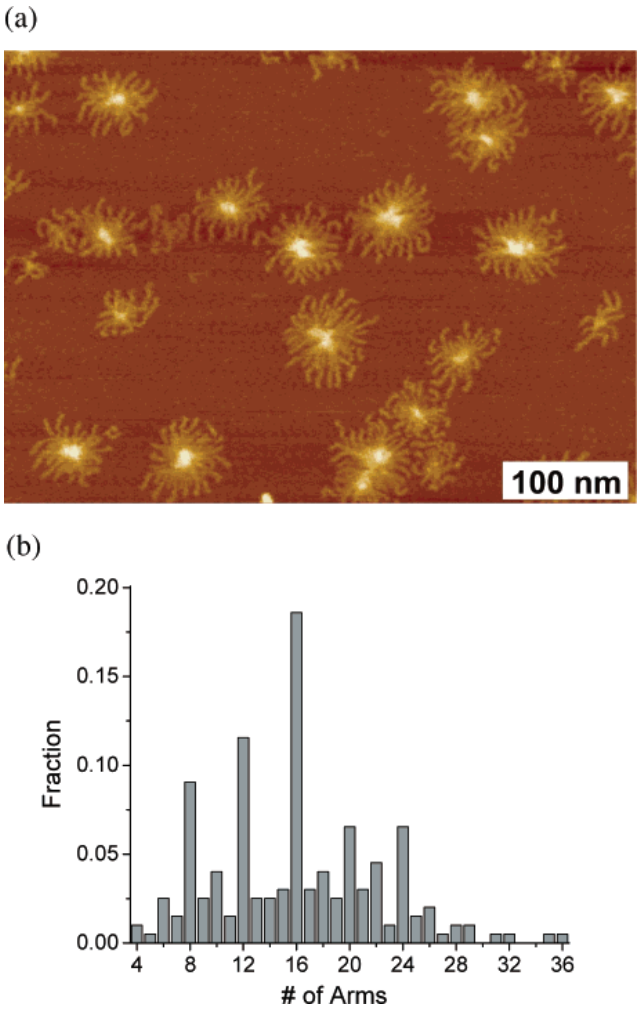

Figure 5. (a) Atomic force microscopy height micrograph of an amphiphilic star block copolymers based on PBMA, PPEGMA and Boltorn H40. **(b)** Distribution of the number of arms, as evaluated from AFM images. "Reprinted with permission from (Kreutzer, G.; Ternat, C.; Nguyen, T. Q.; Plummer, C. J. G.; Månson, J. A. E.; Castelletto, V.; Hamley, I. W.; Sun, F.; Sheiko, S. S.; Herrmann, A.; Ouali, L.; Sommer, H.; Fieber, W.; Velazco, M. I.; Klok, H. A. *Macromolecules* **2006**, *39* (13), 4507–4516.). Copyright (2018) American Chemical Society."

Using SAXS experiments on aqueous solutions, these authors indicated that the star block copolymers can be regarded as unimolecular micelles and through NMR spectroscopy they evaluated the ability of the polymers to encapsulate and release hydrophobic guests. These star amphiphilic block copolymers have been employed to study hydrophobic fragrances encapsulation in water. Diffusion coefficients of four different fragrance molecules in the free form and in the presence of the polymer have been determined trhought NMR spectroscopy and the degree of encapsulation depends on the hydrophobicity of the guest molecule. The fragrance molecules are mainly located in the hydrophobic core of the polymer, which is tightly packed, whereas the hydrophilic shell is flexible and takes up only a small percentage.[34]

Carletto et al,[35] prepared polymethyl methacrylare-block-polystyrene arms with cross-linked divinylbenzene core. The authors observed that several factors affecting the polymer aggregation and solubility such as the length, the composition of the arms and the polymerization catalyst used. On the other hand, using ATRP strategies, Gao et al[36] have been prepared three-arm star block copolymers based on polystyrene and poly(ethylene oxide) chains to evaluate its amphiphilic capability.

Poree et al,[37] evaluated the transdermal drug delivery capability of star block copolymer micelles as an alternative to the more common oral and intravenous routes. For this, the authors synthesized 6- and 12-arm star amphiphilic block copolymers using sequential ATRP of polar oligo(ethylene glycol) methacrylate and nonpolar lauryl methacrylate. The polymerization was carried out using brominated macroinitiators based on 2,2-bis(hydroxymethyl) propionic acid. These star block copolymers demonstrate the ability to encapsulate polar entities in nonpolar media. Furthermore, their transdermal carrier capabilities were demonstrated, verifying penetration of the carriers into the stratum corneum.

Liu et al,[38] prepared amphiphilic multiarm star copolymer based on Boltorn H40, poly(L-lactide) and Poly(2-ethoxy-2-oxo-1,3,2-dioxaphospholane) (PEP) (H40-star-PLA-SS-PEP) with disulfide linkages between the hydrophobic polyester core and hydrophilic polyphosphate arms. Due to their amphiphilic structure, H40-star-PLA-SS-PEP was able to self-assemble into micelles in aqueous solution. These structures were used to evaluate the glutathione-mediated intracellular drug delivery and the micelles show potentiality to improve the antitumor efficacy of hydrophobic chemotherapeutic drugs.

To disperse an oil phase in water, Li et al.[34] prepared a series of well-defined amphiphilic multiarm star copolymer based on poly(ethylene oxide) and poly(butyl acrylate). These star structures produce the formation of stable water-in-oil emulsions. On the other hand, Narrainen et al.[39] studied the micellization behavior of amphiphilic block copolymers based on poly(*n*-butyl

methacrylate) [P(*n*-BMA)] and poly[(2-dimethylamino)ethyl methacrylate] (PDMAEMA) on functionalized bromo P(*n*-BMA) macroinitiator cores prepared from monofunctional, difunctional, and trifunctional initiators: 2-bromo-2-methylpropionic acid 4-methoxyphenyl ester, 1,4-(2-bromo-2-methyl-propionate) benzene, and 1,3,5-(2-bromo-2-methylpropionato)benzene. Fluorescence spectroscopy and dynamic light scattering showed that the micellar capability and micelle size depended essentially on the molecular weight of the copolymer and arms number.

2.5 Star non-block branched Copolymers

This class of copolymer have been less study than star block branched copolymers. The amphiphilic behaviour of these copolymers is provided by selecting differentiate polarities between core entity and copolymer shell. Another alternative, as the case of linear non-block copolymers, is selecting monomer with large pendant group. Below are some relevant examples of synthesis and properties of these copolymers.

Kowalczuk et al,[40] synthesized amphiphilic star copolymers composed of a hyperbranched poly(arylene oxindole) (PArOx) core. Shells were different length arms formed by poly[di(ethylene glycol) methyl ether methacrylate] (PDEGMA) or copolymer poly [di(ethylene glycol) methyl ether methacrylate-ran-oligo(ethylene glycol) methyl ether methacrylate] P(DEGMA-ran-OEGMA). The amphiphilic behaviour of this system is due to the hydrophobic core and hydrophilic shells. These thermo-responsive star non-block branched copolymers showed good properties in solution and the amphiphilic capability was study by light scattering techniques, AFM and cryo-TEM. Different results indicate that star non-block branched copolymers obtained are prospective carriers for biomolecules.

Combining self-condensing vinyl polymerization (SCVP) and reversible addition–fragmentation chain transfer (RAFT), Narrainen et al,[39] designed and synthesized amino acid-based hyperbranched polymers based on tert-butyl carbamate (Boc)-L-valine acryloyloxyethyl ester (Boc-Val-HEA) and S-(4-vinyl)benzyl S'-butyltrithiocarbonate (VBBT) with variable degrees of branching (DB), molecular weights (Mn), and chainend functionalities. Removing Boc groups from the polymers results in water-soluble pH-responsive cationic hyperbranched architectures with tunable pH responsiveness. Dynamic light scattering (DLS), atomic force microscopy (AFM) and scanning electron microscopy (SEM) reveal the interesting self-assembly of star polymers in aqueous media with amino acid-based cores and water-soluble thermo-responsive arms.

2.6 Cylindrical branched copolymers

Cylindrical brunched copolymers are branched polymers consisting of several linear polymer chains connected to a linear polymeric backbone (figure 6).[41,42] This kind of structures are involved in various biological functions, including the lung and particular processing.

The linear polymeric backbone is generally a functional polymer chain and the bonded chains can be linear homo- or copolymers structures. In the case of copolymers, these can present their own microstructure, such as alternating, block, statistical and sequential (figure 6a). On the other hand, based on chains distribution anchored to the backbone, linear branched copolymers can be classified as random brush copolymers and gradient brush copolymers (figure 6a). In the first category, a uniform density of chains are bonding along the backbone and in the second category; the polymeric chains are forming a gradient along the backbone. the first-mentioned category.

Cylindrical branched copolymers can be prepared principally by three synthetic approaches, grafting from, grafting through and grafting to. In grafting from reactions, the backbone polymer contains reactive sites to initiate the polymerization of the side copolymer chains (figure 6b). Grafting to reactions connect an end functional of preformed copolymer chains with a backbone polymer with reactive sites for connecting side copolymer chains (figure 6b). Finally, in Grafting through reactions, a typical copolymerization occurs with macromonomer precursors (figure 6b). In order to prepare structures with cylindrical shapes, in the synthetic procedures, the backbone should be much longer than the lateral anchored chains.

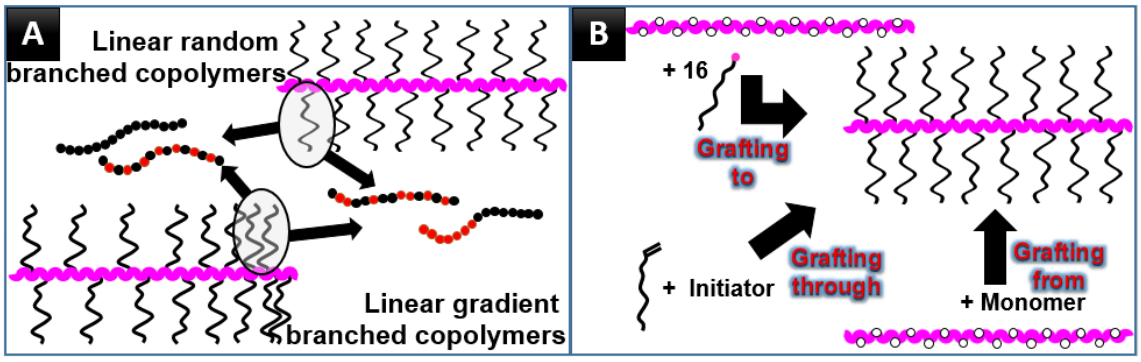

Figure 6. Schematic representation of cilindrical copolymers with random- and gradient-branched distribution (a) and the most common synthetic approaches (b)

In the literature, the number of monomers employed to obtain cylindrical brunched polymers is not very extent and these macromolecules have been prepared in general to produce functional materials. Based on our consideration, below are listed the most relevant examples. A distinctive observation of this class of macromolecules with densely grafted polymeric side chains, is that

interactions between side chains lead to extended backbone conformations[43,44] and reduced density of entanglements.[45]

According to the above characteristic Li et al,[46] reported the synthesis, characterization, and properties of cylindrical-brush polymers based on poly-N-isopropyl-acrylamide (PNIPAM) side chains, in which the side-chain repulsion can be controlled easily by variation of the temperature due to the well-known lower critical solution temperature in aqueous solution. PNIPAM brushes were grafting from the macroinitiator poly-2-bromoisobutyryloxyethyl methacrylate (PBIEM). This macroinitiator can be prepared by ATRP of hydroxyethylmethacrylate and subsequent reaction with a-bromoisobutyric acid bromide. The AFM image in figure 7 clearly shows the cylindrical structure of the obtained copolymer by Li.

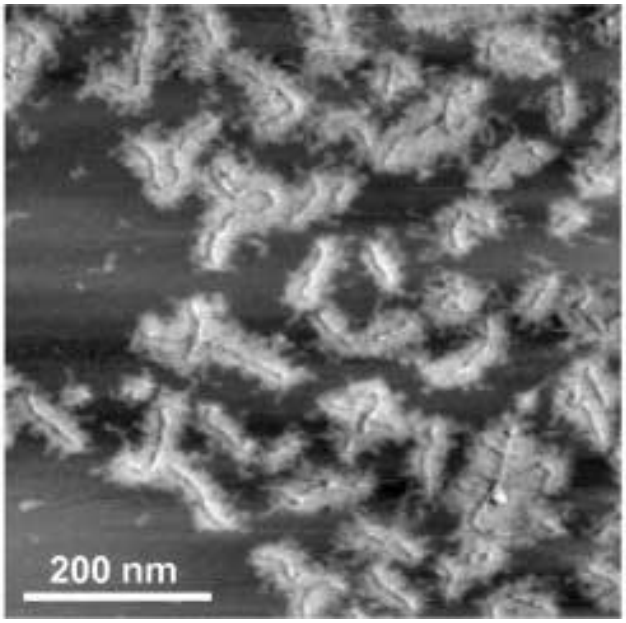

Figure 7. AFM image of the cylindrical PNIPAM brush polymers spin casted from a dilute solution in acetone. "Reprinted with permission from (Li, C.; Gunari, N.; Fischer, K.; Janshoff, A.; Schmidt, M. *Angew. Chemie - Int. Ed.* **2004**, *43* (9), 1101–1104). Copyright (2018) John Wiley & Sons Inc."

In cylindrical brunched polymers, the conformational degree and physical-chemical properties can be controlled by steric repulsion of grafted side chains. In this context, the polymers can be either flexible or stiff, depending on the length of the side chains and their grafting density. Cylindrical brunched polymers can be designed to switch their conformation in response to environmental changes, e.g. solvent, temperature, pH, ionic strength. Gunari et al,[47] reported the complex formation of cylindrical brush polymers with poly(L-lysine) (PLL) side chains and sodium dodecylsulfate (SDS). These authors found that due to the hydrophobicity of the b-sheets formed by the PLL side chain–SDS complexes, increasing amount of added surfactant the cylindrical polymers first adopt a helical conformation followed by a spherically collapsed

structure. Additionally, Cong et al,[48] systematically investigated the influence of surfactant, salt, and pH on the supramolecular structure of cylindrical brush polymers with poly(L-lysine) (PLL). These authors found that salt additions destroy the helical structures as do pH conditions below 4 and above 6. The most probable reason is that the polymer surfactant complexes start to disintegrate. Finally, Cong et al,[49] reported the synthesis of a core-shell cylindrical brush copolymer with poly(2-hydroxyethyl methacrylate) (PHEMA) backbone and polystyrene-block-poly(ε-caprolactone) (PS-b-PCL) diblock side chains with ATRP grafting from method.

2.7 Cylindrical Branched Block Copolymers

Cylindrical branched block copolymers are the most studied cylindrical branched copolymer. Several authors have described the preparation and uses of cylindrical branched block copolymers. Based in our consideration, below are listed the most relevant examples. Wooley et al. developed the synthesis of cylindrical branched block copolymers based on poly(acrylic acid) with core-shell and block distribution. These authors investigated their self-assembly in aqueous solutions.[50,51] In some articles, cylindrical branched block copolymers produced spherical aggregates often characterized in the dried state.[50,52] In this state, the information obtained on the micellar composition and morphology is not representative of the actual state. On the other hand, Fenyves et al,[53] explore a new class of giant polymeric surfactants with cylindrical branched architecture. These amphiphilic block copolymers containing polylactide (PLA) and poly(ethylene oxide) (PEO) side chains were synthesized by a grafting-from method. Critical micelle concentration of these materials was determined to be approx. 1 nM indicating an enhanced thermodynamic stability of the produced micelle aggregates.

Gromadzki et al,[54] synthesized amphiphilic methacrylate-based cylindrical branched block copolymers using grafting-from ATRP. For this, the authors firstly prepare poly(2-(2-bromoisobutyryloxy)ethyl methacrylate) PBIEM as the macroinitiator and next tert-butyl methacrylate (tBuMA) was polymerized from PBIEM. After the chlorine-terminated PBIEM-graft-P(tBuMA)-Cl macroinitiators were subsequently copolymerized with 2-(dimethylamino ethyl) methacrylate (DMAEMA) yielding densely grafted copolymers with diblock copolymer side chains PBIEM-graft-P(tBuMA)-block-PDMAEMA. The hydrolysis of tert-butyl groups produce the ionic amphiphilic methacrylate-based cylindrical branched block copolymers.

Chenet al,[55] combining step-growth polymerization and reversible addition fragmentation chain transfer (RAFT) polymerization in a ‘‘grafting from’’ methodology to produce amphiphilic cylindrical branched block copolymers based on styrene and tert-butyl acrylate block copolymer arms from poly(N-alkyl urea peptoid) backbone. The tert-butyl groups were removed using

trifluoroacetic acid affording hydrophilic polyacrylic acid segments. The molecular brushes were observed to generate stable micelles in aqueous solution.

Radzinski et al,[56] produced amphiphilic cylindrical branched block copolymers via ring-opening metathesis polymerization using grafting through process. These authors studied different parameters on the grafting process and they optimized conditions yielded amphiphilic cylindrical branched block copolymers with controllable molecular weights, polydispersity and high conversions. These authors,[57] also studied the kinetics parameters on the polymerization and the lifetime of the catalyst.

Tang et al,[58] synthesized amphiphilic cylindrical branched block copolymers based on helical polypeptide backbone and polylactide-b-poly-(ethylene glycol) block copolymer side chains via a grafting-to method. This complex structure has been synthesized by ring-opening polymerization (ROP). Using Langmuir-Blodgett (LB) technique and atomic force microscopy (AFM), the authors have allowed for direct imaging of the synthesized copolymer and the characterization of their molecular weight (MW) distribution. These authors observed that temperature variation can cause partial and reversible unfolding of the helical backbones and the temperature effect is greatly diminished for the copolymers with longer side chains.

Tang et al,[59] also prepared PNIPAM lateral chains integrated to poly[oligo(ethylene glycol) methacrylate] (POEGMA) as the core using successive atom transfer radical polymerization (ATRP). These authors found that POEGMA core existence gives double phase transition temperature to the unimolecular micelle formed.

Zehm et al,[60] prepared amphiphilic cylindrical branched block copolymers coupling RAFT and NMP (nitroxide-mediated polymerization) techniques. This combination allows to prepared complex amphiphilic polymers. The resulting polymers were composed of a thermosensitive poly(N-isopropylacrylamide) brush as hydrophilic block and a polystyrene brush as hydrophobic block.

2.8 Cylindrical Branched Statistic Copolymers

This class of copolymer can be prepared by grafting from, grafting thought and grafting to methods. This copolymers are the easiest to prepare and can be obtained by controlled and uncontrolled methods.

Iborra et al,[61] using grafting to method, obtained a copolymer based on lauryl methacrylate and poly(ethylene glycol) methyl ether methacrylate, prepared by solution radical copolymerization. Emulsification studies thought DLS showed different sizes of the formed micelles depending on solvent polarity due to polymer-polymer or polymer-solvent interactions and rheological characterization was undertaken to study the viscoelastic properties of the dispersed systems.

Additionally, this copolymer allowed to disperse small amounts of an organic solvent in water forming only one phase. Finally, due to the amphiphilic properties of this macrosurfactant, highly stable dispersions of carbon nanotubes in water were prepared.

Xia et al,[62] synthesized polylactide (PLA) and poly(*n*-butyl acrylate) (P*n*BA) side chains at similar MWs. In contrast, brush block copolymers containing approximately equal volume fractions of these MMs self-assembled into highly ordered lamellae with domain spacing over 100 nm. Their assemblies suggested that the block structure adopted an extended conformation in the ordered state.

Yamamoto et al,[63,64] obtained dual responsive cylindrical branched statistic copolymers based on di(ethylene glycol) methyl ether methacrylate (MEO2MA), tri(ethylene glycol) methyl ether methacrylate (MEO3MA) and MAA grafting from poly(2-(2-bromoisobutyroyloxy)ethyl methacrylate (PBIEM) macroinitiators using atom transfer radical polymerization (ATRP). The authors observed that the lower critical solution temperature (LCST) of this system decreased with the increasing molar fraction of MAA in the copolymer and the responsive nature of the copolymer is enhanced by the dense graft structure of a brush copolymer.

Gromadzki et al,[54] aforementioned in before section, also synthesized amphiphilic methacrylate-based cylindrical branched statistical copolymers using grafting-from ATRP. These authors did not find clear differences between PBIEM-graft-P(MAA)-block-PDMAEMA and PBIEM-graft-P(MAA)-stat-PDMAEMA.

Using grafting-from via ATRP, Pietrasik et al,[65] synthesized amphiphilic cylindrical branched statistic copolymers with side chains consisting of two copolymers: 2-(dimethylamino)ethyl methacrylate with methyl methacrylate, and N,N-dimethylacrylamide with butyl acrylate. Poly(2-(2-bromoisobutyryloxy) ethyl methacrylate) and poly(2-(2-bromopropionyloxy)ethyl methacrylate) were used as macroinitiators. These authors found thought DLS studies in water an unusual concentration-dependent LCST suggesting that, due to the compact structure of molecular brushes, an intramolecular collapse can occur.

3. Conclusions

In this mini-review, we have discussed some advances in the preparation of amphiphilic macromolecules, with special emphasis in copolymers with complex architectures, star and cylindrical. Their controlled compositions and architectures are produced by sequential addition of controlled/living polymerization techniques and the combination of controlled polymerization techniques with facile coupling chemistry. One of the most fascinating features of amphiphilic copolymers with complex architectures is their ability to self-assemble into nanoscale ordered structures with various morphologies and behaviours. Amphiphilic copolymers have been

employed as macrosurfactants with good results in many areas and the polymeric systems have some advantages compared to small molecule surfactants, amphiphilic polymers produce a better control over lyophilic/lyophobic balance and this context generates more thermodynamically stable structures, producing a lower critical micelle concentration (CMC) than small molecule analogues. When the polymer architecture presents more complexity, generally their amphiphilic capability produced small spherical micelles and less critical micellar concentration (CMC). In the last decade increase the number of papers that report the preparation of amphiphilic macromolecules with complex architectures and for the future will be crucial the design and synthesis of complex material to replace the materials known today.

Acknowledgments: A.I., G.R.V. and J.M.G. acknowledge the financial support from CONICET, Y-TEC, ANPCyT (PICT-2015-0346) and UNLP.

A.I. is currently working on his PhD thesis supported by CONICET and Y-TEC at UNLP under the supervision of Prof. Omar Azzaroni and Dr. Juan M. Giussi.

G.R.V. is currently working on his PhD thesis supported by CONICET at UNLP under the supervision of Prof. Marcelo Ceolín and Dr. Juan M. Giussi.

References

(1) Schramm, L. L.; Stasiuk, E. N.; Marangoni, D. G. *Annu. Rep. Prog. Chem., Sect. C Phys. Chem.* **2003**, *99* (2), 3–48.

(2) Kronberg, B.; Holmberg, K.; Lindman, B. *Surface Chemistry of Surfactants and Polymers*; John Wiley & Sons, Ltd., 2014.

(3) Riess, G. *Prog. Polym. Sci.* **2003**, *28* (7), 1107–1170.

(4) Odian, G. *Principles of Polymerization*, 4th Editio.; John Wiley & Sons, Inc.: New York, 2004.

(5) "BASF - Product information the chemicals catalog - Pluronics". BASF Corporation Website. Retrieved 2018-05-22.

(6) Tadros, T. F. *Emulsion Formation and Stability*; Wiley-VCH, 2013.

(7) Sternhagen, G. L.; Gupta, S.; Zhang, Y.; John, V.; Schneider, G. J.; Zhang, D. *J. Am. Chem. Soc.* **2018**, *140* (11), 4100–4109.

(8) Matsuoka, H.; Matsutani, M.; Mouri, E.; Matsumoto, K. *Macromolecules* **2003**, *36* (14), 5321–5330.

(9) Matsuoka, H.; Maeda, S.; Kaewsaiha, P.; Matsumoto, K. *Langmuir* **2004**, *20* (18), 7412–7421.

(10) Kaewsaiha, P.; Matsumoto, K.; Matsuoka, H. *Langmuir* **2005**, *21* (22), 9938–9945.

(11) Zhou, J.; Wang, L.; Wang, C.; Chen, T.; Yu, H.; Yang, Q. *Polymer (Guildf).* **2005**, *46*

(24), 11157–11164.

(12) Gargallo, L.; Opazo, A.; Radic, D. *Eur. Polym. J.* **1990**, *26* (7), 727–730.

(13) Leiva, A.; Gargallo, L.; Radic, D. *J. Macromol. Sci. Part B* **1998**, *37* (1), 45–57.

(14) Ahmad, H.; Hasan, M. K.; Miah, M. A. J.; Ali, A. M. I.; Tauer, K. *Polymer (Guildf).* **2011**, *52* (18), 3925–3932.

(15) Matsumoto, A.; Murakami, N.; Aota, H.; Ikeda, J.; Capek, I. *Polymer (Guildf).* **1999**, *40* (20), 5687–5690.

(16) Inoue, K. *Prog. Polym. Sci.* **2000**, *25* (4), 453–571.

(17) Hawker, C. J. *Angew. Chem., Int. Ed. Engl.* **1995**, *34* (13/14), 1456–1459.

(18) Jones, M.-C.; Leroux, J.-C. *Soft Matter* **2010**, *6* (23), 5850.

(19) Matyjaszewski, K.; Gaynor, S. G. *Macromolecules* **1997**, *30* (23), 7042–7049.

(20) Gao, H.; Tsarevsky, N. V.; Matyjaszewski, K. *Macromolecules* **2005**, *38* (14), 5995–6004.

(21) Ueda, J.; Kamigaito, M.; Sawamoto, M. *Macromolecules* **1998**, *31* (20), 6762–6768.

(22) Li, M.; Jahed, N. M.; Min, K.; Matyjaszewski, K. *Macromolecules* **2004**, *37* (7), 2434–2441.

(23) Giussi, J. M.; Azzaroni, O.; Hensel-Bielowka, S.; Wojnarowska, Z.; Knapik, J.; Paluch, M. *Polymer (Guildf).* **2016**, *100*, 227–237.

(24) Gao, H.; Matyjaszewski, K. *Prog. Polym. Sci.* **2009**, *34* (4), 317–350.

(25) Kolb, H. C.; Finn, M. G.; Sharpless, K. B. *Angew. Chemie - Int. Ed.* **2001**, *40* (11), 2004–2021.

(26) Sumerlin, B. S.; Tsarevsky, N. V.; Louche, G.; Lee, R. Y.; Matyjaszewski, K. *Macromolecules* **2005**, *38* (18), 7540–7545.

(27) Xia, J. *Macromolecules* **1999**, *32* (13), 4482–4484.

(28) Liu, C.; Zhang, Y.; Huang, J. *Macromolecules* **2008**, *41* (2), 325–331.

(29) Xiao, Y.; Hong, H.; Javadi, A.; Engle, J. W.; Xu, W.; Yang, Y.; Zhang, Y.; Barnhart, T. E.; Cai, W.; Gong, S. *Biomaterials* **2012**, *33* (11), 3071–3082.

(30) Li, X.; Qian, Y.; Liu, T.; Hu, X.; Zhang, G.; You, Y.; Liu, S. *Biomaterials* **2011**, *32* (27), 6595–6605.

(31) Pang, Y.; Liu, J.; Su, Y.; Zhu, B.; Huang, W.; Zhou, Y.; Zhu, X.; Yan, D. *Sci. China Chem.* **2010**, *53* (12), 2497–2508.

(32) Prabaharan, M.; Grailer, J. J.; Pilla, S.; Steeber, D. A.; Gong, S. *Biomaterials* **2009**, *30* (29), 5757–5766.

(33) Kreutzer, G.; Ternat, C.; Nguyen, T. Q.; Plummer, C. J. G.; Månson, J. A. E.; Castelletto, V.; Hamley, I. W.; Sun, F.; Sheiko, S. S.; Herrmann, A.; Ouali, L.; Sommer, H.; Fieber, W.; Velazco, M. I.; Klok, H. A. *Macromolecules* **2006**, *39* (13), 4507–4516.

(34) Fieber, W.; Herrmann, A.; Ouali, L.; Velazco, M. I.; Kreutzer, G.; Klok, H. A.; Ternat, C.; Plummer, C. J. G.; Manson, J. A. E.; Sommer, H. *Macromolecules* **2007**, *40* (15), 5372–5378.

(35) Carletto, A.; Cardozo, A. F.; Suriano, R.; Manoury, E.; Turri, S.; Poli, R. *Isr. J. Chem.* **2012**, *52* (3–4), 328–338.

(36) Gao, H.; Min, K.; Matyjaszewski, K. *Macromol. Chem. Phys.* **2007**, *208* (13), 1370–1378.

(37) Poree, D. E.; Giles, M. D.; Lawson, L. B.; He, J.; Grayson, S. M. *Biomacromolecules* **2011**, *12* (4), 898–906.

(38) Liu, J.; Pang, Y.; Huang, W.; Huang, X.; Meng, L.; Zhu, X.; Zhou, Y.; Yan, D. *Biomacromolecules* **2011**, *12* (5), 1567–1577.

(39) Narrainen, A. P.; Pascual, S.; Haddleton, D. M. *J. Polym. Sci. Part A Polym. Chem.* **2002**, *40* (4), 439–450.

(40) Kowalczuk, A.; Mendrek, B.; Zymełka-Miara, I.; Libera, M.; Marcinkowski, A.; Trzebicka, B.; Smet, M.; Dworak, A. *Polym. (United Kingdom)* **2012**, *53* (25), 5619–5631.

(41) Sheiko, S. S.; Sumerlin, B. S.; Matyjaszewski, K. *Prog. Polym. Sci.* **2008**, *33* (7), 759–785.

(42) Zhang, M.; Müller, A. H. E. *J. Polym. Sci. Part A Polym. Chem.* **2005**, *43* (16), 3461–3481.

(43) Rathgeber, S.; Pakula, T.; Wilk, A.; Matyjaszewski, K.; Beers, K. L. *J. Chem. Phys.* **2005**, *122* (12).

(44) Zhang, B.; Gröhn, F.; Pedersen, J. S.; Fischer, K.; Schmidt, M. *Macromolecules* **2006**, *39* (24), 8440–8450.

(45) Hu, M.; Xia, Y.; McKenna, G. B.; Kornfield, J. A.; Grubbs, R. H. *Macromolecules* **2011**, *44* (17), 6935–6943.

(46) Li, C.; Gunari, N.; Fischer, K.; Janshoff, A.; Schmidt, M. *Angew. Chemie - Int. Ed.* **2004**, *43* (9), 1101–1104.

(47) Gunari, N.; Cong, Y.; Zhang, B.; Fischer, K.; Janshoff, A.; Schmidt, M. *Macromol. Rapid Commun.* **2008**, *29* (10), 821–825.

(48) Cong, Y.; Gunari, N.; Zhang, B.; Janshoff, A.; Schmidt, M. *Langmuir* **2009**, *25* (11), 6392–6397.

(49) Cong, H.; Li, L.; Zheng, S. *Polym. (United Kingdom)* **2015**, *79*, 99–109.

(50) Li, Z.; Ma, J.; Cheng, C.; Zhang, K.; Wooley, K. L. *Macromolecules* **2010**, *43* (3), 1182–1184.

(51) Li, Z.; Lee, N. S.; Wooley, K. L. *J. Am. Chem. Soc.* **2010**, *132*, 21–23.

(52) Wu, D.; Zhao, C.; Tian, J.; Zhao, H. *Polym. Int.* **2009**, *58* (11), 1335–1340.

(53) Fenyves, R.; Schmutz, M.; Horner, I. J.; Bright, F. V.; Rzayev, J. *J. Am. Chem. Soc.* **2014**, *136* (21), 7762–7770.

(54) Gromadzki, D.; Štěpánek, P.; Makuška, R. *Mater. Chem. Phys.* **2013**, *137* (3), 709–715.

(55) Chen, X.; Ayres, N. *J. Polym. Sci. Part A Polym. Chem.* **2011**, *49* (14), 3030–3037.

(56) Radzinski, S. C.; Foster, J. C.; Matson, J. B. *Polym. Chem.* **2015**, *6* (31), 5643–5652.

(57) Radzinski, S. C.; Foster, J. C.; Chapleski, R. C.; Troya, D.; Matson, J. B. *J. Am. Chem. Soc.* **2016**, *138* (22), 6998–7004.

(58) Tang, H.; Li, Y.; Lahasky, S. H.; Sheiko, S. S.; Zhang, D. *Macromolecules* **2011**, *44* (6), 1491–1499.

(59) Tang, H.; Zhang, B.; Wu, P. *Soft Matter* **2014**, *10* (37), 7278–7284.

(60) Zehm, D.; Laschewsky, A.; Liang, H.; Rabe, J. P. *Macromolecules* **2011**, *44* (24), 9635–9641.

(61) Iborra, A.; Díaz, G.; López, D.; Giussi, J. M.; Azzaroni, O. *Eur. Polym. J.* **2017**, *87*, 308–317.

(62) Xia, Y.; Olsen, B. D.; Kornfield, J. A.; Grubbs, R. H. *J. Am. Chem. Soc.* **2009**, *131* (51), 18525–18532.

(63) Yamamoto, S. I.; Pietrasik, J.; Matyjaszewski, K. *Macromolecules* **2008**, *41* (19), 7013–7020.

(64) Yamamoto, S. I.; Pietrasik, J.; Matyjaszewski, K. *Macromolecules* **2007**, *40* (26), 9348–9353.

(65) Pietrasik, J.; Sumerlin, B. S.; Lee, R. Y.; Matyjaszewski, K. *Macromol. Chem. Phys.* **2007**, *208* (1), 30–36.

Gabriel Rios Valer obtained his Degree in Engineering physics (2015) at the Universidad Nacional de Ingeniería, UNI (Perú). His first and unique research exchange stay (2013) was carried out at the Istituto de Cristallografia, CNR, Bari (Italy) in Prof. Cinzia Giannini's group (XMI Lab), where Gabriel performed studies (data acquisition and analysis) for obtaining the structural, micro-structural and morphological information by means of X-Ray Powder Diffraction, SAXS and WAXS techniques for the new nanostructured materials (CuO) synthetized by himself as a thesis preparation student of Prof. José Solis (Laboratorio de Materiales Funcionales, Energías Renovables y Eficiencia Energética de la Facultad de Ciencias de la UNI). Currently Gabriel is a PhD student at Universidad Nacional de La Plata (UNLP) and work as scholarship holder at Soft Matter Laboratory in the Instituto de Investigaciones Fisicoquímicas Teóricas y Aplicadas (INIFTA) under Marcelo Ceolín and Juan M. Giussi supervision.

Agustin Iborra got his degree in chemistry (2015) and started his PhD in chemistry cofinanced by CONICET and Y-TEC at the Universidad Nacional de La Plata (UNLP, Argentina) under Omar Azzaroni and Juan M. Giussi supervision. His project is about "Design and preparation of amphiphilic macromolecules" to improve recovery factors in oil industries. His PhD begins learning and specializing in atom transfer radical polymerization (ATRP) in SoftMatter Lab at the Instituto de Fisicoquimica Teoricas y Aplicadas. During 2017, He did a stay at Institute of Physical Chemistry of the University of Göttingen (Germany) where he learned about reversible addition-fragmentation chain transfer polymerization (RAFT) in Professor P. Vana's Laboratory. In 2018, Agustin trained about different characterization techniques for 6 month in Sergio Moya's Laboratory in The Center for Cooperative Research in Biomaterials-CIC biomaGUNE, located in San Sebastián (Spain). He plan present his PhD during 2020.

Juan Martín Giussi obtained his Degree in Chemistry (2007) and his PhD in Chemistry (2012) at the Universidad Nacional de La Plata (UNLP) (Argentina). His first postdoctoral position (2012-2013) was carried out at the Instituto de Ciencia y Tecnología de Polímeros of Madrid (España) in Prof. C. Mijangos department, where Juan performed studies in nano-molding and synthesis of polymers in confinement for biomedical applications. His second postdoctoral position (2013-2015) was done at the Instituto de Investigaciones Fisicoquímicas Teóricas y Aplicadas (INIFTA) of La Plata in Prof. O. Azzaroni laboratory. In INIFTA, Juan learned and specialized in controlled polymerization techniques and synthesis of stimuli-responsive microgels. In 2015, he obtained his CONICET researcher position at Soft Matter Laboratory, research is focused on Molecular Design, Synthesis and Characterization of amphiphilic macromolecules for industrial. Juan is also university teacher assistant in Organic Chemistry at Chemistry Department of the Facultad de Ciencias Exactas (UNLP).

Anales de la Asociación Química Argentina

División Jóvenes Profesionales

Mini-Review

REMOTE ACTUATION OF EPOXY NANOCOMPOSITES WITH FUNCTIONAL PROPERTIES

F. Altuna[1]*, J. Puig*[1], C. E. Hoppe[1] and R. J. J. Williams[1]

[1]Institute of Materials Science and Technology, INTEMA, UNMDP-CONICET, Av. Juan B. Justo 4302, B7608FDQ, Mar del Plata, Argentina.
Autor Corresponsal: faltuna@fi.mdp.edu.ar; julietapuig@fi.mdp.edu.ar

Resumen Gráfico - Graphical abstract

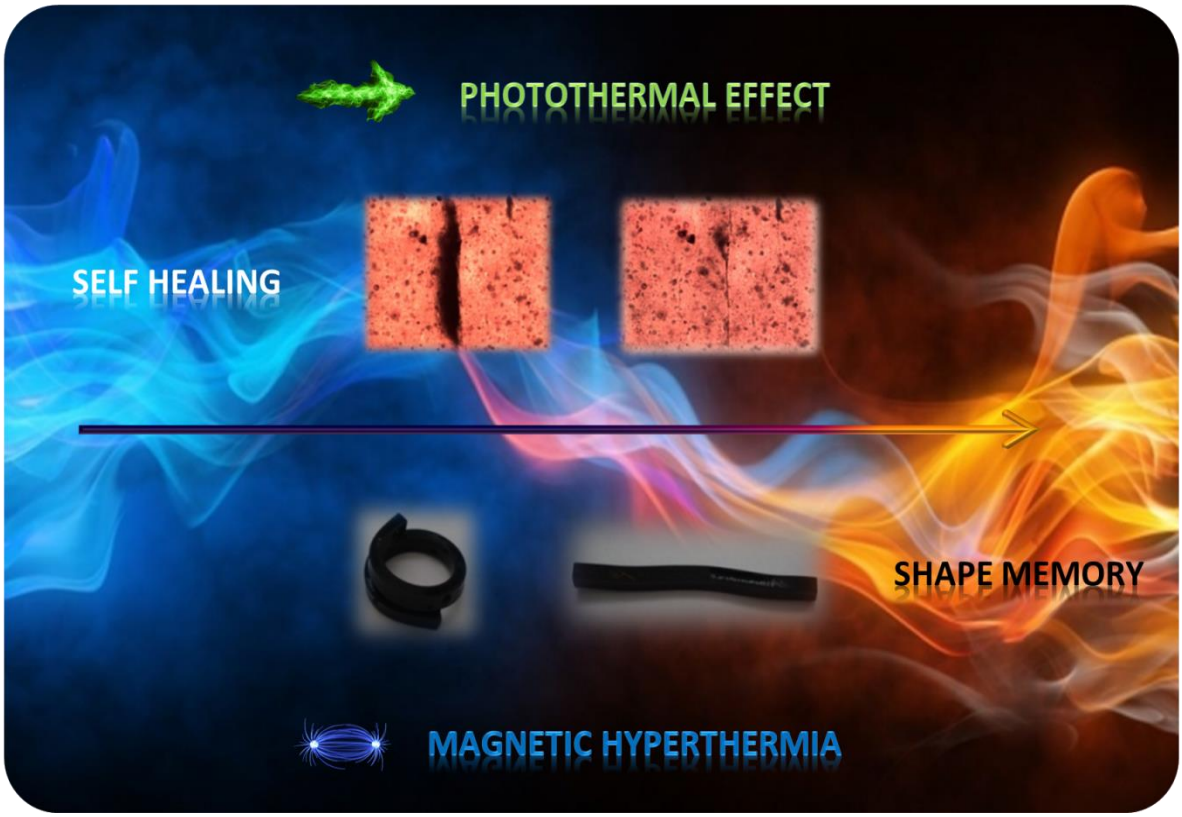

Resumen

Las redes epoxi son una familia de compuestos con uso extensivo en aplicaciones tales como recubrimientos, adhesivos y materiales compuestos avanzados. Exhiben diferentes propiedades funcionales tales como la capacidad de modificar su forma en respuesta a estímulos externos (epoxi con memoria de forma o SME por sus siglas en inglés), o su capacidad para intercambiar segmentos en su estructura química cuando se calientan a temperaturas superiores a la temperatura crítica (vitrímeros epoxi o EV). Los vitrímeros constituyen uno de los descubrimientos más importantes en el campo de los polímeros de los últimos años. Se comportan de diferente manera según se varíe la temperatura por encima o debajo de la temperatura crítica. Por encima de la misma pueden fluir e intercambiar segmentos de cadenas elásticas sin modificar la densidad de entrecruzamiento. Esto es lo que precisamente les otorga propiedades de auto-curado, reciclado y soldado. Los SME y EV se activan en ciclos de

calentamiento/enfriamiento. La incorporación de nanopartículas capaces de convertir radiación IR o visible en calor (efecto fototérmico) hace posible la actuación remota de estos materiales inteligentes. Similarmente, la incorporación de nanopartículas magnéticas hace posible el mismo efecto por medio de la hipertermia magnética. La síntesis de materiales inteligentes a partir de nanocompuestos basados en matrices de epoxi requiere la funcionalización apropiada de las nanopartículas para producir una dispersión homogénea en la matriz de epoxi. En este artículo discutiremos los desarrollos más recientes en los nanocompuestos EV y SME que pueden ser activados.

Abstract
Epoxy networks are one of the most important families of thermosetting polymers with an extensive use as adhesives, coatings and matrices of advanced composites. In recent years, smart materials based on epoxy formulations were developed. They exhibit different functional properties such as the capacity of modifying their shape in response to an external stimulus (shape-memory epoxies, SME) or the capacity of interchanging segments of their chemical structures when heated above a critical temperature (epoxy vitrimers, EV). Vitrimers are one of the most important recent discoveries in the field of polymers. They behave as conventional thermosets below the critical temperature but they can flow at higher temperatures interchanging segments of elastic chains while keeping a constant crosslink density. This enables their self-healing, recycling and welding as well as the relaxation of strained chains. SME and EV are activated by adequate heating/cooling cycles. Incorporation of specific nanoparticles (NPs) capable of converting IR or visible light radiation into heat (photothermal effect) makes it possible the remote actuation of these smart materials. Similarly, incorporation of magnetic NPs can be used to produce the remote heating by exposure to an alternating magnetic field (magnetic hyperthermia). The photothermal effect provides also the possibility of local heating and, therefore, a local response (e.g., localized shape recovery or the self-healing of a localized area). Besides, the synthesis of smart epoxy nanocomposites requires the appropriate functionalization of NPs to produce their uniform dispersion in the epoxy matrix. In this article, we review recent selected papers dealing with the development of EV and SME nanocomposites that can be remotely activated.

Palabras Clave: *Vitrímeros epoxi, activación remota,epoxis con memoria de forma.*

Keywords: *epoxy vitrimers,remote activation, shape memory epoxies.*

1.Introduction

Epoxies are one of the most important families of thermosetting polymers with conventional uses as adhesives, coatings and matrices of composites for advanced applications. In recent years, their applications have been expanded to the new field of stimuli-responsive materials. This is a consequence of the versatility of epoxy formulations for designing networks with a large variety of controlled physicochemical properties. In the present article we will place the focus on two of these new families of advanced materials: shape memory epoxies (SME),[1–3] and epoxy vitrimers (EV).[4–7]

The shape memory is a characteristic feature of polymer networks. When they are heated above the glass transition they can be deformed to a temporary shape by employing an adequate tension. If they are cooled under tension to temperatures below the glass transition, the temporary shape is frozen with elastic energy stored in the strained chains. If tension is removed and the material is heated again above the glass transition, the elastic chains turn back to their equilibrium conformations and the material recovers its initial shape. If the change of shape is

prevented by a constraint, the material exerts a tension equivalent to the one used to produce the initial deformation. Materials that can change their shapes in a desired way or that can exert a force on an external constraint have found several practical applications. SME are one of the most important families of shape memory polymers due to their high versatility for tuning the location of the glass transition temperature, their excellent mechanical properties at temperatures below and above the glass transition and the high values of shape fixity and recovery. Formulations can include liquid crystalline monomers that introduce a new thermal transition enabling the generation of multiple-shape materials exhibiting two or more different temporary shapes frozen either by the glass transition or by an isotropic-liquid crystal transition. This gives new possibilities for practical applications.

The discovery of epoxy vitrimers (EV)[4–6] has completely changed the usual description of thermosetting polymers as materials that cannot be reprocessed or welded like thermoplastic polymers. The most important family of epoxy vitrimers is based on the reaction of carboxylic acids with epoxy groups generating *β*-hydroxyester groups (Scheme 1). Under the action of specific catalysts and at temperatures above a specific temperature (usually called topology freezing transition temperature, T_v, arbitrarily defined by a timescale adapted for practical applications), these groups can undergo transesterification reactions as shown in Scheme 2. This allows the interchange of chain segments enabling the material to flow and keeping a high viscosity associated to its crosslinked structure. The rheological behavior of vitrimers is equivalent to the one of inorganic glass with the same capacity of being thermoformed (the name vitrimers given to these materials derives from this property). This new family of materials behaves as a typical thermosetting epoxy network at temperatures below T_v. However, above this temperature the material can be recycled, welded, self-healed or thermoformed. As strained chains can be relaxed to equilibrium configurations by transesterification reactions, the temporary shape of an SME can be converted to a permanent shape by a simple thermoforming process. This enables to produce complex shapes out of a mold. Besides transesterification reactions, several other chemistries were recently proposed to produce a similar behavior in different types of polymer networks. However, epoxy vitrimers keep their position at the frontier of practical applications.

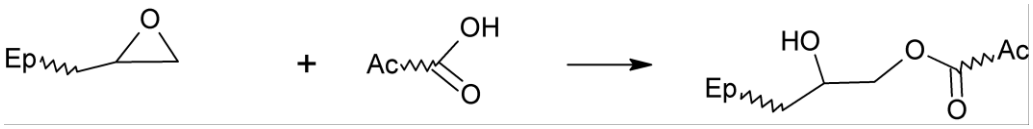

Scheme 1. Reaction of a carboxylic acid with an epoxy group generating a *β*-hydroxyester group.

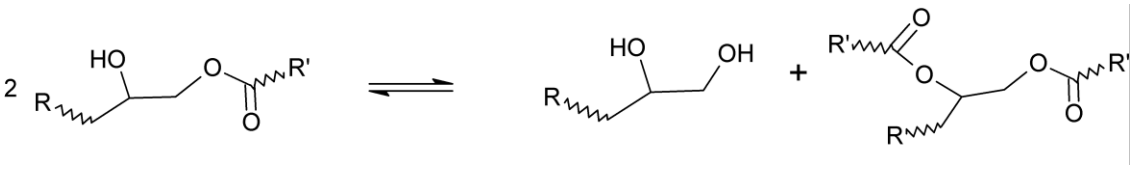

Scheme 2. Transesterification reactions of *β*-hydroxyester groups.

Remote triggering of the actuation of these smart epoxy networks requires the dispersion of adequate nanoparticles (NPs) that can respond to external fields generating heat. Herein we will discuss examples of the use of the photothermal effect or magnetic hyperthermia to produce the remote heating of nanocomposites based on SME or EV. The photothermal effect consists on the conversion of light into heat by electrically conductive nanostructures, such as metal NPs and nanowires (NWs), carbon nanotubes (CNTs) and graphene, when they are irradiated with light of a wavelength matching that of its surface plasmon resonance (SPR).[8–11] At SPR the population of "hot electrons" that can couple with the phonons of the lattice significantly increases giving place to a fast increase of the lattice temperature.[12] The low thermal conductivity of the polymeric matrix surrounding the NPs prevents the generated heat to be quickly transferred to the environment, and therefore a significant temperature increase is produced. The whole process displays a very fast dynamics, related to the relatively small volume fraction of NPs in the material.[9,12]

Magnetic hyperthermia is based on the generation of heat due to losses during magnetization reversal process of the magnetic NPs, under exposure to an alternating magnetic field. [13,14] This mechanism has found applications in: electronics,[15] energy,[16] and biomedicine,[17,18] and has been already approved for brain cancer therapies.[17,19] Transformation of the magnetic energy provided by the external magnetic source working in the radio-frequencies range, RF (f = 3 KHz – 300 GHz), into heat by magnetic NPs can be produced by three potential mechanisms: Néel (inner fluctuation of the magnetic moment) and Brown (rotation of the whole particle) relaxation mechanisms for single-domain super-paramagnetic (SPM) NPs, or due to hysteresis losses (magnetic domain and domain wall motion processes) for multi-domain ferro-magnetic (FM) NPs respectively.[20] In systems formed by magnetic nanofillers dispersed in rigid substrates, rotation is forbidden and Neel relaxation is the only mechanism enabling heating of the material.

In this review article we describe some selected articles from the recent literature dealing with the remote heating of EV and SME nanocomposites produced by the photothermal effect or by magnetic hyperthermia.

2.Remote Activation of EV and SME Nanocomposites by the Photothermal Effect

Remote activation of transesterification reactions in EV nanocomposites was first reported by Yang et al.[21,22] They added 0.1-3.0 wt% multi-walled carbon nanotubes (MWCNTs) to a vitrimer synthesized from a commercial epoxy resin based on diglycidyl ether of bisphenol A (DGEBA) crosslinked with adipic acid and with 1,5,7-triazabicyclo[4.4.0]dec-5-ene (TBD) as a transesterification catalyst.[6,23] Though the reaction between a difunctional epoxy resin and a difunctional acid leads to linear chains, a crosslinked structure is obtained due to transesterification reactions.[24] These CNT-vitrimers could be efficiently welded by irradiating them with infrared light (λ=808 nm; 3.8 W/cm^2) for times varying from 30 s to 3 min depending on the MWCNTs content. Vitrimers containing only 1% of MWCNTs reached a temperature of about 180 ºC when infrared light was applied for 20 s with a power of 0.84 W/cm^2. Figure 1 shows experiments that illustrate the remote activation of properties by the photothermal effect. Figure 1a shows the welding of two ribbon-shaped specimens using infrared light. Lap-shear tests proved that 30 s of irradiation (0.84 W/cm^2) provided a better bonding than 10 min of direct heating in an oven at 180ºC. Figure 1b shows that bonding can be restricted to selected areas by simply using a mask. Figure 1 (c and d) shows the healing of damaged samples and the mechanical tests for as-synthesized, cut and healed samples, respectively. Good levels of healing were in all cases obtained by triggering the materials response by infrared light. However, the authors found, unexpectedly, that direct heating at 180 ºC in an oven produced lower levels of healing, even after 1 h.

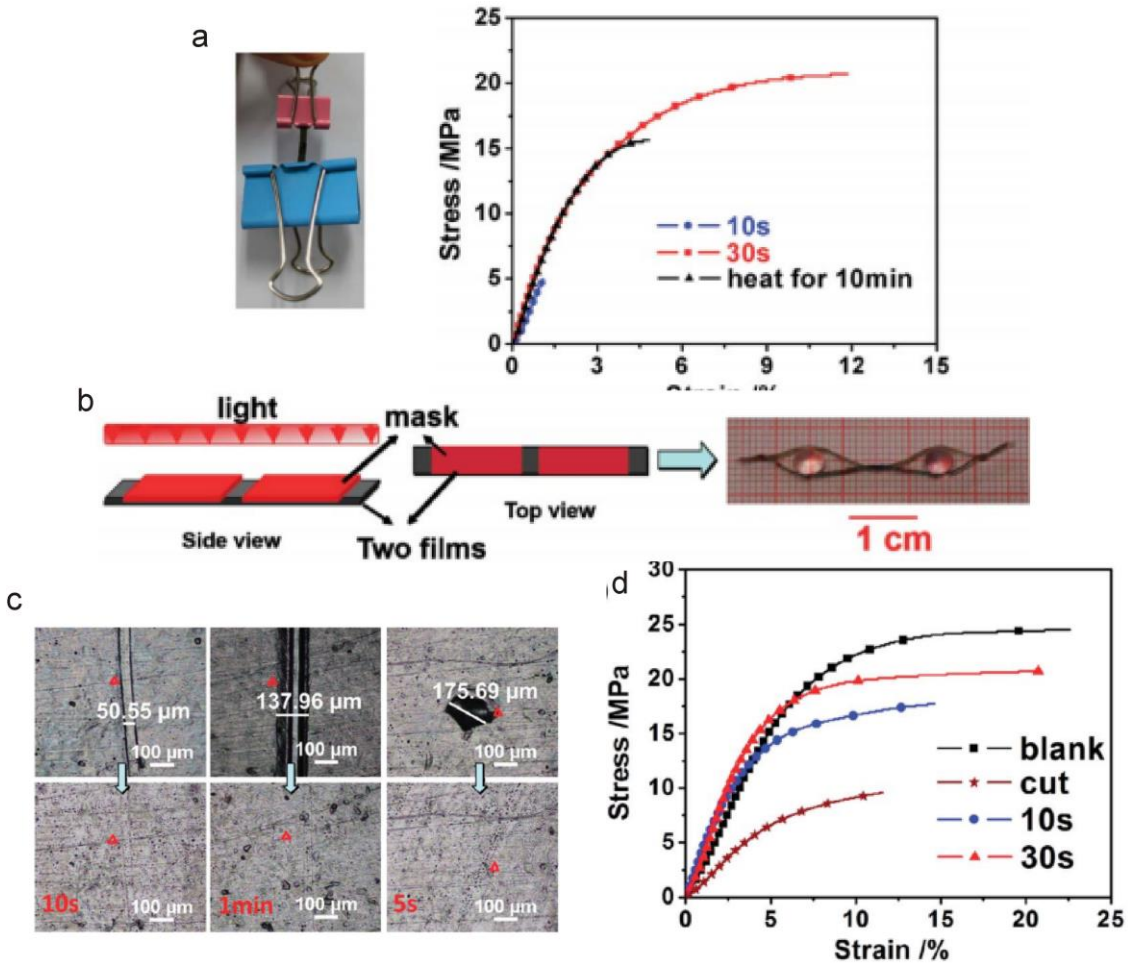

Figure 1. (a) Healed CNT-vitrimer specimen of 6 mg holding a weight of 14 g, and the corresponding lap shear tests. **(b)** Different figures that can be obtained using masks and irradiating with infrared light. **(c)** Healing of damaged samples of CNT-vitrimer composites with infrared light with an intensity of 15.2 W/cm^2. From left to right: a razor blade cut (50 µm width) healed for 10 s, a wider cut (130 µm) healed for 1 min and a needle pierce (140 µm in diameter), healed for 5s. **(d)** Stress-strain curves of virgin, cut and healed CNT-vitrimer. Repr. from Ref. [21] with permission from the Royal Society of Chemistry.

The incorporation of metallic NPs constitutes another route for the light-triggering of the self-healing of EV. We successfully employed polyvinylpyrrolidone (PVP)-capped gold NPs, (Au@PVP) NPs, with a mean diameter of 13.1 nm to activate transesterification reactions by visible light irradiation.[25] The polymeric network was obtained by crosslinking epoxidized soybean oil (ESO) with citric acid (CA), whose self-healing ability was previously demonstrated[7]. One remarkable advantage of Au NPs over carbon-based nanostructures is that even very low amounts of gold lead to significant temperature increases, and thus the material remains with a high degree of transparency in wide regions of the visible spectrum. ESO-CA-Au@PVP nanocomposites with 0.02 and 0.08 wt% Au displayed a SPR band centered at 538-545 nm. Upon illumination with a green laser (λ=532 nm; 1.74 W/cm^2) the bulk temperature measured within the sample (at about 1 mm of the irradiated surface) increased quickly (3-4

minutes) from 22ºC to more than 80ºC for nanocomposites with 0.02wt% Au and to around 130ºC for 0.08 wt% Au. Moreover, nanocomposites with 0.08 wt% Au underwent thermal degradation on the surface, indicating that temperature reached values above 200ºC. Figure 2a and b shows, respectively, optical micrographs of a cracked sample before and after irradiation and the stress-strain curves for tensile tests of the neat matrix, and virgin and healed nanocomposites with 0.02 wt% Au. Due to the lack of a transesterification catalyst, reactions were relatively slow. An additional advantage of photothermal heating is that thanks to the confined thermal expansion of the irradiated area, the fracture surfaces become in close contact without the need of external pressure.[25,26] This is probably the explanation for the poor healing observed by Yang et al. when their CNT-vitrimers were subjected to direct heating.[21]

Using a similar concept based on the use of Au NPs, Wang et al. introduced polydopamine-modified Au microspheres (averaging 1300 nm in diameter) in a vitrimer matrix based on DGEBA, sebacic acid and TBD[27]. They used infrared light (λ=808 nm; 3.5 W/cm^2) to trigger self-healing, and found that 120 s of infrared irradiation yielded a more effective healing than direct heating in an oven for 10 min at 180ºC (Figure 2c and d).

In another study, we developed two different SME nanocomposites that could be remotely activated by green light irradiation.[28] AuNPs were incorporated in two different epoxy matrices as photohermal fillers. In the first strategy, PEO (poly(ethylene oxide)) was used as stabilizing ligand of NPs to minimize aggregation. This polymer was selected due to its high solubility in epoxy networks based on DGEBA. DGEBA was cured with a mixture of n-dodecylamine (DA) and m-xylylenediamine (MXDA) to give a shape memory thermoset with excellent recovery and fixation ratios.[3] This formulation combined large strains with relatively large stresses, a desirable property for an SME. Activation temperature was 41 °C (the glass transition temperature T_g of the matrix), a value located near room temperature that is useful for practical applications. Incorporation of a very low amount of Au@PEO NPs (0.01, 0.05 and 0.1 wt%) did not produce any significant change in the thermal or mechanical properties of the polymer. The temperature increase of the nanocomposites under green light irradiation (DPSS laser at 532 nm), is shown in Figure 3. The three samples showed high temperature increases after 400 s irradiation (power density close to 2 W/cm^2), reaching 140ºC for the highest NPs loading (0.1 wt%). A bar of the sample containing 0.01 wt% Au@PEO NPs was bended above T_g and cooled to room temperature (temporary shape). As shown in Figure 4, recovery of the initial shape occurred after a few seconds irradiation with the green light laser.

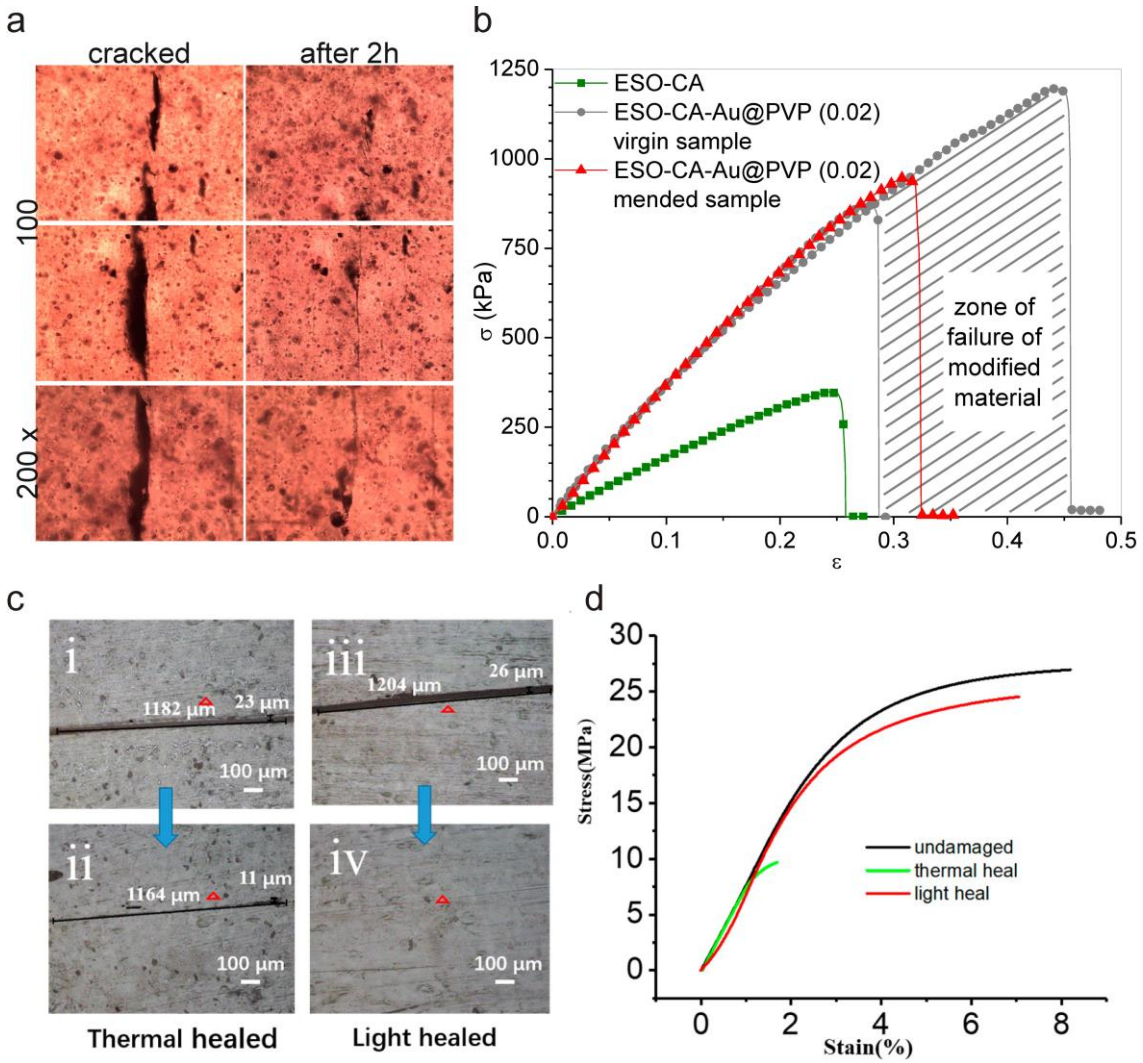

Figure 2. (a) Optical microscopy images of a healed crack after irradiation with a green laser with an intensity of 1.74 W/cm^2. Scale bars lengths represent 0.2 mm. **(b)** Strain-stress curves of the neat polymer and the virgin and healed (after complete cut through) nanocomposite. **(c)** Comparison between direct (10 min, 180ºC) and photothermal (infrared light, 120 s, 3.5 W/cm^2) heating for the vitrimer with gold microspheres. **(d)** Strain-stress curves of the virgin material and samples healed through direct heating and infrared radiation. (a) and (b) repr. with permission from Ref. [25] (©2016 IOP Publishing LTD.) and (c) and (d) repr. from Ref. [27] (©2018 Multidisciplinary Digital Publishing Institute)

The second strategy was to employ an amphiphilic epoxy matrix to generate a uniform dispersion of Au NPs coated with dodecyl chains (Au@DD NPs).[29] An epoxy matrix was obtained by homopolymerization of DGEBA with benzyldimethylamine (BDMA) in the presence of 5 wt% of a linear polymer (LAP) containing pendant dodecyl chains. This LAP was obtained by reaction of DGEBA with dodecylamine in stoichiometric ratio. During homopolymerization of DGEBA, the LAP was covalently bonded to the network by chain-transfer reactions, generating a transparent material with a T_g of 43ºC.[29] Au@DD NPs (0.04 wt%) could be uniformly dispersed due to the compatibility between the alkyl chains of the

network and those stabilizing the Au NPs. The temperature increase was recorded with an embedded thermocouple (Figure 5). About 38 % of the maximum power and less than 20 s were needed to increase the temperature above T_g. A bar of the SME nanocomposite was bended in three different sections to demonstrate the localized shape recovery under exposure to green light (Figure 6). The first irradiation step was carried out for 15 s at the first bended section; the second step was performed for 19 s at the second bended section, and the last step for another 18 s at the third bended section. This enabled a complete recovery of the initial shape. This work demonstrated the possibility of local control on actuation with very low concentrations of Au NPs.

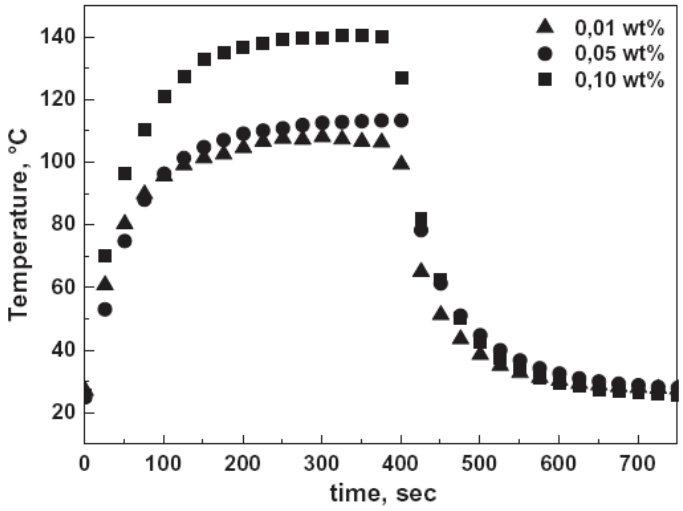

Figure 3. Temperature increase or SME containing different amounts of Au@PEO NPs. Temperature was recorded with a thermocouple inserted in the material before polymerization. Reprinted from ref [28] ©2015 with permission from Elsevier.

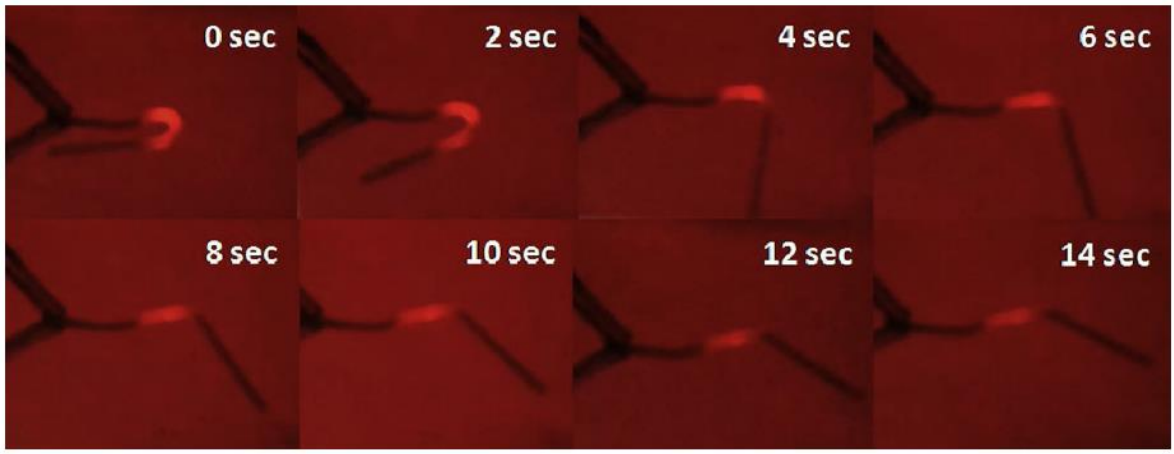

Figure 4. Shape recovery of an SME nanocomposite containing 0.01 wt% Au@PEO NPs, previously folded at 180°, when irradiated with green light at the bended section (photos were taken with a red filter). Reprinted from ref [28] ©2015 with permission from Elsevier.

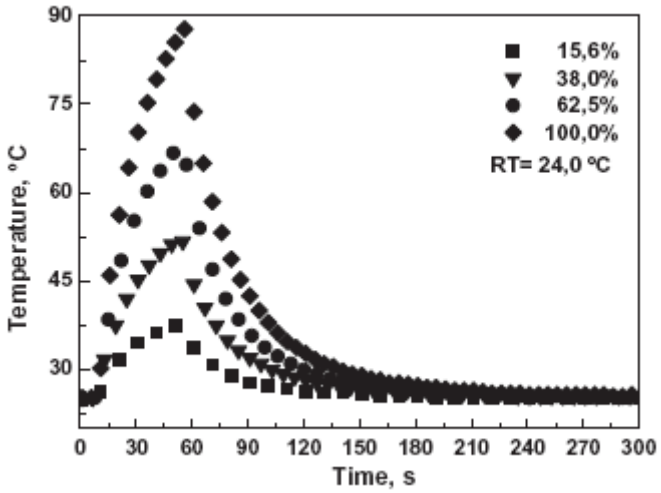

Figure 5. Temperature increase in the SME nanocomposite containing 0.04 wt% Au@DD NPs, recorded with an embedded thermocouple. The irradiation started at 10 s and was stopped at 52 s. Curves correspond to different irradiation powers (100% corresponds to about 700 mW). Reprinted from ref [28] ©2015 with permission from Elsevier

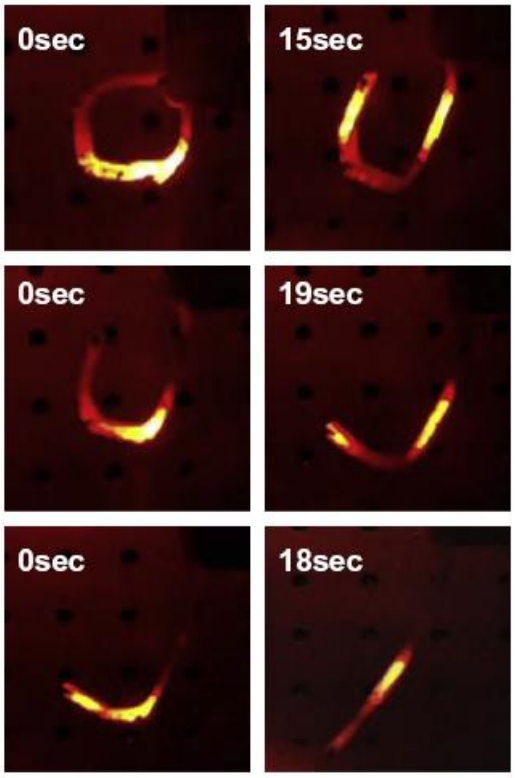

Figure 6. Shape recovery of a SME containing 0.04 wt% Au@DD by irradiation with green light at the previously bended section (photographs were taken with a red filter). Reprinted from ref [28] ©2015 with permission from Elsevier.

Pei et al. first realized that the remote actuation of shape memory of epoxy vitrimers enables access to complicated architectures that would hardly be possible to obtain by other means.[30]

They used three different diepoxide precursors, sebacic acid and TBD as catalyst of the transesterification reactions, for obtaining the three EV with different T_g values, comprised between 30 ºC and 50 ºC. Two of the EV were liquid crystalline networks with isotropic-liquid crystal transition temperatures (T_i) of 65 and 100°C. They were used to weld parts of different networks, giving place to shape memory structures with different shape recovery temperatures, where the original permanent shape could be recovered in steps of increasing temperature (Figure 7a).

The incorporation of CNTs offered the possibility of locally heating the samples by infrared light irradiation (λ=808 nm; 0.28 W/cm^2), obtaining a remote shape recovery of one of the segments of the strip while the others were sequentially activated by direct heating (Figure 7b).

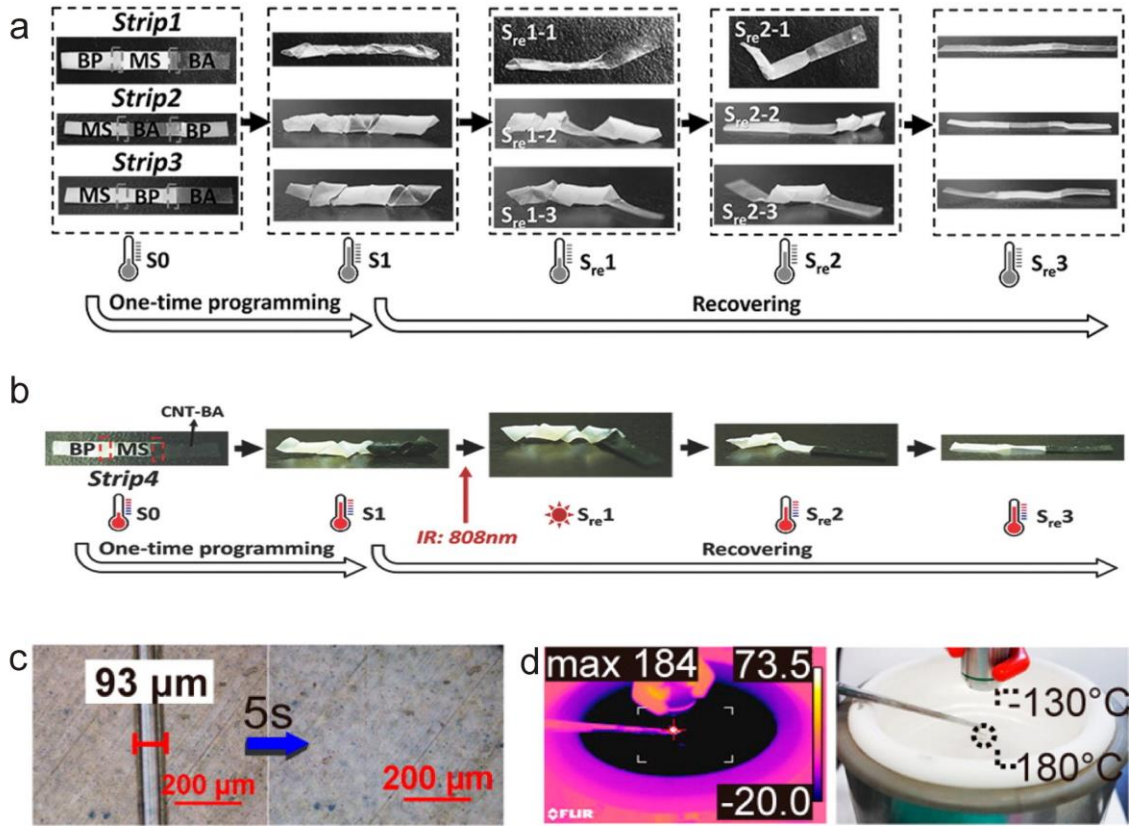

Figure 7. (a) Demonstration of the multi-shape memory behavior of strips formed by three vitrimers with different shape recovery temperatures activated sequentially by a temperature increase; **(b)** Demonstration of multi-SM behavior of a strip with CNTs in one of its three segments that is first activated through infrared radiation; **(c)** Healing of a cut (93 μm width) in the EV nanocomposite by infrared light irradiation; **(d)** IR and optical images of the liquid crystalline vitrimer nanocomposite irradiated in a nitrogen vapor atmosphere at -130ºC. (a) and (b): Reproduced from Ref. [30]. Copyright 2016 ©-VCH Verlag GmbH & Co. KGaA, Weinheim. (c) and (d): Reprinted with permission from Ref. [31]. ©2016 American Chemical Society.

The same research group synthesized an EV nanocomposite with an isotropic-liquid crystal transition temperature, adding MWCNTs to a matrix based on diglycidyl ether of 4, 4′-dihydroxybiphenol (DGE-DHBP) crosslinked with sebacic acid and employing TBD as transesterification catalyst. [31] Figure 7c shows the light induced (λ = 808 nm) self-healing of a 93 μm crack, and Figure 7d depicts the high temperatures (enough to activate the shape recovery) reached through the photothermal effect, even when the surroundings are in a nitrogen vapor atmosphere at -130ºC.

Yang et al. described the utilization of graphene for the remote heating of an EV nanocomposite based on DGEBA-sebacic acid and TBD as transesterification catalyst.[32] The photothermal effect produced by graphene enabled shape recovery by infrared light irradiation (λ = 808 nm; 0.1 W/cm^2)[32]. They clearly showed how shape memory could be combined with the stress relaxation produced by transesterification reactions to produce a box that could be deployed and closed by an adequate thermal cycle (Figure 8). The first sequence shows a simple shape recovery sequence. The bar was deformed at 70 ºC, cooled to freeze the temporary shape and heated again to 70 ºC to recover the permanent shape. The second sequence shows the reconfiguration of the permanent shape by a thermoforming step at 200 ºC. At this temperature, transesterification reactions are active and relax the initially strained elastic chains to their equilibrium values, fixing the new permanent shape. Then temperature was decreased to 70 ºC, a new temporary shape was created that was frozen by cooling to room temperature. By a new heating at 70 ºC, the permanent shape produced at 200 ºC was recovered. The third sequence shows the generation of a new permanent shape at 200 ºC, the generation of a temporary shape at 70 ºC (similar to the permanent shape generated in the previous sequence), its fixation by cooling to room temperature and the recovery produced by a new heating at 70 ºC. The final sequence shows the possibility of generating a box using the properties of the EV. The box may be first formed by welding four faces to a central face. By folding these faces at 70 ºC, an open box is generated. Heating at 200 ºC for 30 min eliminates residual tensions and the box becomes the permanent shape. The box may be opened again by reducing temperature to 70 ºC and cooling to room temperature to freeze the temporary shape.

Heating to 70 ºC produces the folding of faces to obtain again the box (permanent shape). As the nanocomposite contains MWCNTs, the heating steps to 70 ºC may be performed by the photothermal effect employing IR radiation.

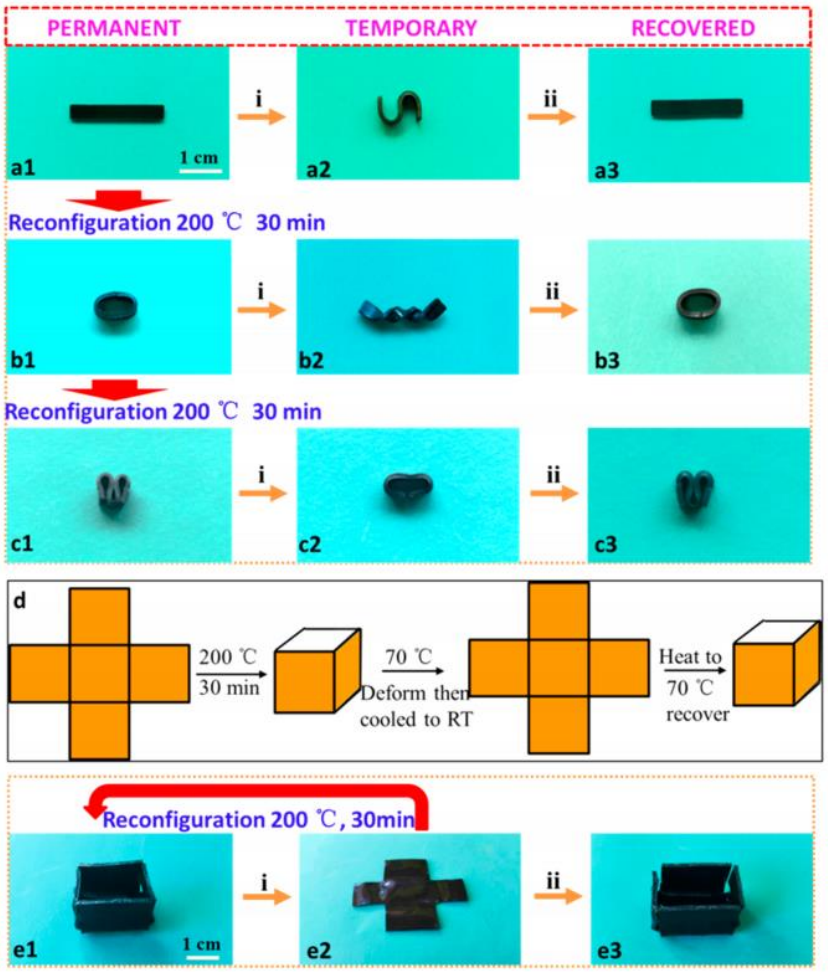

Figure 8. Permanent and temporary shapes of an EV nanocomposite containing MWCNTs (explanation of different shapes is given in the text). Reprinted with permission from Ref. [32]. ©2016 American Chemical Society..

Another strategy to obtain a multi-stimuli responsive EV was described by Chen et al.[33] Instead of nano- or microstructures, they used an amino-capped aniline trimer (ACAT) and/or the absorption of a Cu^{+2} salt to produce the photothermal effect using IR radiation (λ=808 nm). The neat EV was synthesized using DGEBA, suberic acid and TBD as transesterification catalyst. Formulations modified with ACAT not only allowed using infrared light to generate heat, but also provided the material with other functional properties such as electrochromism, metal ions sorption ability and pH and voltage responsiveness. Moreover, it was found that ACAT could also exert a catalytic effect, speeding up the transesterification reactions thanks to the presence of amino groups. Temperature increases from room temperature to more than 200ºC were measured in the EV with an ACAT content of 10 mol %, for an irradiation power density of 0.9 W/cm^2.

The shape memory behavior of different EV is shown in Figure 9. As expected, the unmodified EV was not responsive to IR radiation (sequence I). After absorption of Cu^{+2}, the EV exhibited shape recovery for an irradiation power of 0.19 W/cm^2 (sequence II). The EV modified with

ACAT showed shape recovery using a lower light intensity (0.09 W/cm^2, sequence III). The EV modified with ACAT and with absorbed Cu^{+2} exhibited shape recovery at a still lower light intensity (0.06 W/cm^2, sequence IV).

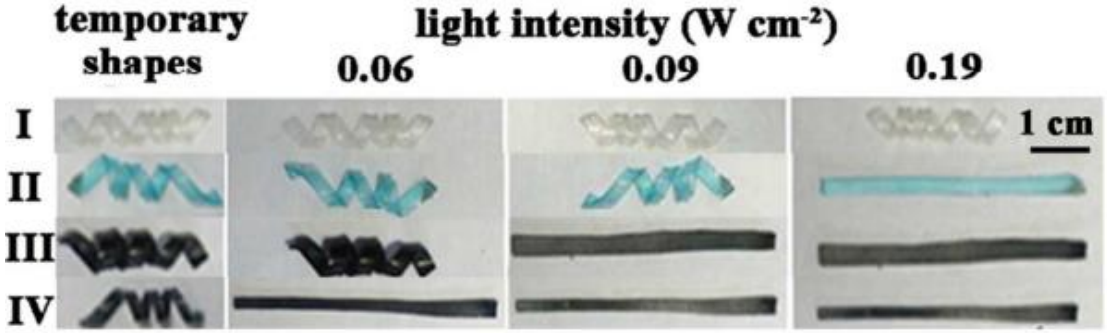

Figure 9. Shape recovery at different light intensities of the neat EV (I), EV after absorbing Cu^{+2} (II), ACAT-modified EV (III), and ACAT-modified EV after absorbing Cu^{+2} (IV). Reproduced from Ref. [33] Published by the Royal Society of Chemistry.

3.Remote Activation of SME Nanocomposites Using Magnetic Hyperthermia

Instead of employing light, the remote heating may be produced by introducing magnetic NPs in the formulation and using an alternating magnetic field (magnetic hyperthermia). Vialle et al. investigated the remote activation of SME nanocomposite foams.[34] A commercial epoxy formulation was modified with the addition of different magnetic fillers: a) Magsilica (silica with embedded iron oxide) with a particle size between 5-30 nm and b) magnetite NPs with an average size of 250 nm.

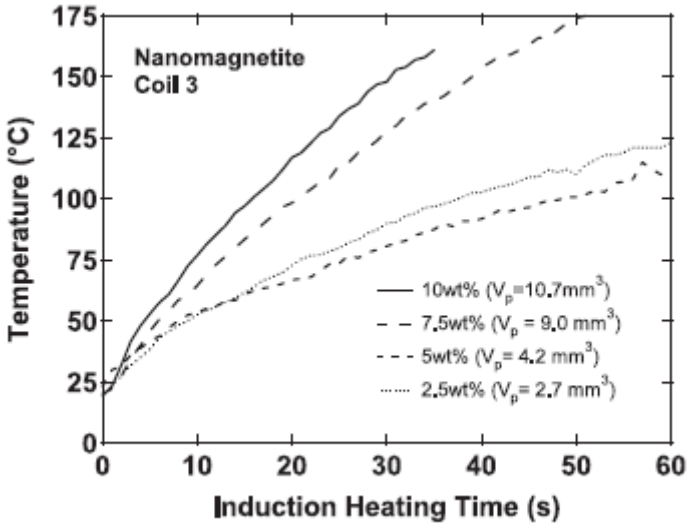

Figure 10. Heating response of a SME foam containing different concentrations of magnetite NPs, exposed to a RF magnetic field. Reproduced from Ref. [35]. Copyrigth 2009 IOP PUBLISHING, LTD.

The heating response of various formulations was monitored using different magnetic coils and configurations. Nanocomposites obtained with magnetite NPs performed significantly better than those obtained with silica embedded-iron oxide NPs. Figure 10 shows the heating response of SME nanocomposites with different contents of magnetite filler (from 2.5 to 10 wt %) in a 330 kHz magnetic field. The heating rate increased with the filler content enabling fast recovery rates (less than 20 s) for SME foams containing 10 wt % magnetite NPs.

He et al.[35] described the synthesis of a bar of a SME with three segments of different compositions (Figure 11). The segment at the left was modified with 0.4 wt% CNT (T_g = 59 ºC), the central segment was made by the unmodified SME (T_g = 60.7 ºC) and the segment at the right contained 5 wt% magnetite NPs (T_g = 44.7 ºC). As magnetite NPs induce heat at a frequency of 296 kHz and CNTs at 13.56 MHz, both segments could be independently activated. Figure 11 shows the shape recovery of the multicomposite. When a deformed sample (temporary shape 1) was exposed to a 13.56 MHz RF field, only the region containing CNTs was heated, allowing a complete recovery of that segment (temporary shape 2). Subsequent exposure to 296 KHz RF field led to a selective heating and recovery of the magnetite/epoxy segment (temporary shape 3). Finally, by heating in an oven (temporary shape 3), the neat epoxy segment was recovered leading to the permanent shape. The multiple shape memory behavior could be selectively activated varying the frequency of the alternating magnetic field.

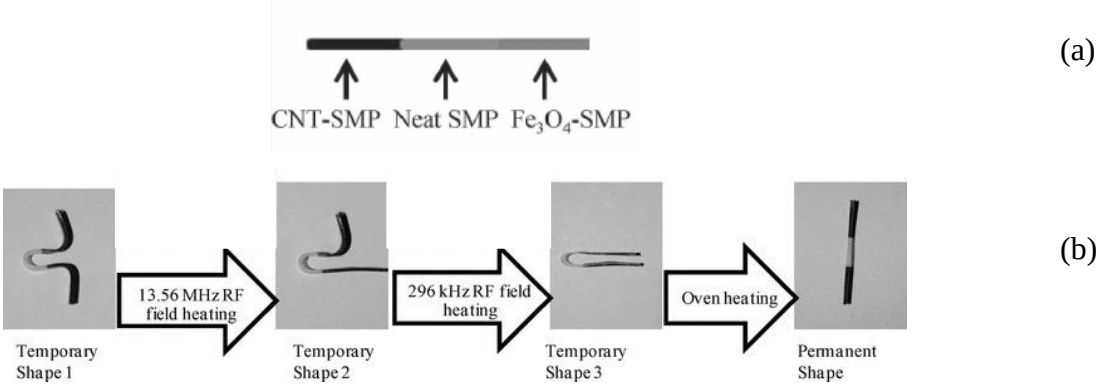

Figure 11. Selective shape recovery of a bar containing three segments of different composition, exposed to an alternating magnetic field of variable frequencies. Reproduced from Ref. [36]. Copyright © 2011 WILEY-VCH Verlag GmbH & Co. KGaA, Weinheim.

Achieving uniform dispersions of magnetic NPs in SME is not a trivial task. A common synthesis of magnetite NPs uses oleic acid (OA) as a stabilizing ligand. The resulting Fe_3O_4@OA NPs are hydrophobic and difficult to disperse in polar epoxy formulations. By pre-reacting DGEBA with 20 wt% OA, the magnetite NPs could be uniformly dispersed in the epoxy matrix.[36] The unreacted epoxy functionalities were homopolymerized in the presence of BDMA

leading to a SME nanocomposite with T_g = 51 ºC. A TEM image of the SME with 8 wt% of Fe_3O_4@OA NPs shows the presence of a uniform dispersion of NPs (Figure 12).

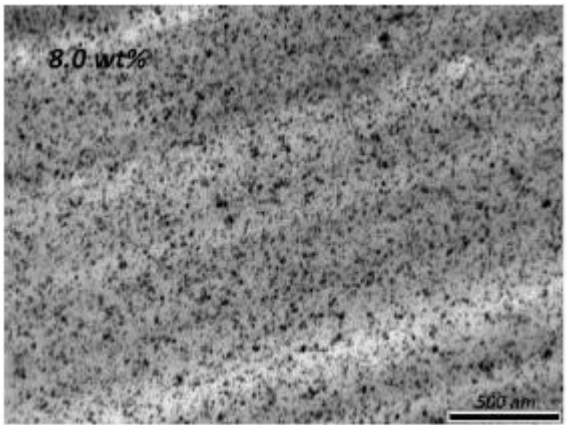

Figure 12. TEM image of an ultrathin cut of the SME nanocomposite containing 8 wt% Fe_3O_4@OA. Reprinted with permission from Ref.[36] ©2012 American Chemical Society.

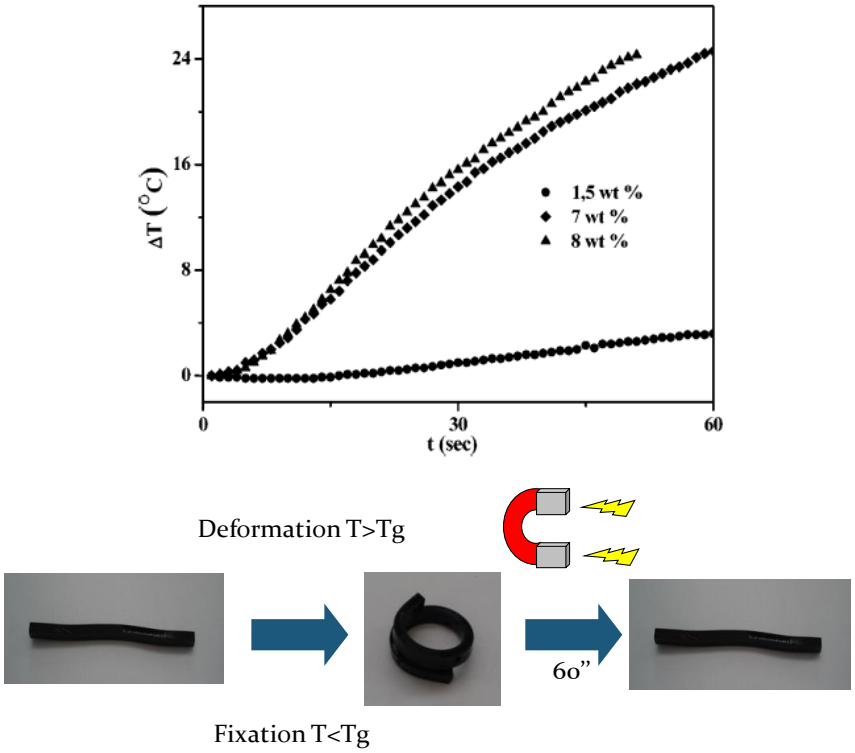

(a)

(b)

Figure 13. (a) Temperature increase for SME nanocomposites with different wt% magnetite NPs exposed to an alternating magnetic field. **(b)** Photographs showing the recovery process. Reprinted with permission from Ref.[36] ©2012 American Chemical Society

The magnetic heating of the SME nanocomposites was produced employing values of frequency and field strength in the range of biomedical applications (293 kHz and 30 mT). A maximum ΔT

~ 25 °C was recorded with a fiber optic sensor for nanocomposites with 7 and 8 wt% NPs after about 60 s, enough to produce the shape recovery (Figure 13).

Conclusions and Future Trends

Epoxy vitrimers (EV) containing NPs or compounds that generate heat when exposed to light or alternating magnetic fields of appropriate frequencies, can be remotely activated generating useful properties for practical applications. As described by the selected examples, these materials can be welded, recycled, self-healed and can relax stresses allowing thermoforming or the conversion of temporary shapes into permanent ones. Conventional SME can be also modified with a similar set of NPs enabling the remote activation of shape memory, necessary for some applications in medicine or in space. Key issues in the synthesis of these smart materials are related to the control of the dispersion level and the thermal response of the nano/microstructures embedded in the polymeric network. Variables as concentration, size, shape, and chemical nature of the stabilizing ligands influence the dispersion and response of the nanofillers employed to produce the remote actuation.

Publications and patents in this field have increased exponentially in recent years together with practical applications. Although the tremendous potential of these systems is clear, some points need further research work. Among them, precise mathematical models that can account for the heat transfer processes taking place in materials heated through magnetic hyperthermia or photothermal effect, are required. Thermal profiles in solid, stiff materials will depend on many variables related with both, the filler and the matrix, in a different way to that expected for colloidal dispersions or gels. A clear picture of this behavior will enable a more rational design of the required devices and a more delicate tuning of the activation rate without using high amounts of fillers and without affecting other important characteristics of the polymer, like transparency or mechanical properties. On the other hand, it will be necessary revising and adapting methods of incorporation of fillers in the polymeric matrix in order to control the dispersion level (models accounting for the influence of aggregation processes will be also necessary at this point) and avoid the use of organic solvents and high energy processing methods. Finally, possibilities of scaling-up, life-cycle analysis and costs associated with these technologies are important issues to consider for specific applications.

Notes and references

(1) Karger-Kocsis, J.; Kéki, S. Recent Advances in Shape Memory Epoxy Resins and Composites. In *Multifunctionality of Polymer Composites*; Elsevier, 2015; pp 822–841.

(2) Rousseau, I. A.; Xie, T. Shape Memory Epoxy: Composition, Structure, Properties and Shape Memory Performances. *J. Mater. Chem.* **2010**, *20* (17), 3431.

(3) Leonardi, A. B.; Fasce, L. A.; Zucchi, I. A.; Hoppe, C. E.; Soulé, E. R.; Pérez, C. J.; Williams, R. J. J. Shape Memory Epoxies Based on Networks with Chemical and Physical Crosslinks. *Eur. Polym. J.* **2011**, *47* (3), 362–369.

(4) Montarnal, D.; Capelot, M.; Tournilhac, F.; Leibler, L. Silica-Like Malleable Materials from Permanent Organic Networks. *Science (80-.).* **2011**, *334* (6058), 965–968.

(5) Capelot, M.; Montarnal, D.; Tournilhac, F.; Leibler, L. Metal-Catalyzed Transesterification for Healing and Assembling of Thermosets. *J. Am. Chem. Soc.* **2012**, *134* (18), 7664–7667.

(6) Capelot, M.; Unterlass, M. M.; Tournilhac, F.; Leibler, L. Catalytic Control of the Vitrimer Glass Transition. *ACS Macro Lett.* **2012**, 789–792.

(7) Altuna, F. I.; Pettarin, V.; Williams, R. J. J. Self-Healable Polymer Networks Based on the Cross-Linking of Epoxidised Soybean Oil by an Aqueous Citric Acid Solution. *Green Chem.* **2013**, *15* (12), 3360–3366.

(8) Richardson, H. H.; Hickman, Z. N.; Govorov, A. O.; Thomas, A. C.; Zhang, W.; Kordesch, M. E. Thermooptical Properties of Gold Nanoparticles Embedded in Ice: Characterization of Heat Generation and Melting. *Nano Lett.* **2006**, *6* (4), 783–788.

(9) Govorov, A. O.; Richardson, H. H. Generating Heat with Metal Nanoparticles. *Nano Today* **2007**, *2* (1), 30–38.

(10) Baffou, G.; Quidant, R.; Girard, C. Heat Generation in Plasmonic Nanostructures: Influence of Morphology. *Appl. Phys. Lett.* **2009**, *94* (15), 153109.

(11) Coronado, E. A.; Encina, E. R.; Stefani, F. D. Optical Properties of Metallic Nanoparticles: Manipulating Light, Heat and Forces at the Nanoscale. *Nanoscale* **2011**, *3* (10), 4042.

(12) Hartland, G. V. Optical Studies of Dynamics in Noble Metal Nanostructures. *Chem. Rev.* **2011**, *111* (6), 3858–3887.

(13) Nemati, Z.; Alonso, J.; Rodrigo, I.; Das, R.; Garaio, E.; García, J. Á.; Orue, I.; Phan, M.-H.; Srikanth, H. Improving the Heating Efficiency of Iron Oxide Nanoparticles by Tuning Their Shape and Size. *J. Phys. Chem. C* **2018**, *122*, 2367–2381.

(14) Kafrouni, L.; Savadogo, O. Recent Progress on Magnetic Nanoparticles for Magnetic Hyperthermia. *Prog. Biomater.* **2016**, *5*, 147–160.

(15) Ko, S. H.; Park, I.; Pan, H.; Grigoropoulos, C. P.; Pisano, A. P.; Luscombe, C. K.; Fréchet, J. M. J. Direct Nanoimprinting of Metal Nanoparticles for Nanoscale Electronics Fabrication. *Nano Lett.* **2007**, *7*, 1869–1877.

(16) Gibson, R. F. A Review of Recent Research on Mechanics of Multifunctional Composite Materials and Structures. *Compos. Struct.* **2010**, *92*, 2793–2810.

(17) Mahmoudi, K.; Bouras, A.; Bozec, D.; Ivkov, R.; Hadjipanayis, C. Magnetic Hyperthermia Therapy for the Treatment of Glioblastoma: A Review of the Therapy's History, Efficacy and Application in Humans. *Int. J. Hyperth.* **2018**, 1–13.

(18) Khan, S.; Danish Rizvi, S.; Ahmad, V.; Baig, M.; Kamal, M.; Ahmad, S.; Rai, M.; Zafar Iqbal, A. N.; Mushtaq, G.; Khan, M. Magnetic Nanoparticles: Properties, Synthesis and Biomedical Applications. *Curr. Drug Metab.* **2015**, *16*, 685–704.

(19) magforce®.

(20) Rosensweig, R. E. Heating Magnetic Fluid with Alternating Magnetic Field. *J. Magn. Magn. Mater.* **2002**, *252*, 370–374.

(21) Yang, Y.; Pei, Z.; Zhang, X.; Tao, L.; Wei, Y.; Ji, Y. Carbon Nanotube–vitrimer Composite for Facile and Efficient Photo-Welding of Epoxy. *Chem. Sci.* **2014**, *5* (9), 3486.

(22) Yang, Y.; Pei, Z.; Zhang, X.; Tao, L.; Wei, Y.; Ji, Y. Correction: Carbon Nanotube–vitrimer Composite for Facile and Efficient Photo-Welding of Epoxy. *Chem. Sci.* **2017**, *8* (3), 2464–2464.

(23) Kiesewetter, M. K.; Scholten, M. D.; Kirn, N.; Weber, R. L.; Hedrick, J. L.; Waymouth, R. M. Cyclic Guanidine Organic Catalysts: What Is Magic About Triazabicyclodecene? *J. Org. Chem.* **2009**, *74* (24), 9490–9496.

(24) Altuna, F.; Hoppe, C.; Williams, R. Epoxy Vitrimers: The Effect of Transesterification Reactions on the Network Structure. *Polymers (Basel).* **2018**, *10* (1), 43.

(25) Altuna, F. I.; Antonacci, J.; Arenas, G. F.; Pettarin, V.; Hoppe, C. E.; Williams, R. J. J. Photothermal Triggering of Self-Healing Processes Applied to the Reparation of Bio-Based Polymer Networks. *Mater. Res. Express* **2016**, *3* (4), 45003.

(26) Zhang, H.; Zhao, Y. Polymers with Dual Light-Triggered Functions of Shape Memory and Healing Using Gold Nanoparticles. *ACS Appl. Mater. Interfaces* **2013**, *5* (24), 13069–13075.

(27) Wang, Z.; Li, Z.; Wei, Y.; Ji, Y. Gold Nanospheres Dispersed Light Responsive Epoxy Vitrimers. *Polymers (Basel).* **2018**, *10* (1), 65.

(28) Leonardi, A. B.; Puig, J.; Antonacci, J.; Arenas, G. F.; Zucchi, I. A.; Hoppe, C. E.; Reven, L.; Zhu, L.; Toader, V.; Williams, R. J. J. Remote Activation by Green-Light Irradiation

of Shape Memory Epoxies Containing Gold Nanoparticles. *Eur. Polym. J.* **2015**, *71*, 451–460.

(29) Puig, J.; Zucchi, I. A.; Hoppe, C. E.; López-Quintela, M. A.; Williams, R. J. J. A Modifier That Enables the Easy Dispersion of Alkyl-Coated Nanoparticles in an Epoxy Network. *Colloid Polym. Sci.* **2013**, *291* (7), 1677–1682.

(30) Pei, Z.; Yang, Y.; Chen, Q.; Wei, Y.; Ji, Y. Regional Shape Control of Strategically Assembled Multishape Memory Vitrimers. *Adv. Mater.* **2016**, *28* (1), 156–160.

(31) Yang, Y.; Pei, Z.; Li, Z.; Wei, Y.; Ji, Y. Making and Remaking Dynamic 3D Structures by Shining Light on Flat Liquid Crystalline Vitrimer Films without a Mold. *J. Am. Chem. Soc.* **2016**, *138* (7), 2118–2121.

(32) Yang, Z.; Wang, Q.; Wang, T. Dual-Triggered and Thermally Reconfigurable Shape Memory Graphene-Vitrimer Composites. *ACS Appl. Mater. Interfaces* **2016**, *8* (33), 21691–21699.

(33) Chen, Q.; Yu, X.; Pei, Z.; Yang, Y.; Wei, Y.; Ji, Y. Multi-Stimuli Responsive and Multi-Functional Oligoaniline-Modified Vitrimers. *Chem. Sci.* **2017**, *8* (1), 724–733.

(34) Vialle, G.; Di Prima, M.; Hocking, E.; Gall, K.; Garmestani, H.; Sanderson, T.; Arzberger, S. C. Remote Activation of Nanomagnetite Reinforced Shape Memory Polymer Foam. *Smart Mater. Struct.* **2009**, *18* (11), 115014.

(35) He, Z.; Satarkar, N.; Xie, T.; Cheng, Y.-T.; Hilt, J. Z. Remote Controlled Multishape Polymer Nanocomposites with Selective Radiofrequency Actuations. *Adv. Mater.* **2011**, *23* (28), 3192–3196.

(36) Puig, J.; Hoppe, C. E.; Fasce, L. A.; Pérez, C. J.; Piñeiro-Redondo, Y.; Bañobre-López, M.; López-Quintela, M. A.; Rivas, J.; Williams, R. J. J. Superparamagnetic Nanocomposites Based on the Dispersion of Oleic Acid-Stabilized Magnetite Nanoparticles in a Diglycidylether of Bisphenol A-Based Epoxy Matrix: Magnetic Hyperthermia and Shape Memory. *J. Phys. Chem. C* **2012**, *116* (24), 13421–13428.

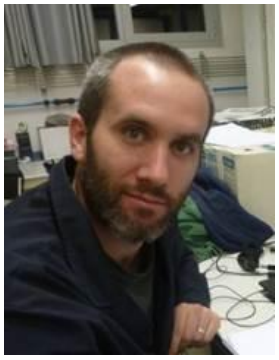

F. I. Altuna es Ing. Químico (UNMdP, 2006) y Dr. en Ciencia de Materiales (UNMdP, 2011). Realizó su tesis doctoral sobre espumas epoxi en la división Ecomateriales del INTEMA, y desde 2012 pertenece a la división Polímeros Nanoestructurados de INTEMA. Actualmente trabaja en la síntesis de polímeros termorrígidos autorreparables con activación remota, bajo la dirección de R. J. J. Williams y C. E. Hoppe

J. Puig es Lic. en Química y Dr. en Ciencia de Materiales. Realizó su tesis doctoral en matrices poliméricas "a medida", para la dispersión y organización de modificadores hidrofóbicos, y desarrollo de materiales funcionales con propiedades tecnológicas de interés. Actualmente es investigadora Asistente del CONICET en la división Polímeros Nanoestructurados (INTEMA), su tema de investigación se basa en la generación de películas nanoestructuradas con propiedades ópticas y térmicas especiales para el desarrollo de ventanas inteligentes.

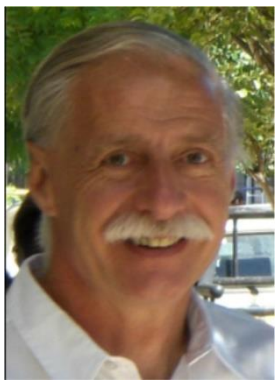

Roberto Williams es investigador superior, actualmente jubilado, del CONICET. Es miembro y fundador del Instituto de Investigaciones en Ciencia y Tecnología de Materiales (INTEMA), especialista en polímeros, con particular énfasis en redes poliméricas entrecruzadas y sus aplicaciones para el desarrollo de materiales funcionales con aplicaciones tecnológicas. El Dr. Williams ha recibido diversas distinciones como el Premio Investigador de la Nación 2011, el Premio Konex de Platino y el Premio Bunge y Born. Es Presidente de la Academia Nacional de Ciencias Exactas, Físicas y Naturales (ANCEFN) y profesor emérito de la UNMdP.

Cristina E. Hoppe es Lic. en Química y doctora en Ciencia de Materiales por la Universidad Nacional de Mar del Plata. Se doctoró en 2004, y a continuación llevó a cabo una estancia posdoctoral de tres años en el grupo de Magnetismo y Nanotecnología de la Universidad de Santiago de Compostela (USC), España. Desde 2008 trabaja en la división Polímeros Nanoestructurados del Instituto de Investigaciones en Ciencia y Tecnología de Materiales (INTEMA) como Investigadora Independiente del CONICET. Sus líneas de trabajo están relacionadas con el diseño, síntesis y propiedades de materiales funcionales basados en sistemas nanoestructurados y redes poliméricas entrecruzadas.

Anales de la Asociación Química Argentina

División Jóvenes Profesionales

Mini-Review

CONDUCTING POLYMERS-BASED ELECTROCHEMICAL PLATFORMS: FROM BIOSENSING TO ENERGY STORAGE

Juliana Scotto,[1,2] Gonzalo E. Fenoy,[1,3] Luciano D. Sappia,[1] Waldemar A. Marmisolle[1,*]

[1]*Instituto de Investigaciones Fisicoquímica Teóricas y Aplicadas (INIFTA) – Departamento de Química – Facultad de Ciencias Exactas – Universidad Nacional de La Plata (UNLP) – CONICET. 64 and 113 –La Plata, Argentina.*

[2] *Instituto de Ciencias de la Salud, Universidad Nacional Arturo Jauretche, Av. Calchaquí 6200, Florencio Varela, Bs. As., Argentina.*

[3] *Instituto de Investigación e Ingeniería Ambiental, Universidad Nacional de San Martín, 25 de mayo y Francia, 1 piso, 1650 Buenos Aires, Argentina.*

[*] *Autor Corresponsal: wmarmi@inifta.unlp.edu.ar, www.softmatter.quimica.unlp.edu.ar*

Resumen Gráfico - Graphical abstract

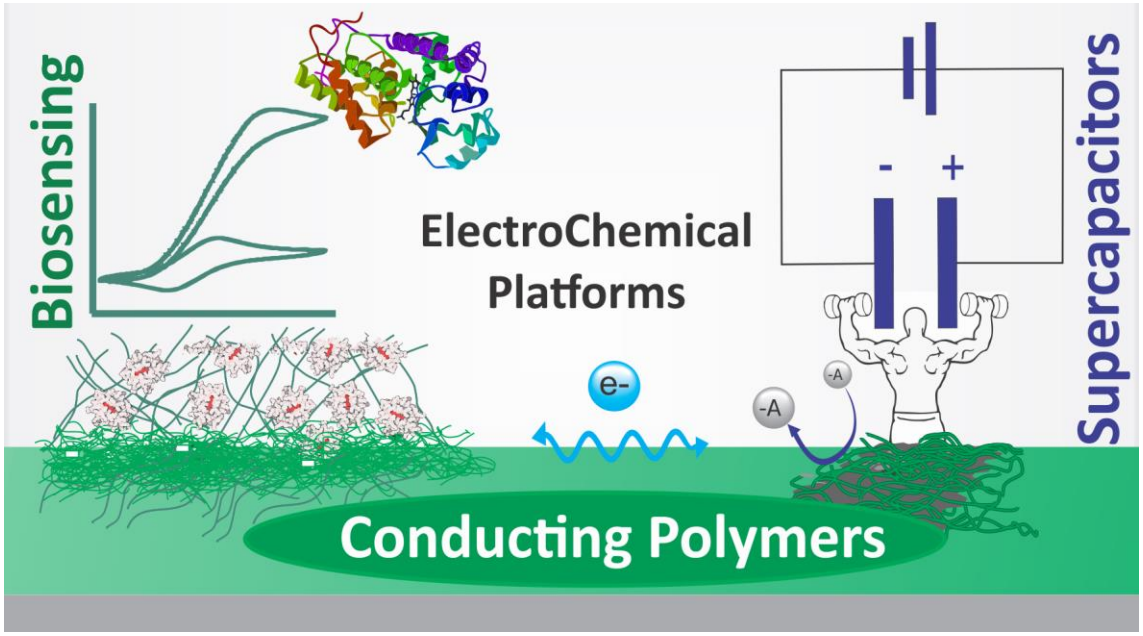

Resumen

A partir su descubrimiento hacia los años 80, los polímeros conductores han sido ampliamente utilizados para la producción de materiales de electrodo en diferentes aplicaciones electroquímicas que van desde el sensado de especies en solución al almacenamiento de energía. La facilidad de síntesis, bajo costo y baja densidad son

algunas de las ventajas del empleo de estos materiales. En particular, su extensa aplicación en dispositivos de biosensado se basa en una serie de ventajas comparativas frente a otro materiales que incluyen la posibilidad de ofrecer entornos moleculares no desnaturalizantes para las proteínas y otras biomoléculas y la capacidad de actuar como transductores fisicoquímicos de las señales químicas en respuestas eléctricas o simplemente mediar la transferencia electrónica entre biomoléculas rédox y las plataformas de sensado. Por otro lado, la naturaleza polielectrolítica y la generación de cargas dependientes del potencial en estos materiales, producen enormes pseudocapacidades que los vuelven adecuados para su utilización en dispositivos de almacenamiento de carga tales como supercapacitores.

Abstract

Since its discovery in the 80´s, Conducting Polymers have been extensively employed for the preparation of electrode materials in different applications from chemical and biochemical sensing to energy storage. Some of the comparative advantages of these materials are the facility of synthesis, low cost and low density.

Particularly, their wide-spread applications in biosensing devices are based on the possibility of providing non-denaturing environments for proteins and other biomolecules and the capacity of acting as physicochemical transductors of chemical signals into electrical out-puts or simply mediating the electron transfer between the biomolecules and the base electrode. On the other hand, the polyelectrolytic nature of conducting polymers and the origin of charges along the polymer chains depending on the applied potential render huge pseudocapacitances, making these materials adequate for the construction of energy storage devices, such as supercapacitors.

Palabras Clave: *Polímeros Conductores, Polianilina, Electroquímica, Sensado, Almacenamiento de Energía.*

Keywords: *Conducting Polymers, Polyaniline, Electrochemistry, Sensing, Energy Storage.*

1. Conducting Polymers

In 1977 Street and co-workers found that the electrical conductivity of films of polymeric sulfur nitride could be increased by bromine oxidation.[1] Some years later,

Heeger and MacDiarmid[‡] applied the same procedure to polyacetylene films $(CH)_n$ yielding a 7 to 12-fold increment in the electrical conductivity.[2,3] In analogy with the doping of semiconductors, this treatment with oxidizing agents was called p-doping (and n-doping for the chemical reduction). The same effect was observed in a series of organic polymers in the subsequent years. Furthermore, similar doping was achieved in the environment of an electrochemical cell, where the doping degree (oxidation degree) can be precisely controlled by electrochemical methods. On the other hand, at the early 80's, the electrochemical polymerization by oxidation of some aromatic monomers as aniline, thiophene and pyrrole was successfully developed, yielding polymer film-modified electrodes.

Nowadays, the polymers that can be reversible oxidized and reduced are referred to as *Electroactive Polymers*.[4] These polymers are usually classified into *Conducting Polymers* (*CPs*) and *Redox Polymers* **(Figure 1)**.[5] Within the first class, they share a common characteristic: they present an extended double bond conjugation and, when they are in a partial oxidation (or reduction) state, they present metallic conductivity. Polyaniline (Pani), polypyrrole (PPy) and polythiophene (Pth) are famous examples of this kind of polymers. During the last 40 years, extensive families of polymers have been developed by employing derivatives of mentioned monomers, such as the case of the PEDOT, synthesized by oxidation of the 3,4-ethylenedioxythiophene.

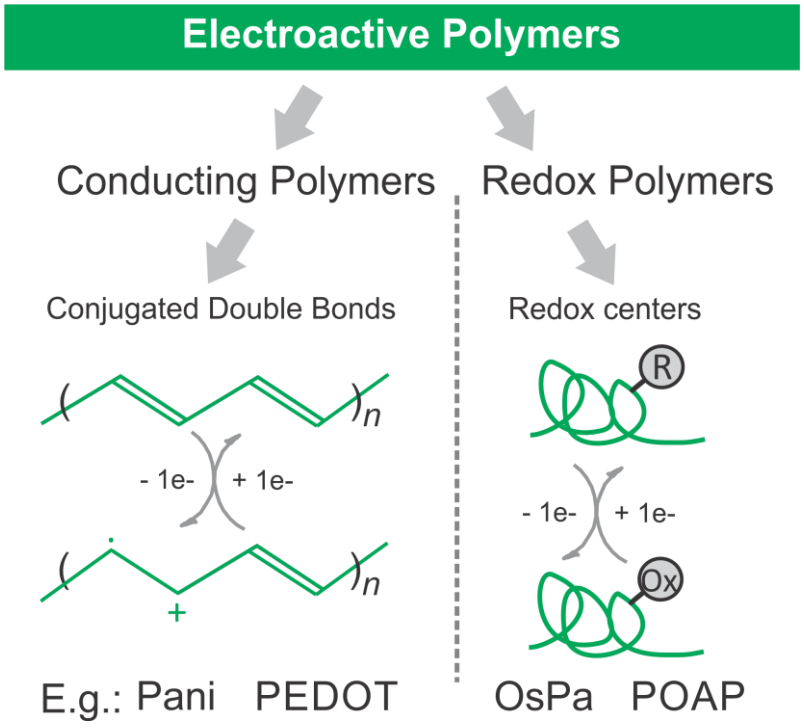

Figure 1. Classification and electrochemical reactions in Electroactive Polymers.

On the other hand, *Redox Polymers* are not conducting materials but they have redox centers in the polymer matrix. These centers can be part of the polymer structure, as in poly-o-aminophenol (POAP),[6] or metallic complexes bound to the polymer chains, as in the case of the osmium complex-modified polyallylamine (OsPA).[7]

2.Pani for Energy Storage Applications

Owing to their excellent electronic and reversible electrochemical properties, CPs have been largely studied for decades.[5,8] Pani has been one of the most investigated CPs as it presents high electronic conductivity, low-cost synthesis and good chemical stability. [9–11] Pani also presents other advantages such as the possibility of further chemical modifications[12] which have propelled its application in different areas.

Pani can be readily obtained by either chemical or electrochemical oxidation of aniline in acidic solutions.[10] The product of the polymerization is an insoluble green solid with high electronic conductivity. This form is called *emeraldine* and it is an intermediate redox state. It can be reduced to *leucoemeraldine* and oxidized to *pernigraniline*.[13,14] The basic structures of the different oxidation states were proposed by MacDiarmid and co-workers in the 80´s.[15] In the leucoemeraldine (L) state, the nitrogen atoms are secondary amines connecting benzenic rings. Leucoemeraldine is usually in its basic form, but at high acidic solutions it becomes protonated (p$Ka \approx 1$)[16] and it is then referred as leucoemeraldine salt (LS). The oxidation of leucoemeraldine leads to the emeraldine form (E), where a quinone-imine structure is obtained by removing two electrons. Emeraldine can exist in its base form (EB) or protonated to the emeraldine salt (ES). Due to its particular chemical and electronic structure, the protonation equilibrium of the backbone nitrogen groups in the emeraldine form is difficult to describe. Moreover, this complex acid base behavior has been found to be dependent on the synthesis[17] and experimental conditions.[17,18] Consequently, a broad dispersion of pK_a values from 3 to 8 has been reported for the emeraldine form. [16,18–20] The protonated emeraldine (emeraldine salt) corresponds to a dicationic structure (bipolaron), which can be internally transformed into a species with radical cations (polarons). In doped Pani, polarons are more stable than bipolarons and they are responsible for the high electronic conductivity.[9,15,21]

Further oxidation of emeraldine yields the pernigraniline form (P), which is unstable in acidic solution.[13,14,22,23] However, the redox transition between the L and E forms is highly reversible in acidic media (**Figure 2**).

The oxidation of leucoemeraldine to emeraldine promotes the generation of mobile charges and requires the ingress of a high proportion of anions in order to maintain the electroneutrality. In fact, the description of the redox response in Pani-like materials is complex as is strongly depends on the pH and the nature of the anions in solution.[24–27] These characteristics have propelled the use of Pani in charge (and energy) storage applications, such as supercapacitors.

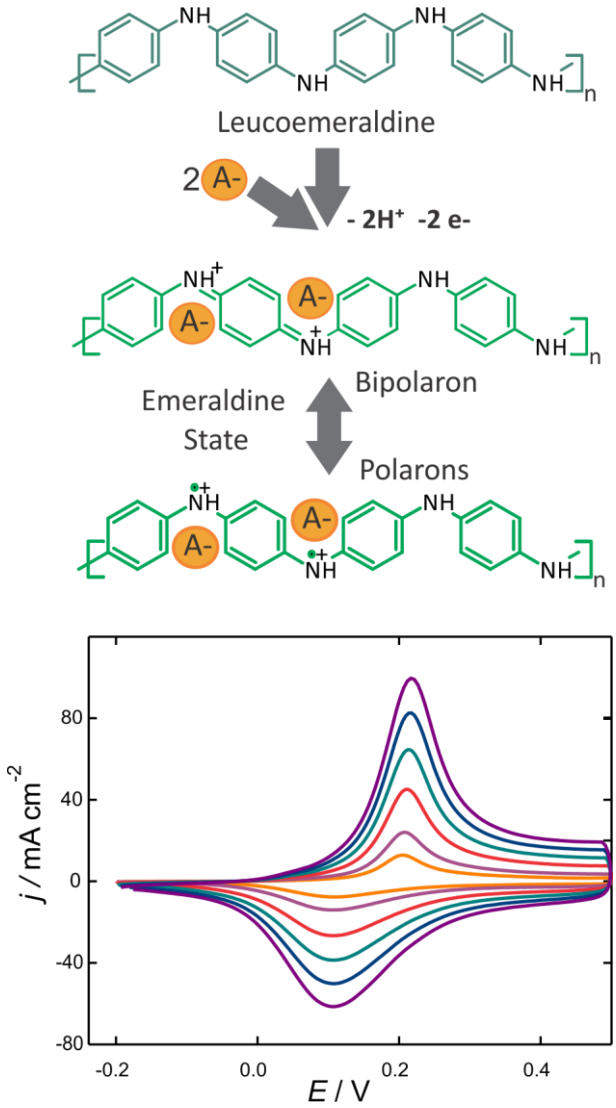

Figure 2. Chemical structures of the first redox transition of Pani. The oxidation implies the ingress of anions from the solution for charge compensation. The voltammetric response of a Pani-modified electrode (50 to 500 mVs^{-1}) in the potential range of this transition is presented at the bottom.

Supercapacitors (SCs) are electrochemical devices able to store charge by a nanometer-scale charge separation between the electrolyte and the electrode material.[28] Frequently, two main mechanisms of charge storage are recognized. In the double-layer mechanism (DL), the charge separation is performed within the so-called electrical double-layer established at the interface between the conducting phase and the electrolyte solution. On the other hand, the charge can be also stored by redox reactions, ion intercalation or ionic sorption promoted by polarization of the electrode. This mechanism involves a faradaic process, yielding the so-called pseudocapacitance, and typically happens in conducting polymers and metal oxides electrodes. Therefore, CPs can store charge not only by a DL mechanism but also by their rapid reversible electrochemical transformations (pseudocapacitance).[29]

Particularly, Pani has become a promising material in energy storage applications as it has one of the highest theoretical specific pseudocapacitances (2000 F g^{-1}) caused by its fast and reversible redox transformations and high surface area.[30] Therefore, Pani has been extensively employed as material for SCs.[31,32]

A serious problem in Pani-based SCs is the mechanical instability caused by the swelling and shrinkage during the doping/dedoping process, which can limit the storage performance and cyclability. This issue can be partially avoided by the incorporation of carbon nanomaterials to create hybrid nanocomposites with enhanced properties. A review on the layer-by-layer integration of Pani and carbon nanomaterials (carbon nanotubes and graphene oxide) for energy storage applications has been recently published.[33]

3.PABA as a versatile building block

Although the electroactivity of Pani is excellent in acidic solution, it becomes poor at pH higher than 3, which represents a clear disadvantage for applications in neutral solutions, such as biosensing. Several strategies have been employed to improve the electroactivity in neutral media; e.g., the incorporation of metal nanoparticles,[34,35] carbon nanomaterials[36–38] or other complex anionic molecules capable of acting as dopants.[39,40] Furthermore, the presence of amine groups in Pani were used in order to confer further chemical functionalization directed to cause an increase in the performance of Pani-containing biodevices. As an example, the formation of a phosphoramidate bond between terminal amino groups and phosphate groups of

artificial single-stranded DNA/RNA oligonucleotides (aptamers), has been employed in a variety of aptasensors.[36,41] In the other approach, the desired functionality can be achieved by employing substituted anilines, whose additional chemical moieties act as self-dopants.[42] An interesting example of substituted polyanilines is the polyaminobenzylamine (PABA), which bears additional pendant amine groups in the structure (**Figure 3**). The protonation of these groups confers additional charges to the polymer structure. Additionally, these pendant primary amines can be easily modified to introduce further chemical moieties or biorecognition elements in a higher extension than that reached in Pani.[43]

Recently, the electrochemical copolymerization of aniline and 3-aminobenzylamine (ABA) has been reported to produce polymer films with higher electroactivity than Pani in neutral solutions.[44] Electrochemically stable films of variable thickness could be obtained by this method. The electroactivity in acid solution was higher for films with a high proportion of aniline, but films obtained from solutions with higher proportion of ABA presented better electrochemical response at neutral pH. The copolymer film-modified electrodes were used for successful mediation for the electro-oxidation of ascorbic acid at pH 7.

On the other hand, a method to obtain water dispersions of polyaminobenzylamine by chemical oxidation of ABA was also described.[45] This procedure does not involve laborious steps, yielding dispersions that remain stable in acidic solutions. The resulting polymer was characterized by diverse spectroscopic techniques and the dispersions were employed for the construction of layer-by-layer assemblies with polyanions. The LbL assemblies presented a linear dependence on the number of deposition cycles, whereas the spectroscopic measurements proved successful integration of the diverse counterparts within the films. These assemblies were found to be electroactive, both in acidic and neutral solutions, as a result of the combination of the doping effect by the polyanions, and the self-doping effect of the protonated amino groups in the PABA backbone. The PABA/polyanions LbL-modified electrodes also showed electrocatalysis of the ascorbic acid oxidation in neutral solutions.

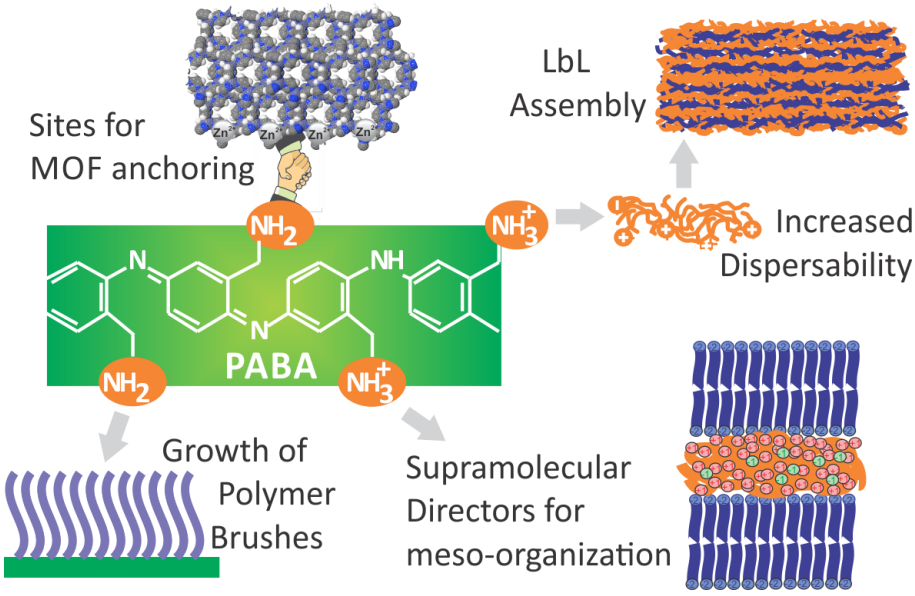

Figure 3. Chemical structure of PABA and schematic representation of the use of this building block in nanoarchitectonics.

This amino-appended polyaniline has resulted to be a versatile building block in electrochemical nanoarchitectonics as it could be satisfactorily integrated into different electroactive platforms (**Figure 3**).

The integration of PABA and a metal organic framework (MOF) for enhancing the oxygen reduction reaction (ORR) was recently demonstrated.[46] In that work, a ZIF-8 microporous film was grown over a PABA-modified electrode. The MOF layer acts as gas reservoir and, via a pre-concentration effect, causes the O_2 to be readily available for the electrochemical reaction of the CP film. The MOF layer was able to provide an efficient pathway for both oxygen diffusion (in the hydrophobic intragrain microporosity) and transport of counterions and solvent (in the intergrain mesoporosity). The extra amino groups in the CP backbone are presumably the responsible for the stable anchoring of the MOF layer via coordination with the zinc ions. The interplay between the electrocatalytic and anchoring properties of PABA and the oxygen storage capabilities of ZIF-8 yielded a new interfacial architecture exhibiting a more efficient response towards the ORR.

Other example of the use of PABA in the design of novel interfacial nanoarchitectures is the anchoring of a polymer brush by surface-initiated atom transfer radical polymerization (SI-ATRP),[47] using the extra amines of an electrochemically synthesized PABA film for the covalent crosslinking of an ATRP initiator. As PABA has extra pendant amino moieties, the grafting of the polyelectrolyte brush poly [2-

(methacryloyloxy)-ethyl-trimethylammonium chloride] (PMETAC) does not affect the backbone nitrogen atoms, which are implicated in the electronic properties. Moreover, as perchlorate anions interact very strongly with the quaternary ammonium pendant groups of PMETAC through ion pairing, the grafting adds the ion-actuation properties of the brush to the modified electrode, keeping the electroactivity. Thus, the conjugation of the electron transfer properties of the conducting polymer with the anion responsiveness of the integrated brush yielded perchlorate actuation of the electrochemical response (**Figure 4**).

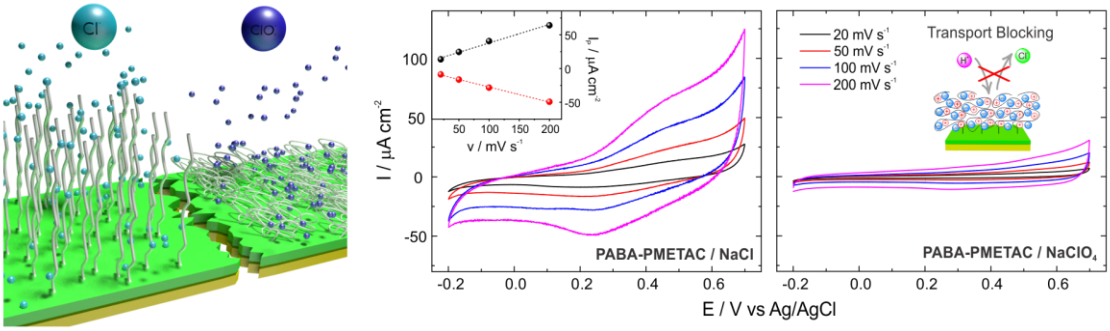

Figure 4. Schematic representation of the reversible conformational changes induced by perchlorate anions on the brush-modified PABA platforms (left) and voltammetric response in the presence and absence of these anions in solution (right).

In a completely different approach, the formation of electrostatic complexes between chemically synthesized PABA and an alkyl-phosphate was employed for the modification of electrodes with self-assembled electroactive polyelectrolyte-surfactant assemblies.[48] The complexes were deposited by spin-coating and the films were extensively characterized by X-ray-based techniques, showing a well-defined lamellar structure, directed by the strong interaction between the phosphate groups and the positive charged amine groups of PABA. These films also presented intrinsic electroactivity as proved by cyclic voltammetry, showing that PABA remains electroactive and ionic transport was still possible across the stratified hydrophobic coatings.

4.PEDOT platforms for biosensing

Conducting polymers-based platforms have been also extensively employed for the construction of biosensors[21] and other biodevices[49] as they can provide an adequate

non-denaturing environment for the immobilization of enzymes and proteins and simultaneously they can act as physicochemical transducer of the chemical signals into a measurable electrical response, or simply mediate the electron transference to the electrode.[21,50,51]

Pani, Ppy, Pth and their derivatives are the most representative polymers employed in the construction of bioelectrochemical devices due to their high electrical conductivity and excellent electrochemical activity, optical properties and chemical and thermal stability.[52] One of the most promising polymers for bioelectronic application is a Pth derivative: poly(3,4-ethylenedioxythiophene) (PEDOT) (**Figure 5**). PEDOT was developed in 1988 at the Bayer AG research laboratories in Germany.[53] It shows high conductivity, good transparency and stability compared with PPy[54] and lower toxicity than Pani and Pth.[55] Moreover, unlike Pani that requires acid media to exhibit good electrochemical activity, PEDOT shows excellent conductivity and electroactivity in neutral solution. These properties combined with a good compatibility with biomolecules, such as enzymes, make PEDOT an appropriated polymer in the design of biosensing platforms. In addition, the remarkable conductivity of PEDOT allows the construction of bioelectrochemical devices without metallic substrates (all- plastic devices).[56–58]

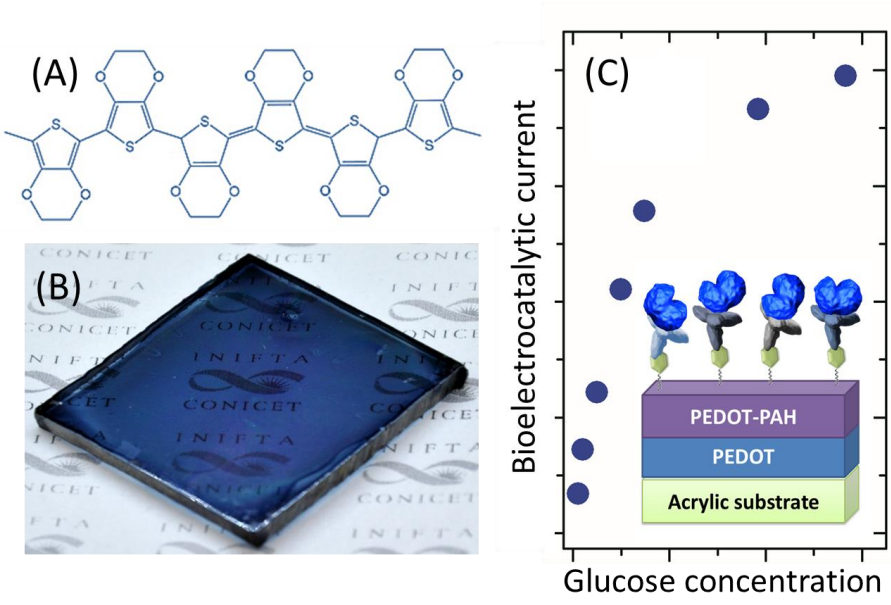

Figure 5. (A) Chemical structure of PEDOT. (B) Image of PEDOT/tosylate-modified plastic substrate. (C) Bioelectrocatalytic current for increasing glucose concentrations for a PEDOT–PAH composite all-plastic electrode modified with concanavalin A and glucose oxidase (scheme).

PEDOT is obtained by oxidative polymerization of 3,4-ethylendioxytiophene (EDOT). There are different methods for the synthesis such as chemical polymerization,[59] electrochemical polymerization,[60] interfacial polymerization,[61] vapor phase polymerization,[62] being the first two the most widely employed. The electrical, mechanical and morphological properties of the resulting polymer depend on the synthesis procedures, reagents and solvents. In particular, the electrochemical deposition is a convenient way to obtain a polymeric-based material in a one-step procedure with superior electrochemical and mechanical properties and it also constitutes a simple method to control the thickness of the film. On the other hand, chemical polymerization is suitable for the large-scale production of materials with selected morphology.

In order to improve the stability and processability of the material, counter-anions are used to dope PEDOT, being the most common dopants polystyrene sulphonate (PSS) and iron/sodium tosylate salts. Commercially available water dispersible PEDOT: PSS was widely employed to fabricate PEDOT-based electrochemical biosensors using different methods to obtain the films such as dip-coating, spin-coating, drop-coating, inkjet-printing and screen-printing.[63] Furthermore, outstanding properties of PEDOT based materials are found when this polymer is combined with different components with synergistic effects. For instance, the incorporation of inorganic nanomaterials shows an improvement in the conductivity and mechanical stability of the films. Metal nanoparticles such as Ag, Au, and Pd have been deposited on the PEDOT surface to obtain platforms with large surface area and leading to an enhancement of the electrochemical response to molecular detection and the immobilization of enzymes in the polymer matrix. On the other hand, in the last years, carbon nanomaterials have received enormous attention because of their unique physicochemical properties. In particular, carbon nanotubes (CNTs), graphene (G), graphene oxide (GO) and reduced graphene oxide (rGO) have been exploited to improve the performance of biosensing platforms with potential applications in health-care sensors. As an example, amperometric enzymatic biosensors for glucose detection were extensively investigated.[64–66] An electrode based on PEDOT nano-fibrous with electrodeposited palladium nanoparticles and immobilized glucose oxidase (GOx) was developed for glucose sensing in a wide linear concentration range.[66] A CNT/PEDOT electrode

incorporating (GOx) and alcohol dehydrogenase was obtained to determine glucose and ethanol concentrations with high sensitivity, showing that the combination of PEDOT and CNTs provides an optimized integration and synergic interaction of these materials.[64] Moreover, in order to obtain a simple and cost-effective biosensor for the determination of ascorbic acid, a one-step electrochemical process was developed for the construction of a PEDOT/G nanocomposite film with large surface area, high electrical conductivity and good biocompatibility. Non-enzymatic sensors were also developed, including Pd-decorated PEDOT nanospheres for H_2O_2 sensing[67] and a PEDOT/graphene oxide nanocomposite with copper nanoparticles, employed in glucose detection with negligible impact from dopamine, ascorbic acid, uric acid, sodium citrate and ethanol.[68]

On the other hand, different redox mediators are usually employed to favor the electron transfer between the sensor active site and the electrode surface.[69–71] Recently, an all-plastic biosensor based on PEDOT and a redox polymer was described.[72] The synergistic combination of CPs and recognition-directed assembly to immobilize redox glycoenzymes was used for the construction of a large-area all- plastic biorecognizable electrode. To this end, PEDOT–poly(allylamine) (PEDOT–PAH) composites were prepared entrapping PAH in the polymer matrix. The PAH amine groups were modified using the divinylsulfone (DVS) cross-linker to anchor concanavalin A (Con A) and glucose oxidase to the composite surface with excellent results. The bioelectrocatalytic oxidation of glucose in the all-plastic platform was compared with the response obtained on a Con A-modified Au electrode with the same assembled, revealing an enhancement of the bioelectrocatalysis when GOx is assembled on the PEDOT–PAH composite (**Figure 5**).

5. Conclusions

Since their discovery, conducting polymers have excited and expanded the field of electrochemistry as they constitute non-expensive stable building blocks for the building up of a variety of electrochemically active components in numerous applications. Due to its particular electronic structure, they arise as light metal-free conducting materials able to be prepared by soft chemical methods, which made them immensely adequate for electrochemical nanoarchitectonics. Moreover, the reversible redox changes in these materials allow their application as active components of charge

storage devices or transducers of electrochemical signals in (bio)sensing platforms. Furthermore, they can be easily derivatized to produce tunable materials with enhanced properties and combined with organic/inorganic nanomaterials to generate more efficient electrode materials.

We have presented a series of examples of interesting electrochemical systems based on the integration of conducting polymers, some of them developed in our laboratory, to illustrate their potential. We hope this work encourages researchers to go deeper into the fascinating world of conducting polymers for electrochemical applications.

Acknowledgments

The authors acknowledge financial support from ANPCyT (PICT-2015-0239), and the Universidad Nacional de La Plata (PPID-X016). J.S., G.E.F. and L.S.S. thank a fellowship from CONICET. W.A.M. is CONICET staff member.

Notes and references

‡ Alan J. Heeger, Alan G. MacDiarmid and Hideki Shirakawa received the Nobel Prize in Chemistry 2000 "for the discovery and development of conductive polymers".

(1) Gill, W. D.; Bludau, W.; Geiss, R. H.; Grant, P. M.; Greene, R. L.; Mayerle, J. J.; Street, G. B. Structure and Electronic Properties of Polymeric Sulfur Nitride SNx Modified by Bromine. *Phys. Rev. Lett.* **1977**, *38* (22), 1305–1308.

(2) Shirakawa, H.; Louis, E. J.; MacDiarmid, A. G.; Chiang, C. K.; Heeger, A. J. Synthesis of Electrically Conducting Organic Polymers: Halogen Derivatives of Polyacetylene, (CH) X. *J. Chem. Soc. Chem. Commun.* **1977**, No. 16, 578.

(3) Chiang, C. K.; Fincher, C. R.; Park, Y. W.; Heeger, A. J.; Shirakawa, H.; Louis, E. J.; Gau, S. C.; MacDiarmid, A. G. Electrical Conductivity in Doped Polyacetylene. *Phys. Rev. Lett.* **1977**, *39* (17), 1098–1101.

(4) Lyons, M. E. G. *Electroactive Polymer Electrochemistry*; Plenum: New York, 1996.

(5) Inzelt, G. *Conducting Polymers: A New Era in Electrochemsitry*, 2nd ed.; Scholz, F., Ed.; Springer-Verlag: Berlin Heidelberg, 2012.

(6) Tucceri, R. Redox Transformation of Poly(o-Aminophenol) (POAP) Film Electrodes under Continuous Potential Cycling. *Procedia Mater. Sci.* **2015**, *8*,

261–270.

(7) Cortez, M. L.; González, G. A.; Ceolín, M.; Azzaroni, O.; Battaglini, F. Self-Assembled Redox Polyelectrolyte-Surfactant Complexes: Nanostructure and Electron Transfer Characteristics of Supramolecular Films with Built-In Electroactive Chemical Functions. *Electrochim. Acta* **2014**, *118* (0), 124–129.

(8) Heinze, J.; Frontana-Uribe, B. A.; Ludwigs, S. Electrochemistry of Conducting Polymers-Persistent Models and New Concepts. *Chem. Rev.* **2010**, *110* (8), 4724–4771.

(9) Bhadra, S.; Khastgir, D.; Singha, N. K.; Lee, J. H. Progress in Preparation, Processing and Applications of Polyaniline. *Prog. Polym. Sci.* **2009**, *34* (8), 783–810.

(10) Ćirić-Marjanović, G. Recent Advances in Polyaniline Research: Polymerization Mechanisms, Structural Aspects, Properties and Applications. *Synth. Met.* **2013**, *177* (3), 1–47.

(11) Stejskal, J.; Trchová, M.; Bober, P.; Humpolíček, P.; Kašpárková, V.; Sapurina, I.; Shishov, M. A.; Varga, M. Conducting Polymers: Polyaniline. In *Encyclopedia of Polymer Science and Technology*; John Wiley & Sons, Inc., 2015.

(12) Jaymand, M. Recent Progress in Chemical Modification of Polyaniline. *Prog. Polym. Sci.* **2013**, *38* (9), 1287–1306.

(13) Kang, E.; Neoh, K. G.; Tan, K. L. Polyaniline: A Polymer with Many Interesting Intrinsic Redox States. *Prog. Polym. Sci.* **1998**, *23* (97), 277–324.

(14) Albuquerque, J. E.; Mattoso, L. H. C.; Balogh, D. T.; Faria, R. M.; Masters, J. G.; MacDiarmid, A. G. A Simple Method to Estimate the Oxidation State of Polyanilines. *Synth. Met.* **2000**, *113* (1–2), 19–22.

(15) Stafström, S.; Brédas, J. L.; Epstein, A. J.; Woo, H. S.; Tanner, D. B.; Huang, W. S.; MacDiarmid, A. G. Polaron Lattice in Highly Conducting Polyaniline: Theoretical and Optical Studies. *Phys. Rev. Lett.* **1987**, *59* (13), 1464–1467.

(16) Marmisollé, W. A.; Florit, M. I.; Posadas, D. Acid-Base Equilibrium in Conducting Polymers. The Case of Reduced Polyaniline. *J. Electroanal. Chem.* **2014**, *734*, 10–17.

(17) Okamoto, H.; Kotaka, T. Structure and Properties of Polyaniline Films Prepared via Electrochemical Polymerization. I: Effect of pH in Electrochemical

Polymerization Media on the Primary Structure and Acid Dissociation Constant of Product Polyaniline Films. *Polymer (Guildf).* **1998**, *39* (18), 4349–4358.

(18) Lindfors, T.; Harju, L. Determination of the Protonation Constants of Electrochemically Polymerized Poly(aniline) and Poly(o-Methylaniline) Films. *Synth. Met.* **2008**, *158* (6), 233–241.

(19) Ping, Z.; Nauer, B. G. E.; Neugebauer, H.; Theiner, J.; Neckel, A. Protonation and Electrochemical Redox Doping Processes of Polyaniline in Aqueous Solutions: Investigations Using in Situ FTIR-ATR Spectroscopy and a New Doping System. *J. Chem. Soc. Faraday Trans.* **1997**, *93* (1), 121–129.

(20) Lindfors, T.; Ivaska, A. Application of Raman Spectroscopy and Sequential Injection Analysis for pH Measurements with Water Dispersion of Polyaniline Nanoparticles. *Anal. Chem.* **2007**, *79* (2), 608–611.

(21) Dhand, C.; Das, M.; Datta, M.; Malhotra, B. D. Recent Advances in Polyaniline Based Biosensors. *Biosens. Bioelectron.* **2011**, *26* (6), 2811–2821.

(22) MacDiarmid, A. G.; Epstein, A. J. Polyanilines: A Novel Class of Conducting Polymers. *Faraday Discuss. Chem. Soc.* **1989**, *88* (0), 317–322.

(23) Huang, W. S.; MacDiarmid, A. G. Optical Properties of Polyaniline. *Polymer (Guildf).* **1993**, *34* (9), 1833–1845.

(24) Scotto, J.; Florit, M. I.; Posadas, D. The Effect of Membrane Equilibrium on the Behaviour of Electrochemically Active Polymers. *J. Electroanal. Chem.* **2016**, *774*, 42–50.

(25) Scotto, J.; Florit, M. I.; Posadas, D. pH Dependence of the Voltammetric Response of Polyaniline. *J. Electroanal. Chem.* **2017**, *785*, 14–19.

(26) Scotto, J.; Inés Florit, M.; Posadas, D. Redox Commuting Properties of Polyaniline in Hydrochloric, Sulphuric and Perchloric Acid Solutions. *J. Electroanal. Chem.* **2018**, No. 2017, #pagerange#.

(27) Scotto, J.; Florit, M. I.; Posadas, D. About the Species Formed during the Electrochemical Half Oxidation of Polyaniline: Polaron-Bipolaron Equilibrium. *Electrochim. Acta* **2018**, *268*, 187–194.

(28) Conway, B. E. *Electrochemical Supercapacitors: Scientific Fundamentals and Technological Applications*; Springer, 1999.

(29) Snook, G. a.; Kao, P.; Best, A. S. Conducting-Polymer-Based Supercapacitor Devices and Electrodes. *J. Power Sources* **2011**, *196* (1), 1–12.

(30) Kumar, N. A.; Baek, J.-B. Electrochemical Supercapacitors from Conducting Polyaniline-Graphene Platforms. *Chem. Commun.* **2014**, *50* (48), 6298–6308.

(31) Gao, Z.; Yang, W.; Wang, J.; Yan, H.; Yao, Y.; Ma, J.; Wang, B.; Zhang, M.; Liu, L. Electrochemical Synthesis of Layer-by-Layer Reduced Graphene Oxide Sheets/polyaniline Nanofibers Composite and Its Electrochemical Performance. *Electrochim. Acta* **2013**, *91*, 185–194.

(32) Sarker, A. K.; Hong, J. D. Layer-by-Layer Self-Assembled Multilayer Films Composed of Graphene/polyaniline Bilayers: High-Energy Electrode Materials for Supercapacitors. *Langmuir* **2012**, *28* (34), 12637–12646.

(33) Marmisollé, W. A.; Azzaroni, O. Recent Developments in the Layer-by-Layer Assembly of Polyaniline and Carbon Nanomaterials for Energy Storage and Sensing Applications. From Synthetic Aspects to Structural and Functional Characterization. *Nanoscale* **2016**, *8* (19), 9890–9918.

(34) Arya, S. K.; Dey, A.; Bhansali, S. Polyaniline Protected Gold Nanoparticles Based Mediator and Label Free Electrochemical Cortisol Biosensor. *Biosens. Bioelectron.* **2011**, *28* (1), 166–173.

(35) Kaushik, A.; Vasudev, A.; Arya, S. K.; Bhansali, S. Mediator and Label Free Estimation of Stress Biomarker Using Electrophoretically Deposited Ag at AgO-Polyaniline Hybrid Nanocomposite. *Biosens. Bioelectron.* **2013**, *50*, 35–41.

(36) Bo, Y.; Yang, H.; Hu, Y.; Yao, T.; Huang, S. A Novel Electrochemical DNA Biosensor Based on Graphene and Polyaniline Nanowires. *Electrochim. Acta* **2011**, *56* (6), 2676–2681.

(37) Feng, X.; Cheng, H.; Pan, Y.; Zheng, H. Development of Glucose Biosensors Based on Nanostructured Graphene-Conducting Polyaniline Composite. *Biosens. Bioelectron.* **2015**, *70*, 411–417.

(38) Ruecha, N.; Rangkupan, R.; Rodthongkum, N.; Chailapakul, O. Novel Paper-Based Cholesterol Biosensor Using Graphene/polyvinylpyrrolidone/polyaniline Nanocomposite. *Biosens. Bioelectron.* **2014**, *52*, 13–19.

(39) Bonastre, A. M.; Sosna, M.; Bartlett, P. N. An Analysis of the Kinetics of Oxidation of Ascorbate at Poly(aniline)-Poly(styrene Sulfonate) Modified Microelectrodes. *Phys. Chem. Chem. Phys.* **2011**, *13* (12), 5365–5372.

(40) Bartlett, P. N.; Wallace, E. N. K. The Oxidation of Ascorbate at Poly(aniline)–poly(vinylsulfonate) Composite Coated Electrodes. *Phys. Chem. Chem. Phys.*

2001, *3* (8), 1491–1496.

(41) Liu, S.; Xing, X.; Yu, J.; Lian, W.; Li, J.; Cui, M.; Huang, J. A Novel Label-Free Electrochemical Aptasensor Based on Graphene-Polyaniline Composite Film for Dopamine Determination. *Biosens. Bioelectron.* **2012**, *36* (1), 186–191.

(42) Deore, B. a; Yu, I.; Freund, M. S. A Switchable Self-Doped Polyaniline: Interconversion between Self-Doped and Non-Self-Doped Forms. *J. Am. Chem. Soc.* **2004**, *126* (1), 52–53.

(43) Marmisollé, W. A.; Irigoyen, J.; Gregurec, D.; Moya, S.; Azzaroni, O. Supramolecular Surface Chemistry: Substrate-Independent, Phosphate-Driven Growth of Polyamine-Based Multifunctional Thin Films. *Adv. Funct. Mater.* **2015**, *25* (26), 4144–4152.

(44) Marmisollé, W. A.; Gregurec, D.; Azzaroni, O.; Moya, S.; Azzaroni, O. Polyanilines with Pendant Amino Groups as Electrochemically Active Copolymers at Neutral pH. *ChemElectroChem* **2015**, n/a--n/a.

(45) Marmisollé, W. A.; Maza, E.; Moya, S.; Azzaroni, O. Amine-Appended Polyaniline as a Water Dispersible Electroactive Polyelectrolyte and Its Integration into Functional Self-Assembled Multilayers. *Electrochim. Acta* **2016**, *210*, 435–444.

(46) Rafti, M.; Marmisollé, W. A.; Azzaroni, O. Metal-Organic Frameworks Help Conducting Polymers Optimize the Efficiency of the Oxygen Reduction Reaction in Neutral Solutions. *Adv. Mater. Interfaces* **2016**, *3* (16), 1600047.

(47) Fenoy, G. E.; Giussi, J. M.; Bilderling, C. von; Maza, E. M.; Pietrasanta, L. I.; Knoll, W.; Marmisollé, W. A.; Azzaroni, O. Reversible Modulation of the Redox Activity in Conducting Polymer Nanofilms Induced by Hydrophobic Collapse of a Surface-Grafted Polyelectrolyte. *J. Colloid Interface Sci.* **2018**, *518*, 92–101.

(48) Lorenzo, A.; Marmisollé, W. A.; Maza, E. M.; Ceolín, M.; Azzaroni, O. Electrochemical Nanoarchitectonics through Polyaminobenzylamine-Dodecyl Phosphate Complexes: Redox Activity and Mesoscopic Organization in Self-Assembled Nanofilms. *Phys. Chem. Chem. Phys.* **2018**, *20* (11).

(49) Desmet, C.; Marquette, C. a.; Blum, L. J.; Doumèche, B. Paper Electrodes for Bioelectrochemistry: Biosensors and Biofuel Cells. *Biosens. Bioelectron.* **2016**, *76*, 145–163.

(50) Ronkainen, N. J.; Halsall, H. B.; Heineman, W. R. Electrochemical Biosensors.

Chem. Soc. Rev. **2010**, *39* (5), 1747.

(51) Iost, R. M.; Crespilho, F. N. Layer-by-Layer Self-Assembly and Electrochemistry: Applications in Biosensing and Bioelectronics. *Biosens. Bioelectron.* **2012**, *31* (1), 1–10.

(52) Shrivastava, S.; Jadon, N.; Jain, R. Next-Generation Polymer Nanocomposite-Based Electrochemical Sensors and Biosensors: A Review. *TrAC - Trends Anal. Chem.* **2016**, *82*, 55–67.

(53) Heywang, G.; Jonas, F. Poly(alkylenedioxythiophene)s—new, Very Stable Conducting Polymers. *Adv. Mater.* **1992**, *4* (2), 116–118.

(54) Yamato, H.; Ohwa, M.; Wernet, W. Stability of Polypyrrole and poly(3,4-Ethylenedioxythiophene) for Biosensor Application. *J. Electroanal. Chem.* **1995**, *397* (1), 163–170.

(55) Groenendaal, L.; Jonas, F.; Freitag, D.; Pielartzik, H.; Reynolds, J. R. Poly(3,4-Ethylenedioxythiophene) and Its Derivatives: Past, Present, and Future. *Adv. Mater.* **2000**, *12* (7), 481–494.

(56) Shim, N. Y.; Bernards, D. A.; Macaya, D. J.; DeFranco, J. A.; Nikolou, M.; Owens, R. M.; Malliaras, G. G. All-Plastic Electrochemical Transistor for Glucose Sensing Using a Ferrocene Mediator. *Sensors* **2009**, *9* (12), 9896–9902.

(57) Gualandi, I.; Marzocchi, M.; Scavetta, E.; Calienni, M.; Bonfiglio, a.; Fraboni, B. A Simple All-PEDOT:PSS Electrochemical Transistor for Ascorbic Acid Sensing. *J. Mater. Chem. B* **2015**, *3* (33), 6753–6762.

(58) Meng, W.; Ge, R.; Li, Z.; Tong, J.; Liu, T.; Zhao, Q.; Xiong, S.; Jiang, F.; Mao, L.; Zhou, Y. Conductivity Enhancement of PEDOT:PSS Films via Phosphoric Acid Treatment for Flexible All-Plastic Solar Cells. *ACS Appl. Mater. Interfaces* **2015**, *7* (25), 14089–14094.

(59) Yoon, H.; Chang, M.; Jang, J. Formation of 1D Poly(3,4-ethylenedioxythiophene) Nanomaterials in Reverse Microemulsions and Their Application to Chemical Sensors. *Adv. Funct. Mater. 17* (3), 431–436.

(60) Xu, G.; Wang, W.; Li, B.; Luo, Z.; Luo, X. A Dopamine Sensor Based on a Carbon Paste Electrode Modified with DNA-Doped poly(3,4-Ethylenedioxythiophene). *Microchim. Acta* **2015**, *182* (3–4), 679–685.

(61) Zuo, Y.; Xu, J.; Zhu, X.; Duan, X.; Lu, L.; Gao, Y.; Xing, H.; Yang, T.; Ye, G.; Yu, Y. Poly(3,4-Ethylenedioxythiophene) Nanorods/graphene Oxide

Nanocomposite as a New Electrode Material for the Selective Electrochemical Detection of Mercury (II). *Synth. Met.* **2016**, *220*, 14–19.

(62) Spain, E.; Keyes, T. E.; Forster, R. J. DNA Sensor Based on Vapour Polymerised Pedot Films Functionalised with Gold Nanoparticles. *Biosens. Bioelectron.* **2013**, *41*, 65–70.

(63) Wen, Y.; Xu, J. Scientific Importance of Water-Processable PEDOT–PSS and Preparation, Challenge and New Application in Sensors of Its Film Electrode: A Review. *J. Polym. Sci. Part A Polym. Chem.* **2017**, *55* (7), 1121–1150.

(64) Barsan, M. M.; Pifferi, V.; Falciola, L.; Brett, C. M. A. New CNT/poly(brilliant Green) and CNT/poly(3,4-Ethylenedioxythiophene) Based Electrochemical Enzyme Biosensors. *Anal. Chim. Acta* **2016**, *927*, 35–45.

(65) Nien, P.; Huang, M.; Chang, F.; Ho, K. Integrating an Enzyme-Entrapped Conducting Polymer Electrode and a Prereactor in a Microfluidic System for Sensing Glucose. *Electroanalysis* **2008**, *20* (6), 635–642.

(66) Santhosh, P.; Manesh, K. M.; Uthayakumar, S.; Komathi, S.; Gopalan, A. I.; Lee, K.-P. Fabrication of Enzymatic Glucose Biosensor Based on Palladium Nanoparticles Dispersed onto poly(3,4-Ethylenedioxythiophene) Nanofibers. *Bioelectrochemistry* **2009**, *75* (1), 61–66.

(67) Jiang, F.; Yue, R.; Du, Y.; Xu, J.; Yang, P. A One-Pot "green" Synthesis of Pd-Decorated PEDOT Nanospheres for Nonenzymatic Hydrogen Peroxide Sensing. *Biosens. Bioelectron.* **2013**, *44*, 127–131.

(68) Hui, N.; Wang, W.; Xu, G.; Luo, X. Graphene Oxide Doped poly(3,4-Ethylenedioxythiophene) Modified with Copper Nanoparticles for High Performance Nonenzymatic Sensing of Glucose. *J. Mater. Chem. B* **2015**, *3* (4), 556–561.

(69) Scavetta, E.; Mazzoni, R.; Mariani, F.; Margutta, R. G.; Bonfiglio, A.; Demelas, M.; Fiorilli, S.; Marzocchi, M.; Fraboni, B. Dopamine Amperometric Detection at a Ferrocene Clicked PEDOT:PSS Coated Electrode. *J. Mater. Chem. B* **2014**, *2* (19), 2861–2867.

(70) García-Hernández, C.; García-Cabezón, C.; Martín-Pedrosa, F.; De Saja, J. A.; Rodríguez-Méndez, M. L. Layered Composites of PEDOT/PSS/nanoparticles and PEDOT/PSS/phthalocyanines as Electron Mediators for Sensors and Biosensors. *Beilstein J. Nanotechnol.* **2016**, *7*, 1948–1959.

(71) Atta, N. F.; Galal, A.; Ali, S. M.; Hassan, S. H. Electrochemistry and Detection of Dopamine at a poly(3,4-Ethylenedioxythiophene) Electrode Modified with Ferrocene and Cobaltocene. *Ionics (Kiel).* **2015**, *21* (8), 2371–2382.

(72) Sappia, L. D.; Piccinini, E.; Marmisollé, W.; Santilli, N.; Maza, E.; Moya, S.; Battaglini, F.; Madrid, R. E.; Azzaroni, O. Integration of Biorecognition Elements on PEDOT Platforms through Supramolecular Interactions. **2017**, *1700502*, 1–11.

Juliana Scotto studied Chemistry at Universidad Nacional de La Plata and she got a PhD in Chemistry in 2016. She is currently a postdoctoral student at Soft Matter Laboratory in INIFTA working on the design of biosensing platforms based on conducting polymers. Also, she carries out teaching and research activities at Universidad Nacional Arturo Jauretche.

Gonzalo E. Fenoy was born in Bragado, Bs. As. He got his Degree in Chemistry in 2015 (UNLP). He is currently PhD student of the UNSAM and CONICET fellow at INIFTA-UNLP. He is working on the integration of conducting polymers and nanomaterials for energy storage and sensing applications.

Luciano Sappia was born in Tucumán, Argentina. He is currently a Post-Doctoral research fellow in the Soft Matter Laboratory in the Instituto de Investigaciones Fisicoquímicas Teóricas y Aplicadas (INIFTA, UNLP-CONICET). Dr. Sappia obtained his PhD and his degree in Biomedical Engineering from the National University of

Tucumán (Argentina). His work is focused in the development of biosensing platforms using the conducting polymer PEDOT.

Waldemar A. Marmisollé was born in Junín, Bs. As., Argentina. He studied Chemistry and he got his PhD in Chemistry from the Universidad Nacional de La Plata in 2011. He is currently a fellow member of CONICET working at the Soft Matter Laboratory in the Instituto de Investigaciones Fisicoquímicas Teóricas y Aplicadas (INIFTA, UNLP-CONICET). His research interests include conducting polymers and soft matter electrochemistry.

Anales de la Asociación Química Argentina

División Jóvenes Profesionales

Mini-Review

POLYELECTROLYTE MULTILAYERS FOR ENHANCING CELL ADHESION AND POTENTIAL APPLICATIONS IN TISSUE ENGINEERING

Nicolás E Muzzio[1,2], Miguel A Pasquale[1], Sergio E Moya[2,*]

[1] *Instituto de Investigaciones Fisicoquímicas Teóricas y Aplicadas (INIFTA), (UNLP, CONICET), Sucursal 4, Casilla de Correo 16, 1900 La Plata, Argentina*

[2] *Soft Matter Nanotechnology group, CIC biomaGUNE, Paseo Miramón 182 C, 20009 San Sebastián, Gipuzkoa, Spain*

* *Autor Corresponsal: smoya@cicbiomagune.es*

Resumen Gráfico - Grafical Abstract

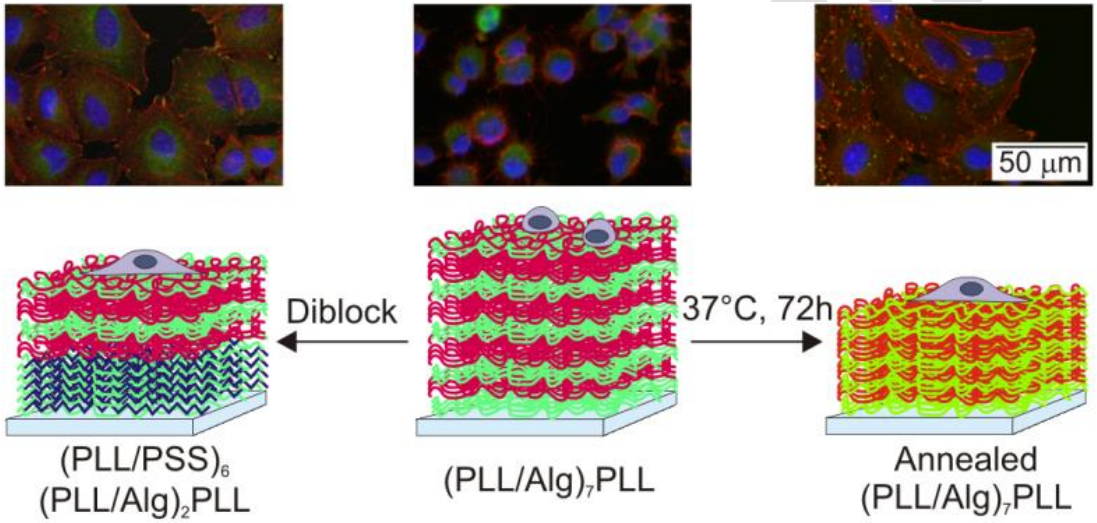

Resumen

Las multicapas de polielectrolitos (MPEs) ensambladas mediante la técnica de Capa por Capa (CpC) ofrecen múltiples opciones para la ingeniería de superficies sin hacer uso de la química covalente. Recientemente, las MPEs han recibido atención como un medio de desarrollar matrices e implantes capaces de promover la adhesión celular, la migración y la diferenciación. En esta revisión se presentará el estado del arte en el uso de multicapas de polielectrolitos para mejorar la adhesión celular. En particular, se mostrarán las diferentes estrategias desarrolladas en nuestro grupo combinando polímeros sintéticos y biológicos, y utilizando el recocido térmico para cambiar las propiedades de estos materiales.

Abstract

Polyelectrolyte multilayers (PEMs) assembled by de Layer by Layer (LbL) technique offer multiple possibilities for surface engineering as an alternative to covalent chemistry. PEMs have recently attracted attention as a mean to engineer scaffolds and implants to make their interface with tissue more amenable for cell adhesion, migration and differentiation. In this review we will present the state of the art on the use of polyelectrolyte multilayers for enhancing cell adhesion. In particular, we will show the different

approaches followed in our group combining synthetic and bio polymers, and the use of thermal annealing.

Palabras Clave: *Multicapas de polielectrolitos, técnica capa a capa, polielectrolitos biológicos, adhesión celular, recocido térmico.*

Keywords: *Polyelectrolyte multilayers, Layer by Layer technique, biological polyelectrolytes, cell adhesion, thermal annealing.*

1. Introduction.

Cell adhesion is a key process in many physiological and pathological processes such as morphogenesis,[1] wound healing,[2] microorganisms infections,[3] and cancer progression.[4] Controlling cell adhesion is also a fundamental issue in the biological and biomedical fields.[5] Different requisites for cell adhesion are needed for diverse types of applications.[6] For instance, for biomaterials that have to interact with blood the adhesion of cells and plasma proteins must be prevented to avoid thrombosis and embolism, but materials used in tissue regeneration are required to act as adherent substrates that first promote cell adhesion and then migration, proliferation and eventually differentiation.

Cells can sense a set of complex biological and physicochemical signals and can integrate them to change their dynamic state.[7] Thus, cell adhesion can be largely affected by the physicochemical properties at the surface of the substrates, such as surface charge and energy, wettability, roughness and stiffness.[7,8] Several strategies like plasma etching,[9] Langmuir-Blodgett,[10] or polymer grafting,[11] have been developed to control cell adhesion by modifying the chemistry, topography and mechanical properties of the substrate interacting with cells. These modifications impact on the interaction of the cell with the substrate material while the latter retains its bulk properties.[12]

Introduced in the 90s by Moehwald, Lvov and Decher, the layer-by-layer (LbL) assembly of polyelectrolyte multilayers provides a simple, versatile and cost-effective technique for the non covalent modification of surfaces and implants and the engineering of scaffolds among other applications.[5,13,14] The LbL assembly is driven by the electrostatic interactions between oppositely charged polyelectrolyte and entropic considerations.[15] By means of the LbL technique, oppositely charged polyelectrolytes (PEs) are sequentially assembled on top of a planar or colloidal charged surface to create a thin polyelectrolyte film, the polyelectrolyte multilayers (PEMs), with thickness and composition controlled in the vertical direction.[16] In addition to synthetic or natural polyelectrolytes,[16,17] nanoparticles,[18] lipid vesicles,[19] biomolecules,[20] and even cells[21] can be used as building blocks provided that they interact with previous and subsequent assembled layers electrostatically or by other type of interactions (i.e., hydrogen bonding, hydrophobic or host-guest interactions).[15] Intrinsic properties of the building

blocks -such as molecular weight of polymers, charge density or polarity- and assembly conditions -such as temperature, ionic strength or pH- can affect the amount of the polymer assembled and the characteristics of the assembled polyelectrolyte layer, i.e. thickness, density, mechanical properties, etc. These physicochemical characteristics of PEMs have a significant impact on cell adhesion and functions.[12]

PEMs fabricated from bio polyelectrolytes, such as chitosan (Chi), hyaluronic acid (HA), alginate (Alg), poly-L-lysine (PLL), among others are very appealing for the modification of surfaces for biological and biomedical applications due to their expected biocompatibility and biodegradability.[22] These PEMs form a cushion on which proteins, growth factors, peptide sequences and other biomolecules can be assembled, controlling cell functionalities such as cell adhesion, migration and proliferation.[14] Moreover, PEMs offer an appropriate mean to mimic the extracellular matrix by incorporation of gradients in their physicochemical properties, which would induce a spatial dependence of cell functionalities.[23] Though PEMs composed of bio polyelectrolytes are very promising materials to be used in tissue engineering and regenerative medicine, they present some limitations, such as poor mechanical properties that tend to prevent cell adhesion.[17]

In this review, we will present the state of the art on the use of polyelectrolyte multilayers for enhancing cell adhesion. We will firstly review the advantages and limitations of the use of synthetic and bio polyelectrolytes, and the impact of the PEM composition on cell adhesion. Then, we will comment different approaches for tuning cell adhesion on PEMs. In particular, we will show two strategies followed in our group based on the combination of synthetic and biopolymers and on the use of thermal annealing. Finally, we will present some strategies to spatially control the physicochemical properties of the PEMs to guide cell adhesion.

2. Cell adhesion on biological and synthetic PEMs

The nature of each component in PEMs, i.e., the polycation and the polyanion composition is one of the factors that determines the physicochemical properties of the final multilayer and, in consequence, its behavior towards cell adhesion. Though there is a huge variety of synthetic and biological polyelectrolytes, each group has a certain number of characteristics.[17] Synthetic polyelectrolytes offer a large choice of chemistries, structures and charge densities. They are susceptible to chemical modifications and can be used in large ranges of pH and ionic strength. Usually, synthetic polyelectrolytes are abundant, cheap and available with highly controlled quality. On the other hand, they are generally non-biodegradable or may have harmful degradation products. Biological polyelectrolytes are biocompatible and naturally degraded by

different kinds of enzymes.[24] As natural constituents, they have interesting structural and functional properties, such as interaction with specific cell receptors or bioactive molecules. Bio polyelectrolytes have, however, some drawbacks, such as a limited pH and ionic strength stability and chemical modifications can be particularly difficult. PEMs made of bio polyelectrolytes tend to render highly hydrated and soft materials that prevent cell adhesion.[14,25,26]

Cell adhesion on PEMs of different composition was assessed in several works, using purely natural, purely synthetic and combined multilayers. Chondrocyte cells adhesion on purely natural Chi/HA films depended on the number of layers and the surface coverage grade.[27] Mesenchymal stromal cells did not adhere to PLL/HA multilayer films with 3, 6 or 9 bilayers.[28] C2C12 myoblasts adhered poorly to $(PLL/HA)_{12}$ films in comparison to glass.[29] The adhesion of human chondrosarcoma cells on poly-L-lysine/poly-L-glutamic multilayer films was also poor.[30] $(Heparin/Collagen)_{10}$ multilayer films reduced the initial adhesion of human bone marrow mesenchymal stem cells whilst stimulated cellular differentiation and mineralization.[31] Adhesion experiments have been also performed on PEMs composed of purely synthetic polyelectrolytes. Poly(sodium 4-styren sulfonate)/poly (allylamine hydrochloride) (PSS/PAH) films presented different behaviors towards C2C12 cells adhesion, proliferation and differentiation depending on the composition of the terminal layer, the number of layers or the molecular weight of the PSS.[32] Cell mortality is favored on PAH-terminated multilayers, probably due to the interaction of the positive amine groups with the negative cell membranes. Poly(allylamine hydrochloride)/poly (acrylic acid) $(PAH/PAA)_9$ films terminated in PAH or PAA were tested with normal, noncancerous fibrocystic disease and cancerous human breast epithelial cell lines.[33] Cell spreading area and morphology depended both on the cell line and on the composition of the last layer. Though the spreading area was poor for both $(PAH/PAA)_9$ and $(PAH/PAA)_9PAH$ films, it was slightly larger for the last one. In a study with combined multilayers composed of PLL and PSS it was found that photoreceptor cell viability was less favorable on PSS terminated films than on PLL ones.[34]

All these articles addressed the adhesion or proliferation of eukaryotic cells on PEMs with distinct chemical composition. The different cell lines and assembly conditions of the multilayers such as pH, ionic strength or number of layer makes hard to compare these studies and to draw clear conclusions of the effect of the chemistry on cell behavior. We reported a systematic study about the impact of the chemistry of PEMs on A549 cell adhesion and proliferation.[16] PEMs of different chemical compositions were obtained by assembling natural polycations and polyanions (PLL; HA; Alg; dextran sulfate, Dex) with the synthetic ones (PAH; PSS; PAA; polyethylenimine, PEI; poly(dyallyldimethylammonium chloride), PDAD). All the multilayers

had the structure (Polycation/Polyanion)$_7$Polycation and were assembled at the same pH and ionic strength. Images of A549 cells, the average cell spreading area and the duplication rate on several of the evaluated PEMs are shown in Figure 1. The average cell spreading area was smaller on PEMs assembled with the natural polyanions HA, Alg and Dex than on PEMs assembled with the synthetic PSS, except when the polycation was PDAD (Fig 1b). Indeed, on PDAD composed PEMs cells exhibited scarce adhesion for all polyanions, probably due to its toxicity.[35,36] For PEMs with PSS, the average cell spreading areas were similar to those obtained for cells adhered on glass.

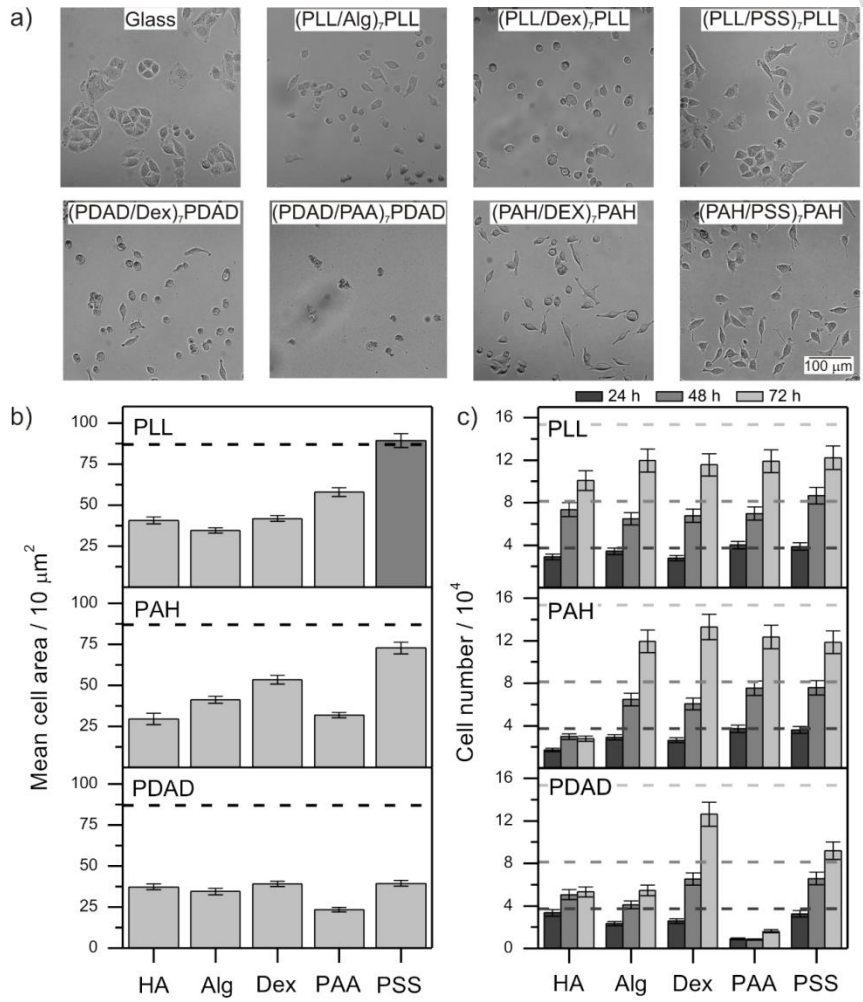

Figure 1. a) Images of A549 cells adhering on glass and purely natural (PLL/Alg, PLL/Dex), purely synthetic (PDAD/PAA, PAH/PSS) and combined (PLL/PSS, PDAD/Dex, PAH/Dex) PEMs. **b)** Mean cell spreading area for A549 cells on PEMs of different composition. For each PEM the average cell adhesion areas were assigned to be smaller (light gray), equal (gray) or larger (dark gray) than on glass employing the ANOVA and Fisher test with 0.05 significance. **c)** Cell proliferation of A549 cells on PEMs coated glass substrates measured by MTT. Cell number was measured after culturing for 24, 48 and 72 h, as indicated in the figure. Dashed lines in b) and c) correspond to the values obtained on glass.

The larger spreading area on PSS based PEMs is consistent with the fact that PSS would increase the stiffness of the multilayer,[37] enhancing cell adhesion. Cell adhesion on PEMs with PAA depended on the polycation. While with the natural PLL the average spreading area was larger than that obtained from PEMs assembled with natural polyanions, with PAH or PDAD the spreading area was lower. PAA retains a large amount of water which makes it a relatively soft material and unsuitable for proper cell adhesion.[38] In that work, we assessed cell proliferation with the methylthiazolyldiphenyl-tetrazolium bromide (MTT) assay 24, 48 and 72 h after seeding on glass and on the different PEMs tested (Fig 1c).

Cell proliferation of cells seeded on all the PEMs was smaller than for cells adhered on glass. Three distinct behaviors for cell proliferation can be distinguished: (i) cell number increased exponentially on glass, PLL/PAA and PEMs assembled with the natural Alg and Dex as polyanions and all tested polycations except PDAD/Alg. (ii) Cell number increased linearly with time on PDAD/Alg multilayers and PEMs with the synthetic PSS as polyanion, except PDAD/PSS. (iii) The rate of cell proliferation diminished with time on PLL/HA, PAH/HA and PEMS assembled with PDAD as polycation, except PDAD/Dex.

To summarize, PEM composition affects cell adhesion and proliferation differently. Cell adhesion on PEMs composed of biological polyelectrolytes was poorer than on glass or on many PEMs with synthetic polyelectrolytes, especially with PSS. On the other hand, cell proliferation was better on natural Alg or Dex based PEMs than on synthetic based PEMs.

3. Strategies to tune cell adhesive properties of PEMs

The development of simple strategies to properly change the physicochemical properties of PEMs made of biological polyelectrolytes without compromising film biocompatibility is fundamental to tune their behavior toward cell adhesion. As diverse cell types preferentially adhere to stiff surfaces and PEMs made from biopolymers usually have low elastic modulus several strategies aim to improve the films mechanical properties have been proposed.

Chemical cross-linking of the multilayers provides stiffness to the PEMs to a degree that correlates with the concentration of cross-linker agent used, leading to an enhancement on cell adhesion. This strategy has been used to enhance the adhesion of placenta and stromal derived mesenchymal stem cells on $(PLL/HA)_9PLL$ films.[28] Preosteoblast and rat skin fibroblast adhesion was also improved on cross-linked Chi/Alg films.[39] The presence of photosensitive groups in one of the polyelectrolytes of the multilayers has been used for photo cross-linking, as an alternative to chemical cross-linking. UV irradiated PEMs composed of PLL and vinylbenzene-grafted hyaluronans showed improved C2C12 cell adhesion in comparison to standard PLL/HA films.[40] Other post-assembly treatments, such as immersion of the PEMs in

concentrated salt solution, has been shown to affect film properties and cell adhesion.[41] Another way to improve the mechanical properties of soft PEMs is the addition of nanoparticles. The mechanical reinforcement of HA/PLL multilayers increases the film Young's modulus in an order of magnitude with a concomitant enhancement of mouse fibroblasts adhesion.[18] Cell adhesion has also been improved with the combination of different blocks of PEMs. HT29 cell adhesion gradually increased when soft natural PLL/HA films were capped with PSS or blocks made of one or two bilayers of PSS/PAH.[42] This fact was attributed to an increase in the elastic module due to the penetration of the PSS into the underlying film.[43]

The use of cross-linking agents, nanoparticles or capping with synthetic polyelectrolytes have the disadvantage that they may not be fully biocompatible. We have reported two strategies to promote cell adhesion while retaining biocompatibility: the use of blocks of polyelectrolytes of different stiffnesses,[16] and the modification of the physicochemical properties of PEMs by thermal annealing.[44–47]

3.1. Di-block PEMs for the enhancement of cell adhesion

With the aim of improving cell adhesion on natural biocompatible films, PEMs were assembled in the form of two blocks with different polyelectrolyte combinations (Fig 2a). The first or inner block was composed of PSS and PLL to reinforce the film mechanical properties, and the outer block was constituted of natural biocompatible polyelectrolytes, like PLL/Alg that displays an exponential like cell proliferation curve (Fig 1c). In this way, in contrast with the capping strategy,[42,43] the top layers of the film facing the cells would be biocompatible.

The assembly of the $(PLL/PSS)_6$ block, $(PLL/Alg)_7PLL$ and $(PLL/Alg)_4PLL$ on top of a $(PLL/PSS)_6$ block was followed by means of the quartz crystal microbalance with dissipation (QCM-D) technique (Figure 2b). Data indicate a rather supralineal growth for the PLL/PSS and the PLL/Alg PEMs assembled on top of glass. The growth of the $(PLL/Alg)_7PLL$ multilayer on top of the PLL/PSS block follows a fairly lineal trend. Thus, the PLL/PSS block underneath affects the growth of the subsequent PLL/Alg block. This fact can also be observed in the atomic force microscopy (AFM) images (Figure 2c). The PLL/PSS PEM is smooth, and this smoothness is retained after the assembly of the PLL/Alg top block. The topography of this PLL/Alg capped film is different from the pure and rough PLL/Alg PEM, highlighting the influence of the inner block of PLL/PSS on the assembly of PLL/Alg layers. Both QCM and AFM data are consistent with the diffusion of the polyelectrolytes throughout the film producing an interdigitated multilayer (Figure 2b).[48,49]

Cell adhesion on $(PLL/Alg)_nPLL$ PEMs (with $1<n<4$) was greatly improved when the polyelectrolytes were assembled on top of a $(PLL/PSS)_6$ block, forming a di-block structure namely $(PLL/PSS)_6(PLL/Alg)_nPLL$ (Figure 3). Fluorescence images (Figure 3a) shows that cells seeded on glass, $(PLL/PSS)_7PLL$ and di-block PEMs exhibit a good cytoskeleton spreading (red) with focal contacts formation (green). In contrast, cells seeded on $(PLL/Alg)_7PLL$ spread poorly and present a diffuse fluorescence image. The average A549 cell spreading area on $(PLL/Alg)_2PLL$ or $(PLL/Alg)_7PLL$ was less than a half of that obtained from cells on glass (Figure 3b). Interestingly, cells seeded on di-block PEMs with n=1 or 2 developed average spreading areas statistically larger than on glass or $(PSS/PLL)_7PLL$ films.

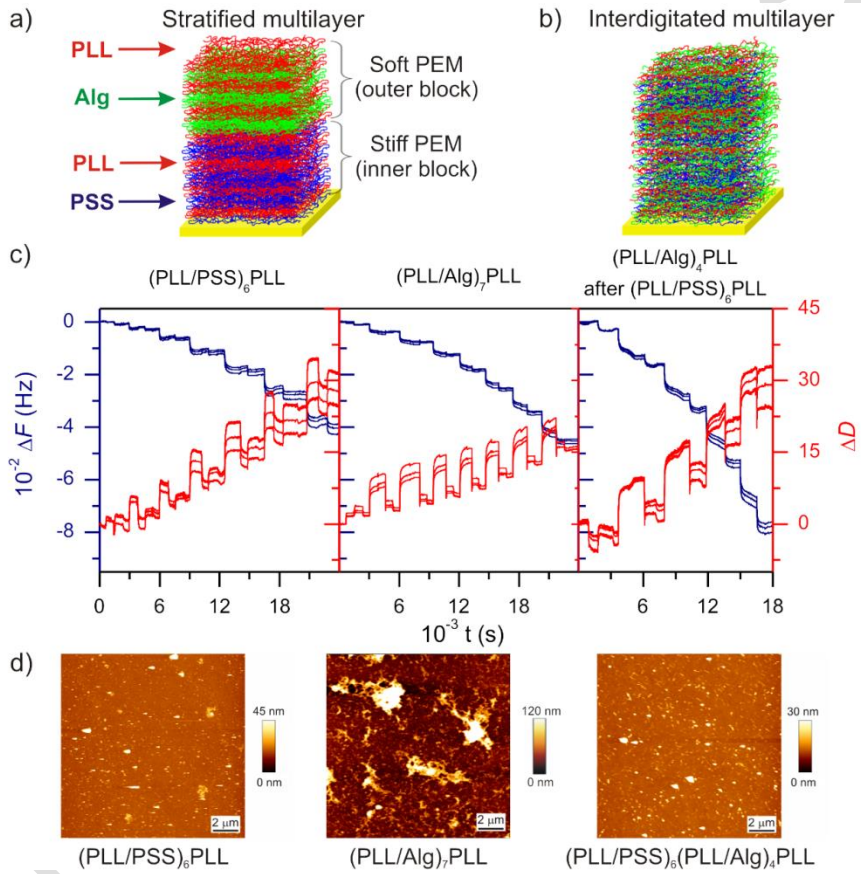

Figure 2. a) Scheme of a di-block polyelectrolyte multilayer. An initial stiff PEM block of $(PLL/PSS)_6$ was first deposited and then a soft PEM block of biocompatible $(PLL/Alg)_nPLL$ was assembled. **b)** Scheme of the possible interdigitation between the blocks. **c)** Frequency and dissipation changes as a function of time for the assembly of $(PLL/PSS)_6PLL$, $(PLL/Alg)_7PLL$ and $(PLL/Alg)_4PLL$ on top of a $(PLL/PSS)_6PLL$ block. **d)** AFM image in dry state of $(PLL/PSS)_6PLL$, $(PLL/Alg)_7PLL$ and $(PLL/PSS)_6(PLL/Alg)_4PLL$.

These results can be interpreted as a consequence of polyelectrolyte interdigitation that generates PEMs with physicochemical properties that are absent in each block separately. We also used the

di-block assembly strategy to improve A549 cell adhesion on PLL/Dex biocompatible PEMs and to enhance the adhesion of C2C12 cell line.[16]

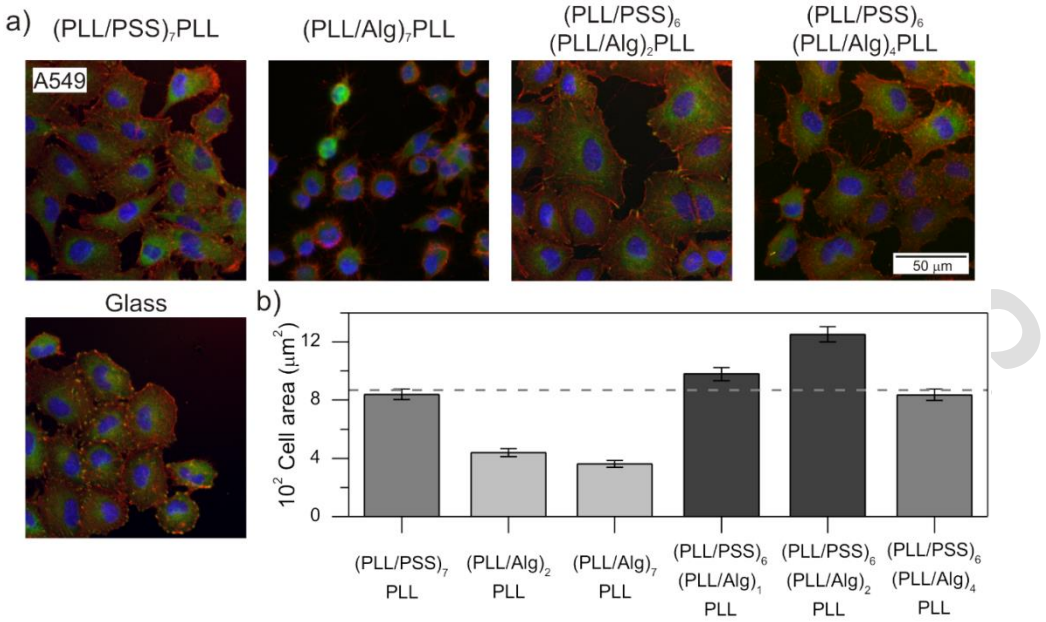

Figure 3. a) Immunostaining of vinculin (green) and staining of actin (red) and cell nucleus (blue) of A549 cells on glass, single and di-block PEMs. b) Mean cell spreading area for A549 cells on single and di-block PEMs. For each PEM the average cell adhesion areas were assigned to be smaller (light gray), equal (gray) or larger (dark gray) than on glass employing the ANOVA-Fisher test with 0.05 significance. Dashed lines correspond to the cell spreading area obtained on glass.

3.2. Cell adhesion improvement by thermal annealing of PEMs

Polyelectrolyte multilayers assembled by the LbL technique are systems outside thermodynamic equilibrium and can be affected by temperature.[50] The post-assembly thermal treatment at 37°C for 3 days generates stable changes in the physicochemical properties of natural polyelectrolyte-based PEMs and induces changes in cell adhesion properties.[44–46] This thermal annealing enhanced the adhesion of A549 and C2C12 cells on biocompatible PLL/Alg and PLL/Dex PEMs.

The changes in the physicochemical properties of $(PLL/Alg)_7PLL$ films upon annealing were assessed with AFM, nanoindentation experiments, water contact angle and zeta potential measurements (Figure 4). AFM images show that after the annealing, the film becomes smoother (Figure 4a) and with height peaks 2 or 3 times shorter than before annealing (Figure 4b). The roughness decreases from a value close to 4.3 nm for the nonannealed film to a value close to 2.3 nm for the annealed one (Figure 4c). The PEM also becomes stiffer, with a Young's modulus one order of magnitude larger after the annealing (Figure 4d). Changes in film wettability were

determined by measuring the water contact angle on air dried samples. The contact angle of the PEMs increases from 36±2.8° to 92±4.6° after the annealing, showing an increase of the film hydrophobicity (Figure 4e). The zeta potential of $(PLL/Alg)_7PLL$ coated colloids changes from about zero on nonannealed films to -14 mV after annealing (Figure 4f), indicating that the density of negatively charged groups on the film surface increased. The above data indicate that the thermal annealing of $(PLL/Alg)_7PLL$ multilayers leads to a reorganization of the film as a consequence of an increase of the polyelectrolyte motility inside the multilayer and a maximization of the polyelectrolyte electrostatic interaction.[51–53]

The reorganization of the $(PLL/Alg)_7PLL$ multilayers induced by the thermal treatment affects its cell adhesive properties (Figure 5). The cytoplasm spreading of A549 and C2C12 cells on nonannealed $(PLL/Alg)_7PLL$ films is poor, as it can be observed in the fluorescence images (Figure 5a). On the other hand, cells seeded on annealed $(PLL/Alg)_7PLL$ PEMs present an extended cytoplasm with well-defined focal contacts and large actin fibers, like the cells seeded on glass. The spreading area of both cell lines on nonannealed $(PLL/Alg)_7PLL$ films is about 2.5 times smaller than the spreading area on glass (Figure 5b).

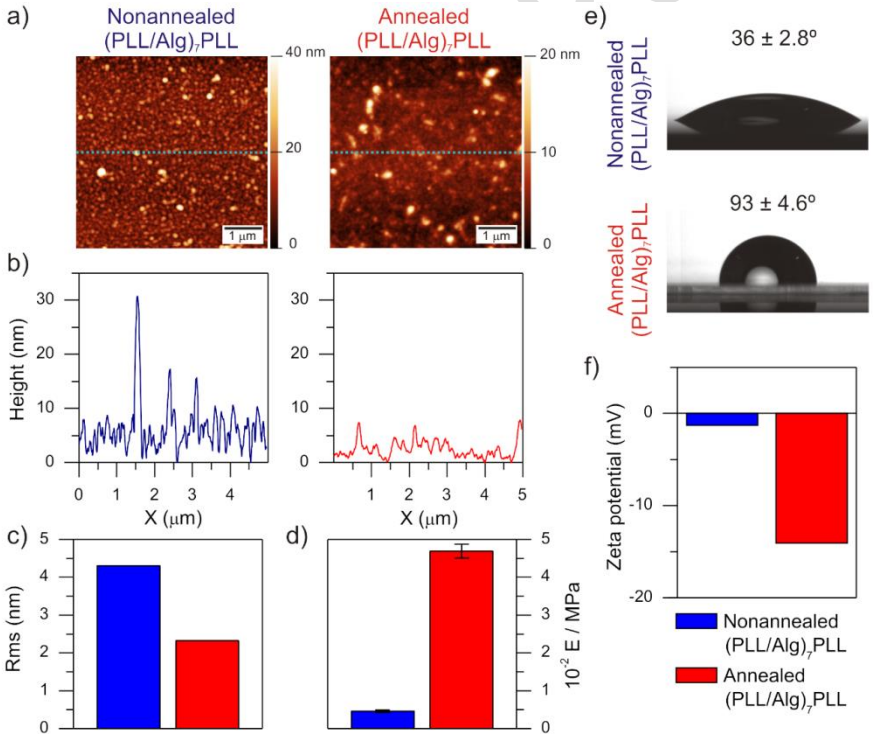

Figure 4. Physicochemical properties of nonannealed and annealed $(PLL/Alg)_7PLL$ multilayers. AFM images **(a)** and roughness profiles **(b)** corresponding to the blue lines in **(a).** Root mean square roughness **(c)** and Young's modulus **(d)** obtained from nanoindentation experiments. Water contact angle measurements **(e)** and surface zeta potential **(f)** of the nonannealed and annealed films.

The vinculin area per cell follows the same trend, being 4 times smaller on nonannealed $(PLL/Alg)_7PLL$ multilayers than on glass. Annealing improves the adhesion of A549 and C2C12 cells, and the adhesion parameters reach values statistically equal to the values found on glass.

Thermal annealing represents a simple and cell-friendly strategy to tune the physicochemical and cell adhesive properties of biocompatible multilayers. This strategy was applied to PEMs composed of others pairs of polyelectrolytes, promoting cell adhesion on PLL/Dex films,[47] and inhibiting it in a cell-dependent manner on Chi/HA PEMs.[46]

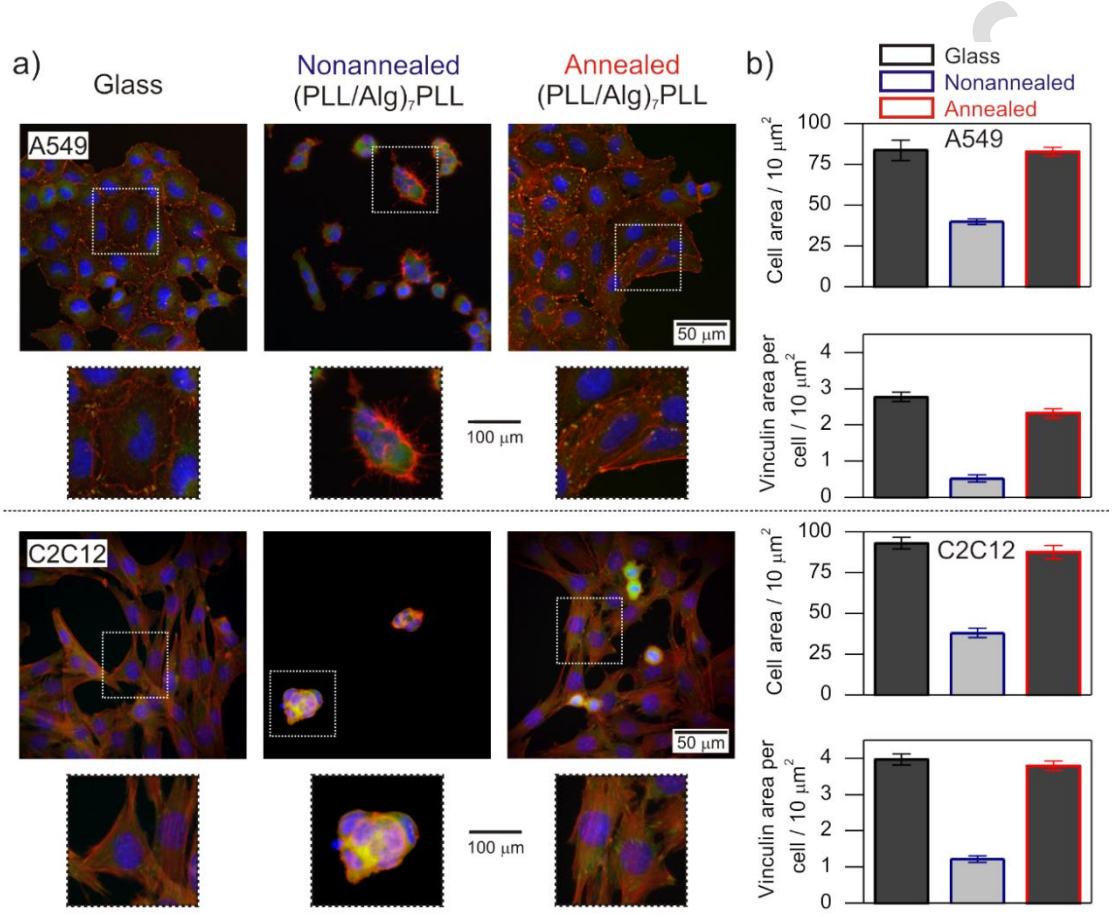

Figure 5. **a)** Immunostaining of vinculin (green) and staining of actin (red) and cell nucleus (blue) of A549 and C2C12 cells on glass, nonannealed and annealed $(PLL/Alg)_7PLL$ multilayers. Enlarged images of the areas indicated by squares are included. **b)** Mean cell spreading area and vinculin area per cell for A549 and C2C12 cells on glass, nonannealed and annealed $(PLL/Alg)_7PLL$ films. For each PEM the average cell adhesion area or vinculin area per cell was assigned to be smaller (light gray), equal (gray) or larger (dark gray) than on glass employing the ANOVA-Fisher test with 0.05 significance.

4. Spatial control of PEMs properties

Surfaces with gradients in their physical properties and with biochemical cues are of great interest for biomedical research and applications as they can better mimic the complexity of the

extracellular matrix and guide cell behavior.[54] As PEMs are promising candidates for a biomaterial mimicking the native extracellular matrix, several types of gradients has been developed with these films.[55]

Gradients in pH assembly of PEI/Heparin/Chi multilayers have been made using microfluidic devices. Cells seeded on the resulting multilayers adhered better on the basic region, which is more stiff and hydrophobic than the acid one.[56] Gradients can also be made with post-assembly treatments. A spatially patterned stiffness has been made on PLL/HA multilayers making a cross-linker agent gradient using a microfluidic device.[55] The resulting multilayer presented a spatially dependent cell adhesion. Microfluidic devices have also been used to spatially pattern biomolecules on top of PEMs. Gradients of bone morphogenic proteins on top of PLL/HA multilayers were used to induce a myogenic or osteogenic commitment of C2C12 cells.[20] Photo-cross-linkable PEMs can also be used to create films with gradients of mechanical properties, which were able to guide cell adhesion and migration.[57] These two cellular functions have been tuned on PSS/PDAD films with a spatially controlled swelling ratio generated by a post-assembly treatment in a salt gradient.[41] Moreover, these gradient substrates were used to study the cell-cell interaction dependence of directional cell migration, demonstrating the utility of these materials on basic cell research.

In our group, we have created a spatially controlled arrangement of physicochemical cues on PEMs surfaces with a temperature gradient treatment after the assembly.[47] PLL/Alg films were placed on a silver sheet with one extreme maintained at 10 °C and the other at 50 °C using thermostated chambers (Figure 6a). The resulting temperature gradient was linear with the distance, with a slope close to 0.002 °C μm^{-1}. The values of water contact angle at the films extremes held at 10 °C and 50 °C were close to those observed in nonannealed and annealed PEMs, respectively (Figure 4e and 6b). At intermediate temperatures the film presented an intermediate value of water contact angle. Thus, a continuous change in the physicochemical properties of the multilayers appears to set in after the application of a thermal gradient.

These changes in the PEM properties affected the adhesion of C2C12 cells seeded on top (Figure 6c). On the film region maintained at the highest temperature cell adhesion was close to that observed on glass. In contrast, on the region maintained at the lowest temperature cell spreading was poor. The most significant changes in the cell spreading area were observed in the region exposed to temperatures between 22 and 30 °C. This is in accordance with the fact that in the case of uniform thermal annealing of PEMs, a treatment at 37 °C is enough to achieve cell spreading areas close to those found on glass (Figure 5).

The application of a thermal gradient to biological polyelectrolyte composed PEMs enable us to locally modify the physicochemical and cell adhesion properties of films, an issue of interest to better mimic the extracellular matrix properties and for rapid testing of cell functionalities.

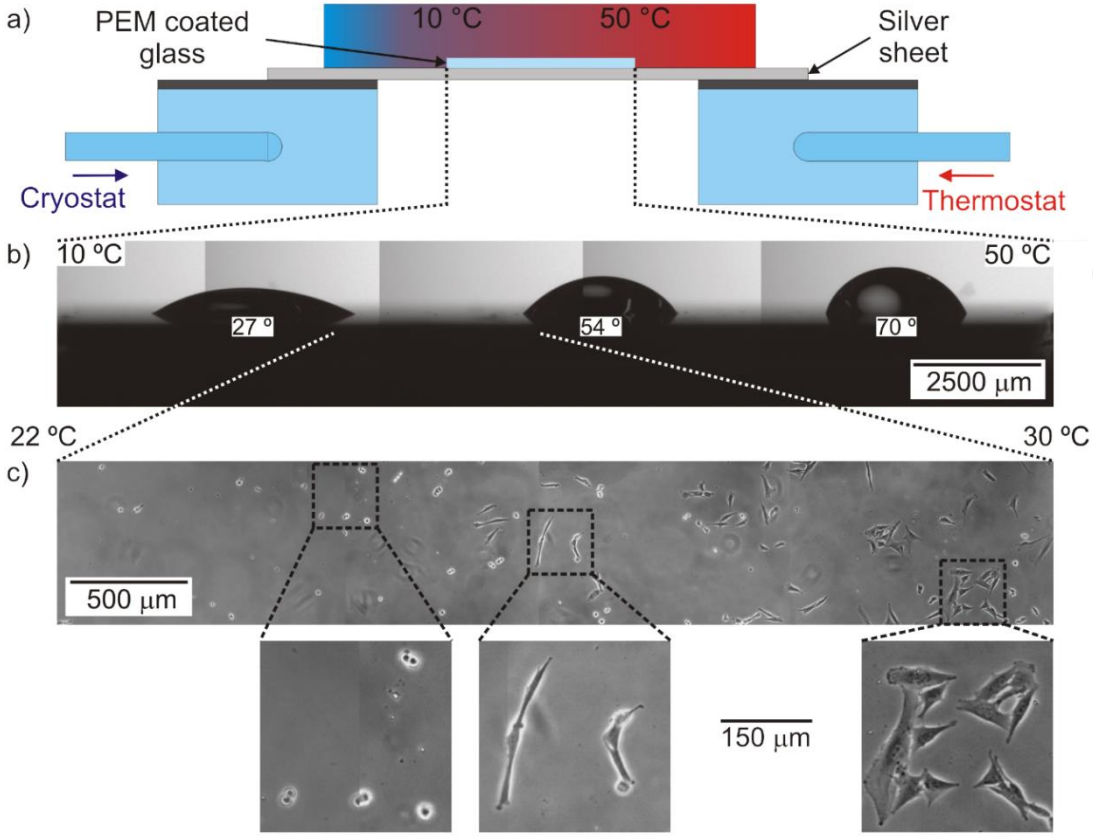

Figure 6. a) Scheme of the experimental setup to produce a temperature gradient on the PEM coated glass. Samples were placed on a silver sheet with one extreme maintained at 50 °C with a chamber connected to a thermostat and the other maintained at 10 °C with chamber connected to a cryostat. Effect of the thermal gradient on the $(PLL/Alg)_7PLL$ surface wettability **(b)** and C2C12 cell adhesion **(c).** The minimum and maximum temperature for all regions are included. Enlarged images of regions indicated by dashed squares in **(c)** are included to appreciate the changes in the cell spreading along the multilayer after the treatment with the temperature gradient.

5. Conclusions

Polyelectrolyte multilayers assembled by the Layer by Layer assembly technique have highly versatile and tunable properties, which make them very attractive materials for various biomedical applications. In this review we have summarized the cell behavior towards purely synthetic, purely natural and combined polyelectrolyte multilayers. As the use of natural polyelectrolytes is highly encouraged because of their biocompatibility and resemblance to the natural extracellular matrix, we have reviewed some of the strategies employed to tune cell

adhesion on natural PEMs. We presented two of the approached followed in our group: the combination of blocks of synthetic and bio polyelectrolytes and the use of thermal annealing. Finally, as surfaces with a spatial patterning of physical and biochemical cues are very interesting for biomedical research and applications, we summarized some of the strategies employed to generate gradients in PEMs properties in order to guide cell behavior.

Acknowledgments

This work was supported by the European Commission in the framework of FP7 PEOPLE-2009 Project TRASNADE Proposal No. 247656.), Consejo Nacional de Investigaciones Científicas y Técnicas (CONICET, Argentina) (Grant No. PIP 0602), and Universidad Nacional de La Plata (UNLP). M.A.P. is staff member of CONICET.

References

(1) Barone, V.; Heisenberg, C.-P. Cell Adhesion in Embryo Morphogenesis. *Curr. Opin. Cell Biol.* **2012**, *24* (1), 148–153.

(2) Boateng, J.; Catanzano, O. Advanced Therapeutic Dressings for Effective Wound Healing - A Review. *J. Pharm. Sci.* **2015**, *104* (11), 3653–3680.

(3) Pizarro-Cerdá, J.; Cossart, P. Bacterial Adhesion and Entry into Host Cells. *Cell* **2006**, *124* (4), 715–727.

(4) Bendas, G.; Borsig, L. Cancer Cell Adhesion and Metastasis: Selectins, Integrins, and the Inhibitory Potential of Heparins. *Int. J. Cell Biol.* **2012**, *2012*, 1–10.

(5) Guo, S.; Zhu, X. Controlling Cell Adhesion Using Layer-by-Layer Approaches for Biomedical Applications. *Mater. Sci. Eng. C* **2017**, *70*, 1163–1175.

(6) Khalili, A. A.; Ahmad, M. R. A Review of Cell Adhesion Studies for Biomedical and Biological Applications. *Int. J. Mol. Sci.* **2015**, *16* (8), 18149–18184.

(7) Silva, E. D.; Gonçalves, A. I.; Santos, L. J.; Rodrigues, M. T.; Gomes, M. E. *Smart Materials for Tissue Engineering Fundamental Principles*; Wang, Q., Ed.; Royal Society of Chemistry: Cambridge, 2017.

(8) Bacakova, L.; Filova, E.; Parizek, M.; Ruml, T.; Svorcik, V. Modulation of Cell Adhesion, Proliferation and Differentiation on Materials Designed for Body Implants. *Biotechnol. Adv.* **2011**, *29* (6), 739–767.

(9) Tamada, Y.; Ikada, Y. Cell Adhesion to Plasma-Treated Polymer Surfaces. *Polymer (Guildf).* **1993**, *34* (10), 2208–2212.

(10) Knight, D. K.; Stutchbury, R.; Imruck, D.; Halfpap, C.; Lin, S.; Langbein, U.; Gillies, E. R.; Mittler, S.; Mequanint, K. Focal Contact Formation of Vascular Smooth Muscle Cells

on Langmuir–Blodgett and Solvent-Cast Films of Biodegradable Poly(ester Amide)s. *ACS Appl. Mater. Interfaces* **2012**, *4* (3), 1303–1312.

(11) Zhang, N.; Pompe, T.; Amin, I.; Luxenhofer, R.; Werner, C.; Jordan, R. Tailored Poly(2-Oxazoline) Polymer Brushes to Control Protein Adsorption and Cell Adhesion. *Macromol. Biosci.* **2012**, *12* (7), 926–936.

(12) Costa, R. R.; Mano, J. F. Polyelectrolyte Multilayered Assemblies in Biomedical Technologies. *Chem. Soc. Rev.* **2014**, *43* (10), 3453.

(13) Lvov, Y.; Decher, G.; Moehwald, H. Assembly, Structural Characterization, and Thermal Behavior of Layer-by-Layer Deposited Ultrathin Films of Poly(vinyl Sulfate) and Poly(allylamine). *Langmuir* **1993**, *9* (2), 481–486.

(14) Gribova, V.; Auzely-Velty, R.; Picart, C. Polyelectrolyte Multilayer Assemblies on Materials Surfaces: From Cell Adhesion to Tissue Engineering. *Chem. Mater.* **2012**, *24* (5), 854–869.

(15) Borges, J.; Mano, J. F. Molecular Interactions Driving the Layer-by-Layer Assembly of Multilayers. *Chem. Rev.* **2014**, *114* (18), 8883–8942.

(16) Muzzio, N. E.; Pasquale, M. A.; Gregurec, D.; Diamanti, E.; Kosutic, M.; Azzaroni, O.; Moya, S. E. Polyelectrolytes Multilayers to Modulate Cell Adhesion: A Study of the Influence of Film Composition and Polyelectrolyte Interdigitation on the Adhesion of the A549 Cell Line. *Macromol. Biosci.* **2016**, *16* (4), 482–495.

(17) Crouzier, T.; Boudou, T.; Picart, C. Polysaccharide-Based Polyelectrolyte Multilayers. *Curr. Opin. Colloid Interface Sci.* **2010**, *15* (6), 417–426.

(18) Schmidt, S.; Madaboosi, N.; Uhlig, K.; Köhler, D.; Skirtach, A.; Duschl, C.; Möhwald, H.; Volodkin, D. V. Control of Cell Adhesion by Mechanical Reinforcement of Soft Polyelectrolyte Films with Nanoparticles. *Langmuir* **2012**, *28* (18), 7249–7257.

(19) Liu, X. Q.; Picart, C. Layer-by-Layer Assemblies for Cancer Treatment and Diagnosis. *Adv. Mater.* **2016**, *28* (6), 1295–1301.

(20) Almodóvar, J.; Guillot, R.; Monge, C.; Vollaire, J.; Selimović, Š.; Coll, J.-L.; Khademhosseini, A.; Picart, C. Spatial Patterning of BMP-2 and BMP-7 on Biopolymeric Films and the Guidance of Muscle Cell Fate. *Biomaterials* **2014**, *35* (13), 3975–3985.

(21) Matsusaki, M.; Kadowaki, K.; Nakahara, Y.; Akashi, M. Fabrication of Cellular Multilayers with Nanometer-Sized Extracellular Matrix Films. *Angew. Chemie - Int. Ed.* **2007**, *46* (25), 4689–4692.

(22) Mano, J. F.; Silva, G. A.; Azevedo, H. S.; Malafaya, P. B.; Sousa, R. A.; Silva, S. S.; Boesel, L. F.; Oliveira, J. M.; Santos, T. C.; Marques, A. P.; Neves, N. M.; Reis, R. L.

Natural Origin Biodegradable Systems in Tissue Engineering and Regenerative Medicine: Present Status and Some Moving Trends. *J. R. Soc. Interface* **2007**, *4* (17), 999–1030.

(23) Khang, G. Evolution of Gradient Concept for the Application of Regenerative Medicine. *Biosurface and Biotribology* **2015**, *1* (3), 202–213.

(24) Picart, C.; Schneider, A.; Etienne, O.; Mutterer, J.; Schaaf, P.; Egles, C.; Jessel, N.; Voegel, J.-C. Controlled Degradability of Polysaccharide Multilayer Films In Vitro and In Vivo. *Adv. Funct. Mater.* **2005**, *15* (11), 1771–1780.

(25) Picart, C.; Senger, B.; Sengupta, K.; Dubreuil, F.; Fery, A. Measuring Mechanical Properties of Polyelectrolyte Multilayer Thin Films: Novel Methods Based on AFM and Optical Techniques. *Colloids Surfaces A Physicochem. Eng. Asp.* **2007**, *303* (1–2), 30–36.

(26) Schneider, A.; Richert, L.; Francius, G.; Voegel, J.-C.; Picart, C. Elasticity, Biodegradability and Cell Adhesive Properties of Chitosan/hyaluronan Multilayer Films. *Biomed. Mater.* **2007**, *2* (1), S45-51.

(27) Richert, L.; Lavalle, P.; Payan, E.; Shu, X. Z.; Prestwich, G. D.; Stoltz, J.-F.; Schaaf, P.; Voegel, J.-C.; Picart, C. Layer by Layer Buildup of Polysaccharide Films: Physical Chemistry and Cellular Adhesion Aspects. *Langmuir* **2004**, *20* (2), 448–458.

(28) Semenov, O. V; Malek, A.; Bittermann, A. G.; Vörös, J.; Zisch, A. H. Engineered Polyelectrolyte Multilayer Substrates for Adhesion, Proliferation, and Differentiation of Human Mesenchymal Stem Cells. *Tissue Eng. Part A* **2009**, *15* (10), 2977–2990.

(29) Ren, K.; Fourel, L.; Rouvière, C. G.; Albiges-Rizo, C.; Picart, C. Manipulation of the Adhesive Behaviour of Skeletal Muscle Cells on Soft and Stiff Polyelectrolyte Multilayers. *Acta Biomater.* **2010**, *6* (11), 4238–4248.

(30) Schneider, A.; Bolcato-Bellemin, A.-L.; Francius, G.; Jedrzejwska, J.; Schaaf, P.; Voegel, J.-C.; Frisch, B.; Picart, C. Glycated Polyelectrolyte Multilayer Films: Differential Adhesion of Primary versus Tumor Cells. *Biomacromolecules* **2006**, *7* (10), 2882–2889.

(31) Ferreira, A. M.; Gentile, P.; Toumpaniari, S.; Ciardelli, G.; Birch, M. A. Impact of Collagen/Heparin Multilayers for Regulating Bone Cellular Functions. *ACS Appl. Mater. Interfaces* **2016**, *8* (44), 29923–29932.

(32) Ricotti, L.; Taccola, S.; Bernardeschi, I.; Pensabene, V.; Dario, P.; Menciassi, A. Quantification of Growth and Differentiation of C2C12 Skeletal Muscle Cells on PSS-PAH-Based Polyelectrolyte Layer-by-Layer Nanofilms. *Biomed. Mater.* **2011**, *6* (3), 31001.

(33) Seo, J.; Lee, H.; Jeon, J.; Jang, Y.; Kim, R.; Char, K.; Nam, J.-M. Tunable Layer-by-Layer Polyelectrolyte Platforms for Comparative Cell Assays. *Biomacromolecules* **2009**, *10* (8), 2254–2260.

(34) Tezcaner, A.; Hicks, D.; Boulmedais, F.; Sahel, J.; Schaaf, P.; Voegel, J.-C.; Lavalle, P. Polyelectrolyte Multilayer Films as Substrates for Photoreceptor Cells. *Biomacromolecules* **2006**, *7* (1), 86–94.

(35) Fischer, D.; Li, Y.; Ahlemeyer, B.; Krieglstein, J.; Kissel, T. In Vitro Cytotoxicity Testing of Polycations: Influence of Polymer Structure on Cell Viability and Hemolysis. *Biomaterials* **2003**, *24* (7), 1121–1131.

(36) Yaroslavov, A. A.; Sitnikova, T. A.; Rakhnyanskaya, A. A.; Yaroslavova, E. G.; Sybachin, A. V.; Melik-Nubarov, N. S.; Khomutov, G. B. Variable and Low-Toxic Polyampholytes: Complexation with Biological Membranes. *Colloid Polym. Sci.* **2017**, *295* (8), 1405–1417.

(37) Nolte, A. J.; Treat, N. D.; Cohen, R. E.; Rubner, M. F. Effect of Relative Humidity on the Young's Modulus of Polyelectrolyte Multilayer Films and Related Nonionic Polymers. *Macromolecules* **2008**, *41* (15), 5793–5798.

(38) Salloum, D. S.; Olenych, S. G.; Keller, T. C. S.; Schlenoff, J. B. Vascular Smooth Muscle Cells on Polyelectrolyte Multilayers: Hydrophobicity-Directed Adhesion and Growth. *Biomacromolecules* **2005**, *6* (1), 161–167.

(39) Hillberg, A. L.; Holmes, C. A.; Tabrizian, M. Effect of Genipin Cross-Linking on the Cellular Adhesion Properties of Layer-by-Layer Assembled Polyelectrolyte Films. *Biomaterials* **2009**, *30* (27), 4463–4470.

(40) Pozos Vázquez, C.; Boudou, T.; Dulong, V.; Nicolas, C.; Picart, C.; Glinel, K. Variation of Polyelectrolyte Film Stiffness by Photo-Cross-Linking: A New Way To Control Cell Adhesion. *Langmuir* **2009**, *25* (6), 3556–3563.

(41) Han, L.; Mao, Z.; Wu, J.; Guo, Y.; Ren, T.; Gao, C. Directional Cell Migration through Cell–cell Interaction on Polyelectrolyte Multilayers with Swelling Gradients. *Biomaterials* **2013**, *34* (4), 975–984.

(42) Vodouhê, C.; Le Guen, E.; Garza, J. M.; Francius, G.; Déjugnat, C.; Ogier, J.; Schaaf, P.; Voegel, J.-C.; Lavalle, P. Control of Drug Accessibility on Functional Polyelectrolyte Multilayer Films. *Biomaterials* **2006**, *27* (22), 4149–4156.

(43) Hemmerle, J.; Ball, V.; Lavalle, P.; Picart, C.; Voegel, J. C.; Schaaf, P.; Senger, B. Stiffening of Soft Polyelectrolyte Architectures by Multilayer Capping Evidenced by Viscoelastic Analysis of AFM Indentation Measurements. *J. Phys. Chem. C* **2007**, *111* (23), 8299–8306.

(44) Muzzio, N. E.; Gregurec, D.; Diamanti, E.; Irigoyen, J.; Pasquale, M. A.; Azzaroni, O.; Moya, S. E. Thermal Annealing of Polyelectrolyte Multilayers: An Effective Approach

for the Enhancement of Cell Adhesion. *Adv. Mater. Interfaces* **2017**, *4* (1).

(45) Diamanti, E.; Muzzio, N.; Gregurec, D.; Irigoyen, J.; Pasquale, M.; Azzaroni, O.; Brinkmann, M.; Moya, S. E. Impact of Thermal Annealing on Wettability and Antifouling Characteristics of Alginate Poly-L-Lysine Polyelectrolyte Multilayer Films. *Colloids Surfaces B Biointerfaces* **2016**, *145*, 328–337.

(46) Muzzio, N. E.; Pasquale, M. A.; Diamanti, E.; Gregurec, D.; Moro, M. M.; Azzaroni, O.; Moya, S. E. Enhanced Antiadhesive Properties of Chitosan/hyaluronic Acid Polyelectrolyte Multilayers Driven by Thermal Annealing: Low Adherence for Mammalian Cells and Selective Decrease in Adhesion for Gram-Positive Bacteria. *Mater. Sci. Eng. C* **2017**, *80*, 677–687.

(47) Muzzio, N. E.; Pasquale, M. A.; Moya, S. E.; Azzaroni, O. Tailored Polyelectrolyte Thin Film Multilayers to Modulate Cell Adhesion. *Biointerphases* **2017**, *12* (4), 04E403.

(48) Zerball, M.; Laschewsky, A.; Von Klitzing, R. Swelling of Polyelectrolyte Multilayers: The Relation Between, Surface and Bulk Characteristics. *J. Phys. Chem. B* **2015**, *119* (35), 11879–11886.

(49) Soltwedel, O.; Ivanova, O.; Nestler, P.; Müller, M.; Köhler, R.; Helm, C. A.; Madlen, M.; Ralf, K.; Helm, C. A. Interdiffusion in Polyelectrolyte Multilayers. *Macromolecules* **2010**, *43* (17), 7288–7293.

(50) Tang, K.; Besseling, N. A. M. Formation of Polyelectrolyte Multilayers: Ionic Strengths and Growth Regimes. *Soft Matter* **2016**, *12* (4), 1032–1040.

(51) Köhler, K.; Shchukin, D. G.; Möhwald, H.; Sukhorukov, G. B. Thermal Behavior of Polyelectrolyte Multilayer Microcapsules. 1. The Effect of Odd and Even Layer Number. *J. Phys. Chem. B* **2005**, *109* (39), 18250–18259.

(52) Köhler, K.; Möhwald, H.; Sukhorukov, G. B. Thermal Behavior of Polyelectrolyte Multilayer Microcapsules: 2. Insight into Molecular Mechanisms for the PDADMAC/PSS System. *J. Phys. Chem. B* **2006**, *110* (47), 24002–24010.

(53) Gao, C.; Leporatti, S.; Moya, S.; Donath, E.; Möhwald, H. Swelling and Shrinking of Polyelectrolyte Microcapsules in Response to Changes in Temperature and Ionic Strength. *Chem. - A Eur. J.* **2003**, *9* (4), 915–920.

(54) Harley, B.; Lu, H. H. Special Issue on Gradients in Biomaterials. *Acta Biomaterialia*. 2017, pp 1–2.

(55) Almodóvar, J.; Crouzier, T.; Selimović, Š.; Boudou, T.; Khademhosseini, A.; Picart, C.; Lopez-Garcia, M.; Walther, P.; Kessler, H.; Geiger, B.; Spatz, J. P. Gradients of Physical and Biochemical Cues on Polyelectrolyte Multilayer Films Generated via Microfluidics. *Lab Chip* **2013**, *13* (8), 1562.

(56) Kirchhof, K.; Andar, A.; Yin, H. B.; Gadegaard, N.; Riehle, M. O.; Groth, T.; Voegel, J.-C.; Picart, C.; Picart, C. Polyelectrolyte Multilayers Generated in a Microfluidic Device with pH Gradients Direct Adhesion and Movement of Cells. *Lab Chip* **2011**, *11* (19), 3326.

(57) Martinez, J. S.; Lehaf, A. M.; Schlenoff, J. B.; Keller, T. C. S. Cell Durotaxis on Polyelectrolyte Multilayers with Photogenerated Gradients of Modulus. *Biomacromolecules* **2013**, *14* (5), 1311–1320.

Miguel A. Pasquale, Dr., is a researcher at the “Instituto de Investigaciones Fisicoquímicas Teóricas y Aplicadas” (INIFTA), CONICET, UNLP, Argentina. He is also Professor at “Universidad Nacional de La Plata”, where he received his doctoral degree in 2004. His major research interest is the study of complex systems of biological interest, particularly the modulation of individual cell phenotypes and cooperative cell behavior by changing the interactions with different environments.

Sergio Moya did undergraduate studies in Chemistry at the Universidad Nacional del Sur, Argentina. He obtained a PhD in Physical Chemistry from the University of Potsdam, working at the Max Planck Institute of Colloids and Interfaces, Germany. He was post doc at the group of Jean Marie Lehn at the College de France, Paris, and at the Nanoscience Center of the University of Cambridge, UK. After postdoctoral work he moved to Mexico where he worked as Conacyt researcher at the Center of Applied Chemistry in Saltillo. Since 2007 he is group leader at CIC biomaGUNE, San Sebastian, Spain. His research interests cover the use of polyelectrolytes in nanofabrication, the development of hybrid materials, bio non bio interactions, nanomedicine and the biological fate of nanomaterials. He is the author of more than 160 articles. He has coordinated several European and international projects.

Nicolás Eduardo Muzzio joined the research group of Prof. Alejandro Arvia in 2010 as an undergraduate student, focusing on cell motility and the dynamic scaling properties of cell colonies. Upon earning his degree in biochemistry from the Universidad Nacional de La Plata in 2013, he joined the Soft Matter Laboratory and obtained a PhD in chemistry under the direction of Prof. Omar Azzaroni and Dr. Miguel Pasquale direction in 2017. Presently, he is working as post doc at the Soft Matter Nanotechnology group at CIC biomaGUNE, Spain. His current research is primarily on the synthesis of new biomaterials that control cell fate towards tissue engineering and cell studies. He is the author of 9 papers in journals of material science, biopolymers, and physical biology.

Anales de la Asociación Química Argentina

División Jóvenes Profesionales

Mini-Review

THE IMPACT THAT CATANIONIC SURFACTANTS HAVE ON THE SOFT MATTER WORLD

Cristian C. Villa[1], Airam K. Cobo Solis[2], Soledad Stagnoli[2], M. Alejandra Luna[2], Fernando Moyano[2], Patricia G. Molina[2], Juana J. Silber[2], R. Dario Falcone[2], N. Mariano Correa[2,*]

[1] *Present Address: Universidad del Quindío, Programa de Química, Carrera 15 Calle 14 Norte, C.P. 630004 Armenia, Colombia.*

[2] *Universidad Nacional de Río Cuarto, Departamento de Química, Universidad Nacional de Río Cuarto, Agencia Postal #3. C.P. X5804BYA Río Cuarto, Argentina*

[*] *mcorrea@exa.unrc.edu.ar*

Resumen Gráfico - Graphical abstract

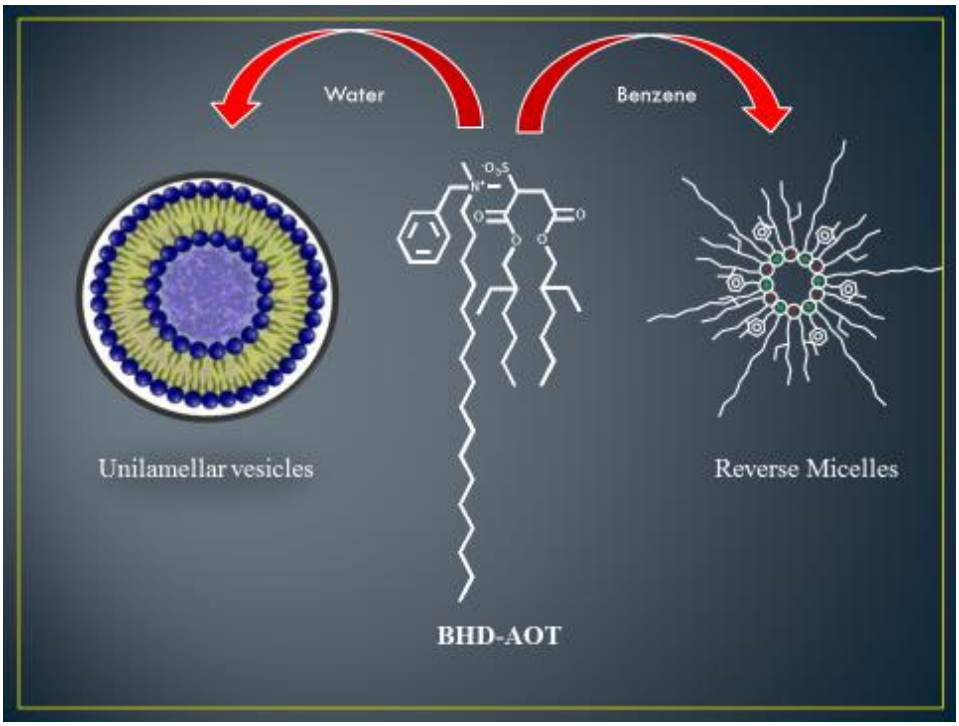

Resumen

Los anfifilos ("surfactantes") cataniónicos, son la clase de surfactantes que resultan de la mezcla equimolar de algún surfactante aniónico y otro catiónico, donde se han removido completamente los contraiones. En nuestro grupo, se ha sintetizado por primera vez, el surfactante cataniónico: 1,4-bis-2-etilhexilsulfosuccinato de bencil-*n*-hexadecildimetilamonio (BHD-AOT), el cual tiene gran utilidad dentro del campo que abarca la "materia blanda". Esto es así porque puede formar micelas inversas o vesículas unilaminares grandes, de manera espontánea, dependiendo del solvente utilizado. Las micelas inversas son agregados supramoleculares que se forman al disolver surfactantes en solventes de baja polaridad. En ellos, la parte polar se ubica hacia el interior mientras que las colas hidrocarbonadas se extienden hacia el solvente orgánico. Las

vesículas son otro tipo de agregados supramoleculares, formados por ciertos surfactantes, en agua, donde una bicapa encierra un volumen de agua que puede atrapar diferentes solutos solubles en dicho solvente. En esta revisión se mostrará resultados relacionados a la síntesis, caracterización y diferentes propiedades que presentan los sistemas creados por BHD-AOT. Además, se mostrarán interesantes aplicaciones en el área de la nanomedicina ya que, como fue probado en el grupo, el surfactante es no-tóxico y puede ser utilizado en sistemas de liberación de droga.

Abstract

Catanionic surfactants are a class of amphiphile which result from the equimolar mixture of a cationic and an anionic surfactant, where the salt formed by the counterions is removed. In our group, for the first time, we have synthetized the unique catanionic surfactant: benzyl-n-hexadecyldimethylammonium 1,4-bis-2-ethylhexylsulfosuccinate (BHD-AOT), which has a tremendous impact in the *soft matter* field. This came out because it can form reverse micelles (RMs) or spontaneous large unilamellar vesicles, depending on the solvent used. RMs are supramolecular assemblies of surfactants formed in nonpolar solvents, in which the polar head groups of the surfactants point inward and the hydrocarbon chains point toward to the nonpolar medium. Vesicles are spherical aggregates formed by some amphiphilic compounds in water, in which the bilayer surrounds an aqueous void volume that can be "loaded" with a wide variety of water-soluble marker molecules. In this review, we will show the synthesis, characterization, and properties of the different organized media created by BHD-AOT and, exciting applications since, as we proved, it is non-toxic and results especially interesting for drug delivery system.

Palabras Clave: *Química Supramolecular, Micelas Inversas, Vesículas, Surfactante Cataniónico.*

Keywords: *Supramolecular Chemistry, Reverse Micelles, Vesicles, Catanionic Surfactants*.

1. Introduction.

Catanionic surfactants are a new kind of molecules with very interesting properties as amphiphiles.[1] It is known that the mixtures of surfactants can exhibit considerable synergistic advantages like solubilization, dispersion, suspension and transportation capabilities, and are used in a wide range of applications in relation to an individual surfactant.[2] This new kind of surfactants is the result of mixtures of oppositely charged surfactants. In the literature, it is easy to find two categories of *catanionic surfactants*: one, known as catanionic mixtures, are simple mixtures of anionic and cationic surfactants without the removal of their respective counterions; the other category corresponds to catanionic systems when surfactants are mixed and the counterions are removed.[1,3,4] The usual way to obtain the latter kind of catanionic surfactants is combining two ionic surfactants in a 1:1 molar ratio; the inorganic salt formed by the remaining counterions is totally removed using a suitable separation method.[1] The amphiphile thus obtained have shown the ability to form different organized systems, such as direct and reverse micelles (RMs)[1,5,6], vesicles[1,7] and liquid crystals.[8]

Within the interesting topic related to the green chemistry lies the synthesis of ionic liquids (ILs)[9] with amphiphilic properties, which can be used to form organized systems.[10,11] Among the

most commonly used molecules, long-chained imidazolium ILs can be mentioned, including charged hydrophilic head group and one or more hydrophobic tails.[10,11] This kind of ILs have been usually referred as "surfactant ionic liquids" (SAILs).[12] In this way, it was synthesized in our lab for the first time, the new catanionic ILs-like surfactant, BHD-AOT resulting from the equimolar mixture of two very well-known surfactants: the anionic sodium 1,4-bis (2-ethylhexyl) sulfosuccinate (Na-AOT) and, the cationic benzyl-n-hexadecyldimethylammonium chloride (BHDC) (Scheme 1). The novelty of this SAIL lies in that the cationic component is an ammonium salt rather than imidazolium salts more commonly found for ILs.[1] This catanionic SAIL shows exceptional properties which will be described in this review.

Respecting the organized systems that the above mentioned SAIL can form depending on the appropriate choice of the external solvent, among the most relevant the following two can be mentioned: reverse micelles (RMs) and vesicles (Scheme 2). RMs are self-assembly systems where a layer of surfactant molecules confines a water nano-droplet with hydrophilic head groups pointing inward to the center which contains the polar solvent and the hydrophobic tails extending outward facing the organic non-polar continuous phase.[13,14] The properties of the RMs are affected by different parameters such as the surfactant class, the non-polar solvent composition, temperature, and water content (which is usually defined as W_0 = [Water]/[Surfactant]). The most common surfactants used to form this kind of supramolecular assemblies are the anionic Na-AOT and the cationic BHDC.[13,15,16] An interesting feature of these surfactants is that they can form RMs without the presence of co-surfactants.[15,17,18] The investigation of RMs has grown considerably due to their applications as mimetic agents and cell biomembranes modeling, drug delivery, oil recovery, and enzymology.[19,21] Also, they can be used as suitable reaction media for both: hydrophilic and hydrophobic substrates, providing "nanoreactors" for a wide variety of systems, including enzymatic ones.[20,22]

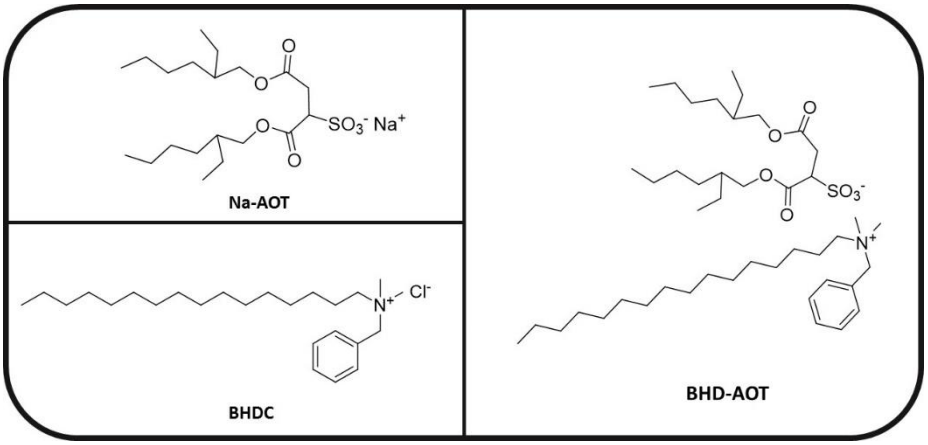

Scheme 1. Structure of ionic surfactants Na-AOT and BHDC, and catanionic surfactant BHD-AOT.

On the other hand, when some surfactants are dissolved in water, they are capable to form a very special kind of organized systems: *the vesicles*.[23] They are spherical aggregates where the lipid bilayer surrounds an aqueous void volume which can be "loaded" with almost any variety of water-soluble molecules. The problems associated with the wide diversity in composition and structure of biological membranes can be avoided using synthetic vesicles, since they can mimic geometry, topology, and skeletal structure of cell membranes, without the presence of ion channels and a multitude of other embedded components.[24] The most common surfactants that form vesicles are the phospholipids. It is worthy to mention here that, phospholipids form spontaneously upon solubilization in water, multilamellar vesicles, and require different methods to be transformed into large unilamellar vesicles (LUV), the kind of system needed for physicochemical studies and/or used as drug delivery device for living organisms.[25,26]

In this review, we will show interesting features of the new catanionic SAIL: BHD-AOT. The work will be divided into various sections as follow: In section 3.1 we will describe the synthesis and the characterization of the SAIL as well the organized systems formed in organic solvent and water; in section 3.2 it will show singularities on the physicochemical properties of the system formed by the catanionic surfactant and, the effect that the cationic moiety has on the structure of water entrapped in RMs; in section 3.3 we will focus on some applications that the system has to offer.

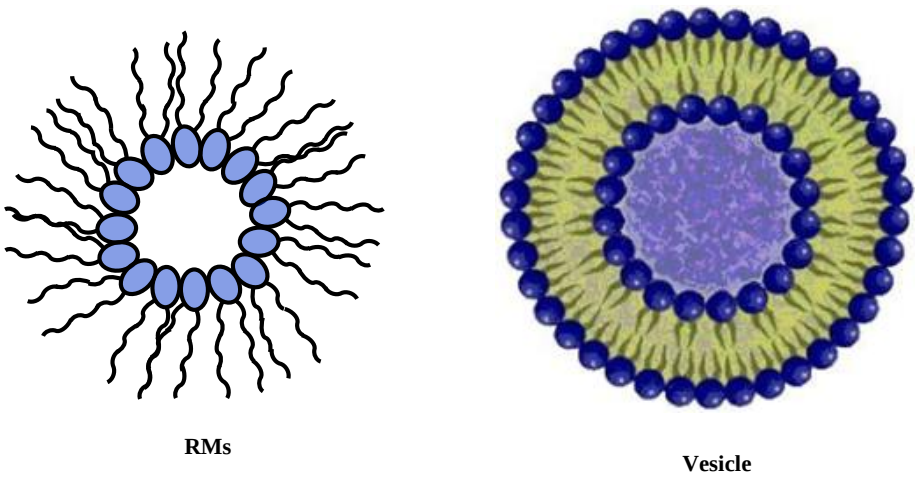

Scheme 2. Schematic representation of RMs and Vesicle.

2. Experimental Section.

In this section is summarized the synthetic methods and methodology used in the papers reviewed.

2.1. Synthesis.

Catanionic IL-like surfactant preparation: The catanionic IL-like surfactants used, benzyl-n-hexadecyldimethylammonium 1,4-bis(2-ethylhexyl)sulfosuccinate (BHD-AOT, Scheme 1) was obtained following the methodology previously reported.[1,27,28] Equimolar solutions of Na-AOT and BHDC were prepared in dichloromethane and combined with magnetic stirring during 72 hours. During the stirring, a white precipitate appeared and it was attributed to salt (NaCl) formation from the original surfactants counterions. The salt was removed firstly by centrifugation and then by liquid-liquid extraction using water until the water fractions were free of chloride ($AgNO_3$ test). Once the salt was eliminated, the dichloromethane was removed by vacuum evaporation and a colorless viscous liquid was obtained. The formation of the catanionic ILs-like surfactant was confirmed by ^{1}H NMR, as we previously reported.[28]

2.2. Methods

RMs preparation: The stock solutions of BHD-AOT in benzene were prepared by mass and volumetric dilution. Aliquots of these stock solutions were used to make individual reverse micelle solutions with different amount of water, defined as W_0 = [water] / [BHD-AOT]. The incorporation of water into each micellar solution was performed using calibrated microsyringes. To obtain optically clear solutions homogenization was carried in an ultrasonic bath, resulting in a single phase.[1]

Vesicles preparation: The solutions of BHD-AOT in water were prepared by mass and volumetric dilution. The opalescence solutions obtained were shacked about 2 minutes at room temperature. All solutions showed stability in a long period of time without visual modification.[1]

3. Results and Discussions

3.1. Characterization of BHD-AOT Reverse Micelles or Vesicles.

The BHD-AOT is a highly viscous liquid with a melting point below 100 ºC and very low vapor pressure which has the characteristics of room temperature IL.[1] As Na-AOT and BHDC are ionic surfactants that form RMs in different nonpolar solvents and, in order to test the amphiphilic properties of BHD-AOT, the catanionic surfactant was dissolved in different media such as: *n*-heptane, chlorobenzene, and benzene. Despite the fact that AOT is completely soluble in aromatic and non-aromatic hydrocarbons, it is very interesting that the catanionic SAIL is soluble only in aromatic solvents. Thus, it seems that the solubility of this new surfactant is

governed by the cationic surfactant moiety. The test of the capability of the system formed to entrap water, it was show that it can be dissolved up to a W_0 value around 1.6.[1] A question that may arise here, is that if actually RMs aggregates are formed as water was dissolved.[29] Dynamic light scattering (DLS) is one of the techniques that can answer this question.[29] The droplets sizes values obtained in the RMs system are shown in Figure 1. From this Figure is possible to observe an increase in the droplets size values when the water content increase. Moreover, the linear tendency observed indicates that RMs are not interacting and the shape is probably spherical. Deviation from the linearity could be due to several factors being the most relevant: droplet–droplet interaction and/or other RMs shape.[29,30]

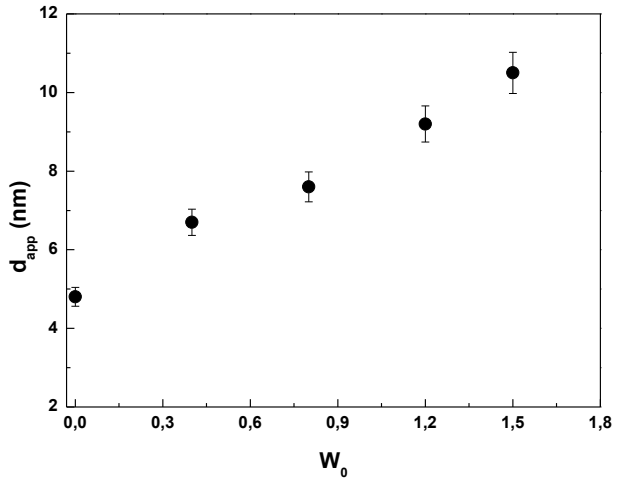

Figure 1. Droplets sizes (d_{app}) values of BHD-AOT RMs varying the water content W_0. [BHD-AOT] = 0.02 M. Data taken from reference 1

In any case, these results confirm the presence of RMs and that water molecules are effectively entrapped in the organized system. In Scheme 3 is presented a cartoon of the schematic representation of the BHD-AOT surfactants distribution in the reverse micelle system.

The situation is different when BHD-AOT surfactant is dissolved in water. An opalescent solution is obtained which was stable for a period of months. In light of these facts, we suppose that the surfactant could form vesicles. In order to confirm this, DLS and small angle x-ray scattering (SAXS) measurements were carried out.[1] In Table 1 it is shown the apparent diameter values, d_{app}, obtained through DLS technique, as a function of the surfactant concentration. It can be seen that the d_{app} value is around 80 nm and the value is relatively constant at all [BHD-AOT] investigated.

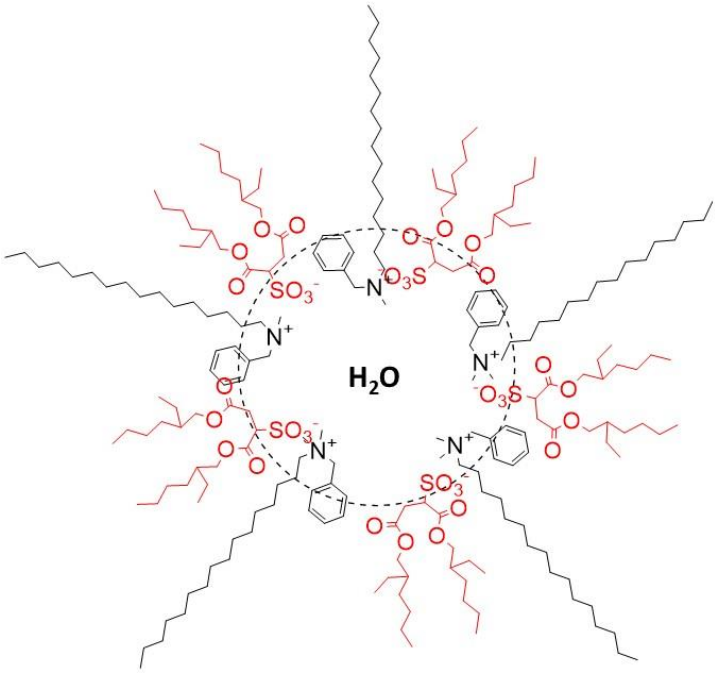

Scheme 3. Schematic representation of BHD cations and AOT anions distribution in the BHD-AOT RMs interface.

Since one characteristic of the vesicles aggregates is the lack of critical aggregate concentration (around 10^{-10} M),[31,33] the d_{app} value of the vesicles at low surfactant concentration should not change in comparison with the values at higher surfactant concentration. Thus, the independence of the d_{app} even at very low [BHD-AOT] indicate that the system created is vesicle and not normal micelles.[34]

The question of whether the vesicle formed by BHD-AOT in water is a multilamellar or unilamellar system, was addressed by using SAXS technique.[1] The SAXS pattern obtained for 5 g/L BHD-AOT vesicles were fitted with several models in order to reproduce the experimental data. The best fit was achieved using a vesicle model with a single diffuse lamellar shell. The structure of the shell was simulated assuming a Gaussian profile for the excess electronic density. The relevant vesicle parameters obtained from the non-linear fit are reported in Table 1. The good fit obtained is consistent with unilamellar vesicles as suggested by DLS experiments (See the low polydispersity index shown in Table 1). Thus, we have obtained, spontaneously unilamellar vesicles of BHD-AOT in water, without the need to add energy to the system, as the traditional methods require.

3.2. Singularities of the Different BHD-AOT Interfaces Formed.

Reverse Micelles. It is interesting to get insights about the nature of the interface of the RMs that the SAIL form in benzene. The interfacial properties depend on, among other parameters, the strength of the water-surfactant interactions. Thus, it was investigated the behavior of water

entrapped in BHD-AOT RMs formed by FT-IR and ^{1}H NMR techniques.[28] FT-IR spectroscopy is a particularly suitable technique to detect interactions and different kind of water molecules, *if present*, because its time scale (10^{-12}-10^{-14} s) is faster than the time scales, e.g., on which water molecules are expected to interchange between discrete layers (between 10^{-7} s and 10^{-11} s).[35]

Table 1. Apparent diameter (d_{app}) and polydispersity index (PDI) values of BHD-AOT vesicles in water at different catanionic concentrations. T = 25°C. Data taken from reference 1

[BHD-AOT] (mg/ml)	**d_{app} (nm)**	**PDI**
0.0001	81 ± 5	0.4
0.05	79 ± 4	0.3
0.1	88 ± 5	0.3
0.5	93 ± 5	0.1
[BHD-AOT] (mg/ml)	**Parameter[a]**	**Value[a]**
5	Vesicle radius (nm)	31.3 ± 14.0
	Shell thickness (nm)	3.3 ± 1.7
	Radius polydispersity	0.15 ± 0.04

[a] Structure parameters of BHD-AOT water vesicles from SAXS experiment. T = 24 °C.

Figure 2A shows the FT-IR spectra of HDO entrapped in BHD-AOT RMs at different W_0, in the region of 2640-2420 cm^{-1}. Figure 2B shows the shifts of the $\nu_{O\text{-}D}$ values for benzene/BHD-AOT/HDO RMs. From Figure 2, it can be observed two facts: i) The O-D band is completely symmetric, which show that there is only one kind of water present in the system and; ii) The O-D stretching frequency values are larger than the corresponding to neat HDO (2519 cm^{-1}).[36]

The fact that the entrapped water in BHD-AOT presents $\nu_{O\text{-}D}$ values larger than neat water, suggest that water molecules are interacting with the surfactant interface breaking its hydrogen bond structure. It is interesting to compare the variation observed with similar studies for the RMs formed by the precursor surfactants, Na-AOT and BHDC. It was previously observed[28] that, the behavior in Na-AOT RMs is opposite to the one observed for BHDC RMs. In benzene/Na-AOT/HDO RMs, the hydrogen bond interaction between the entrapped water and the AOT polar head group at the interface disrupt the hydrogen bond network of water.[13] On the contrary, for water entrapped in benzene/BHDC RMs we observe that $\nu_{O\text{-}D}$ values appear at lower frequencies that neat water. This fact was explained considering that in BHDC RMs, the cationic polar head group is solvated by ion-dipole interactions through the non-bonding electrons pairs of oxygen, which leads to smaller force constant in the O-H bond.[28] Thus, taking

into account these backgrounds our results indicate that in BHD-AOT, the water-catanionic surfactant interaction is mainly due to hydrogen bonding.

BHD-AOT also helps to resolve a long time question about the cause of the asymmetry in the stretching band corresponding to the carbonyl group of AOT. Figure 3 shows the FT-IR spectra corresponding to the carbonyl stretching band for the Na-AOT and BHD-AOT surfactants dissolved in benzene at $W_0 = 0$.[28] From the Figure is possible to see that the C=O band shows a notable difference in its shape in the catanionic surfactant in comparison with the one obtained for Na-AOT. In the Na-AOT system, the C=O band appears as a broad band with the main peak at 1735 cm^{-1} with a shoulder around 1724 cm^{-1}, while in the catanionic surfactant it appears as a symmetrical band with a peak around 1735-1734 cm^{-1}.

These results suggest that the replacement of Na^+ by other large cation with different structure has an impact on the shape of the $\nu_{C=O}$ band. The presence of cations such as BHD^+ with amphiphilic properties, makes that the cations can be located far from the AOT polar head group in comparison with the Na^+ location. This different position of the cations promote that the C=O band appears symmetrical, reinforces the idea that Na^+ located near to the C=O group can be the reason for the asymmetry observed in the AOT band. Also, the water-surfactant interaction inside the RMs was investigated using ^{1}H-NMR technique and following, not only the water protons but the surfactant's protons.[28] Regarding the entrapped water structure, these studies reaffirmed what it was previously observed via FT-IR. The upfield shift of the proton signal (from water) in comparison with neat water was attributed to the entrapped water having its hydrogen bond structure disrupted due to interaction with the surfactant. An increase on the amount of water within the RMs, causes the hydrogen bond structure of neat water to be recovered. A stronger interaction between the entrapped water and the interface leads to fewer water molecules self-interacting, and consequently, to a further upfield shift on the proton signal. This interaction also leads to the upfield shift of the protons signals of the water molecules in the catanionic systems.

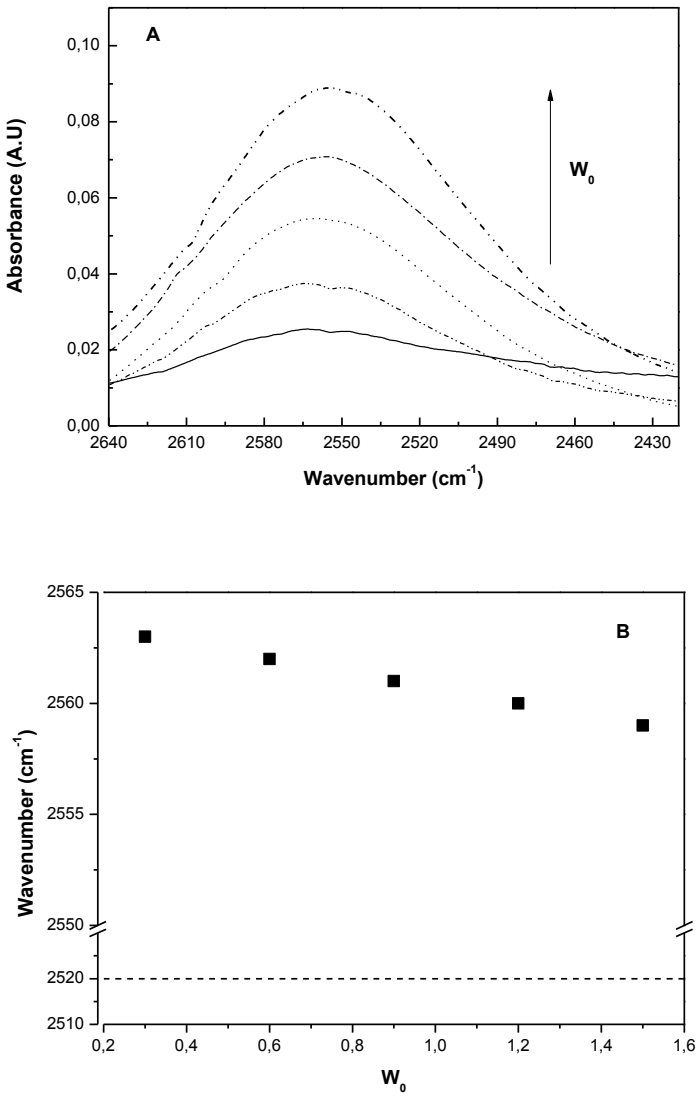

Figure 2. A) FT-IR spectra in the region of 2640-2420 cm^{-1} of HDO entrapped in benzene/BHD-AOT RMs at different W_0 values (0.3; 0.6; 0.9; 1.2; 1.5). [Surfactant] = 0.2 M. B) Shifts of the O-D stretching band upon increasing W_0 values in the benzene/BHD-AOT/HDO RMs. The corresponding value for neat HDO (---) is included as a reference. Data taken from Reference 28.

At this point, and knowing that the counterion has a dramatic impact on the interfacial properties of the RMs, it was synthesized and characterized another catanionic surfactant: cetyltrimethylammonium 1,4-bis-2-ethylhexylsulfosuccinate (CTA-AOT)[28], where the sodium was replaced by the more voluminous cetyltrimethylammonium cation. It was also found that this catanionic surfactant is a SAIL, and it can form RMs when using benzene as solvent. Water can also be encapsulated but, water–surfactant interaction strength is very different to what previously observed for BHD-AOT. Even though hydrogen bond interaction was observed for both catanionic surfactants, the strength of it seemed to be different. For the BHD-AOT RMs, a

stronger water-surfactant interaction can be invoked while for CTA-AOT this interaction appears weaker. This would lead to more water molecules interacting with the interface in BHD-AOT RMs (with its hydrogen bong network disrupted) in comparison with CTA-AOT RMs, where a weaker water-catanionic surfactant interaction allows that the water molecules establish hydrogen bonds to each other, resulting more ¨free" configurations than those obtained in BHD-AOT RMs.[28]

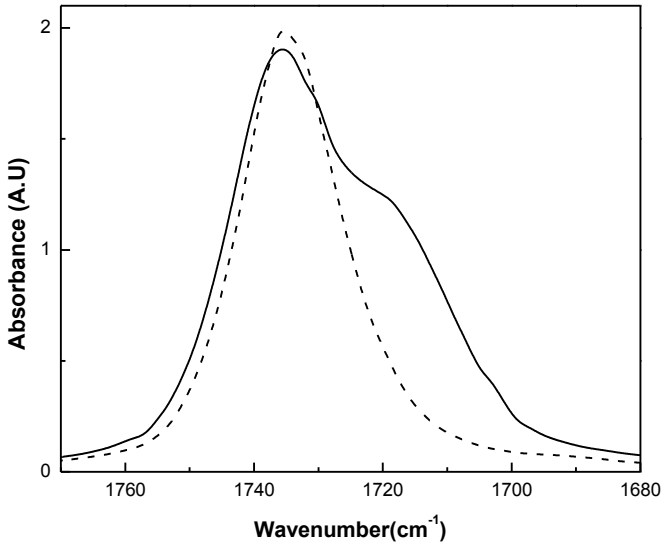

Figure 3. FT-IR spectra in the region of 1690-1770 cm^{-1} for the benzene/Na-AOT (continuous-line) and benzene/BHD-AOT (dashed line) RMs at $W_0 = 0$. [Surfactant] = 0.05 M. Data taken from reference 28

In summary, DLS results reveal the formation of both (BHD-AOT and CTA-AOT) RMs, and that water interacts with the RMs interface since the droplet size increased as W_0 increased. From FT-IR and ^1H NMR experiments, a difference in the magnitude of the water-catanionic surfactant interaction at the interface is observed. Even though for both catanionic surfactants we observed hydrogen bond interaction with the anionic component, their strength is different. For the BHD-AOT RMs, a stronger water-surfactant interaction can be invoked while for CTA-AOT this interaction seems to be weaker. This would lead to more water molecules interacting with the interface in BHD-AOT RMs, with its hydrogen bong network completely disrupted. On the other hand, for CTA-AOT RMs a weaker water-catanionic surfactant interaction allows that the water molecules make a hydrogen bond each other. We hypothesize that the benzyl group present in the BHD^+ moiety in BHD-AOT has a notable impact on the behavior of the catanionic interface in comparison with the interface created in CTA-AOT. These results are interesting since a simple change in the cationic component in the catanionic surfactant, promotes

remarkable changes in the RMs interface. In Scheme 4 it is represented the effect of the cationic surfactant moiety on the structure of water entrapped in two catanionic RMs.

We also study these RMs using a probe molecule and emission spectroscopy. The molecular probe is very peculiar: *trans*-4-[4-(dimethylamino)styryl]-N-methylpyridinium iodide (HC, Scheme 5), which shows differences in their interfaces.[3] While the cationic hemicyanine HC undergoes an intramolecular charge-transfer process upon excitation in CTA-AOT RMs, in BHD-AOT RMs this process is inhibited due to a specific interaction between HC and the polar head group of the BHD^+ cation. This implies that chemical structure of CTA^+ and BHD^+ cations has a great impact on the excited stated from which HC emission occurs. Additionally, the structural differences between both cations impacts on the water-RM interface interaction, which provides a way to acquire control on the solvation process in these RMs.

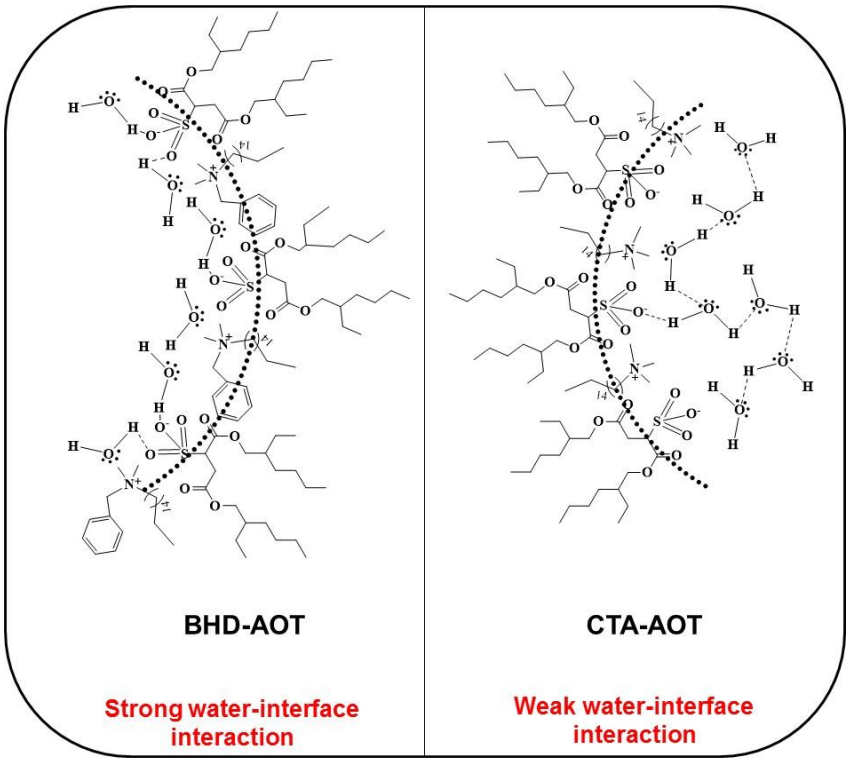

Scheme 4. Schematic representation of the water-interface interaction in BHD-AOT and CTA-AOT RMs systems.

Furthermore, differences in the interfacial fluidity between both catanionic RMs can be observed. Thus, HC senses a more fluid environment as water is added to the CTA-AOT RMs in comparison with BHD-AOT, which corroborates the weak water-interface interaction invoked above, with the consequent increase of the water-water interaction, making a real "pool" with higher fluidity.[3]

Unilamellar Vesicles. The properties of the bilayer of unilamellar vesicles created with BHD-AOT in water were investigated using two different fluorescent probes: HC and 6-propionyl-2-(dimethylaminonaphthalene), PRODAN (Scheme 5). Thus, it was chosen one ionic molecular probe, HC, and other non-ionic, PRODAN. Also, the system spontaneously formed was compared with the traditional vesicles made with phospholipids. [27]

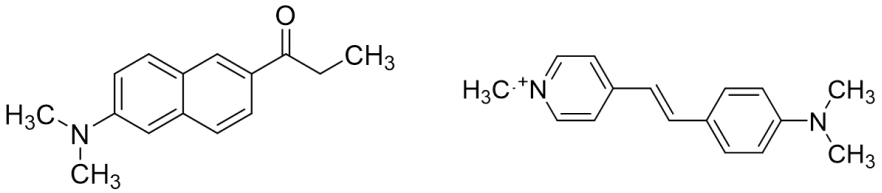

Prodan **HC**

Scheme 5. Structures of PRODAN and HC.

From the emission feature of HC it was concluded that HC senses a slightly more viscous environment in BHD-AOT than in the vesicles made with the traditional phospholipid 1,2-dioleoyl-sn-glycero-3-phosphocholine, DOPC. Apparently, the bilayer composed by both amphiphilic moieties, the anionic AOT and the cationic BHD, make the bilayer slightly more rigid than the phospholipid one. This difference in rigidity suggests a different water penetration into the bilayer (less water penetration in the BHD-AOT bilayer, more rigidity). Also, HC senses a more electron donor and less polar environment in BHD-AOT than in DOPC vesicles (Scheme 6 A).

On the other hand, PRODAN emission profile shows that, in BHD-AOT, it is located in a region of the bilayer where exist as a sole species. By contrast, in DOPC vesicle, PRODAN undergoes a partition process, probably because the bilayer is more fluid (Scheme 6 B). In summary, the results suggest that the BHD-AOT vesicles present a bilayer completely different to the DOPC ones, with low polarity, high viscosity, and more electron donor capacity.

These properties produce large incorporation of ionic and nonionic molecules, which are very promising to use in the future this kind of organized media as nanocarrier in pharmacologic, cosmetic and foods fields.[27]

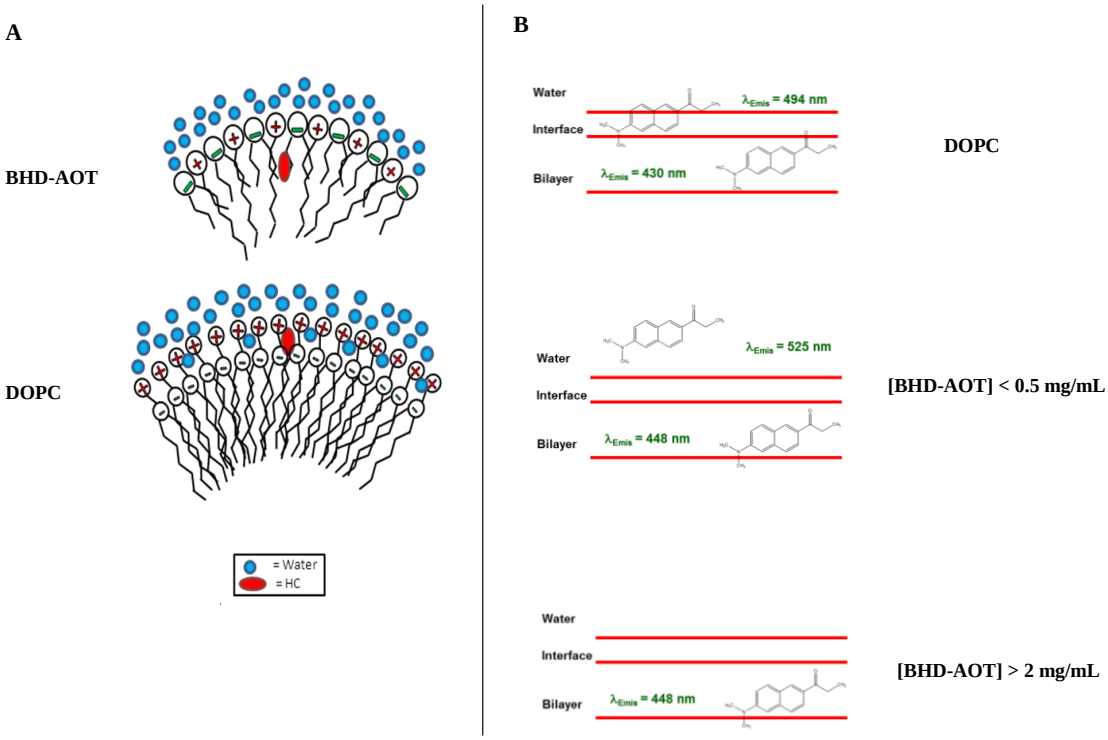

Scheme 6. A Schematic representation of HC location into the BHD-AOT and DOPC vesicles. **B** Schematic representation of PRODAN location into the vesicles of DOPC at [DOPC] = 1 mg/mL; BHD-AOT at [BHD-AOT] < 0.5 mg/mL and BHD-AOT at [BHD-AOT] > 2 mg/mL. Adapted from reference 27

3.3. Different Applications of the BHD-AOT Vesicles.

3.3.1. How can it be retarded a proton transfer reaction?

As it was shown, vesicle bilayer of BHD-AOT has unique properties; therefore, we investigated the effect that the bilayer has on different processes, for example, a proton transfer reaction. In this way, the behavior of 1-Naphthol (NPh) was investigated in large unilamellar vesicles made with BHD-AOT by electrochemical and spectroscopic techniques. This also shows how an alternative and non-conventional approach, the electrochemistry, can be employed with success in different organized media such as vesicles.[37]

The NPh behavior shows that the molecule undergoes a partition process between two phases, water and the large unilamellar vesicles bilayer. Also, by using an electrochemical model we could calculate the partition constant values at pH=6.40 and pH=10.75. The values of the partition constant, which are shown in Table 2 have good agreement with the values obtained by absorbance spectroscopy at the same experimental conditions. Moreover, our model also allows us to calculate the diffusion coefficient in the vesicle for BHD-AOT large unilamellar vesicles, which coincides with the diffusion coefficient obtained through the DLS technique.

Naphtol is an interesting molecule, since it becomes more acidic in the excited state and their pKa decreases by several units in the electronically excited state (pKa* around 0.5) compared to that in the ground state (pKa around 9).[38] As a consequence, the molecule always emits from the anionic species, at practically any pH value. Thus, in aqueous solution (see Scheme 6) NPh undergoes ultrafast deprotonation in 35 ps and, the intensity of the neutral emission of NPh* (at λ=355 nm) is extremely low in aqueous solution, and one observes almost exclusively the anion emission of NPh^{*-} at λ= 460 nm.

Table 2. Values obtained for diffusion coefficient, D_{LUVs}, and NPh partition constant, K_p of BHD-AOT vesicles by using different techniques. Values obtained from reference 37.

Technique	pH	K_p (mL mg^{-1})	D_{LUVs} (cm^2s^{-1})
DLS	6.40		$(2.3\pm0.3)x10^{-7}$
DLS	10.75		$(2.2\pm0.2)x10^{-7}$
Square wave voltammetry	6.40	1.55±0.03	$(2.06\pm0.03)x10^{-7}$
Square wave voltammetry	10.75	0.84±0.01	$(2.08\pm0.03)x10^{-7}$
Absorption Spectroscopy	6.40	1.20±0.20	
Absorption Spectroscopy	10.75	0.70±0.10	

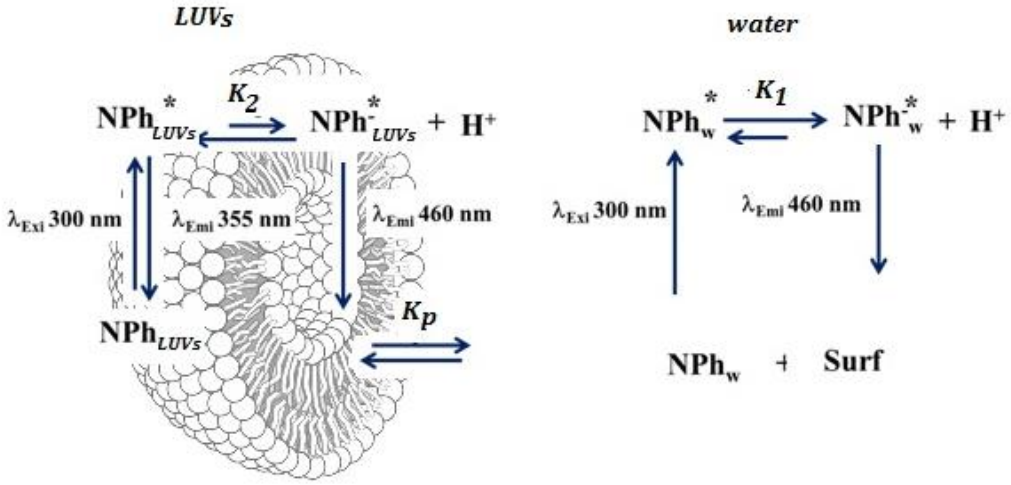

Scheme 6. Representation of the NPh species emission in the different pseudophases. Adapted from reference 37.

Interestingly, the situation is different when NPh is dissolved in BHD-AOT vesicles, at any pH studied. Figure 4 shows the NPh emission spectra at different [BHD-AOT] at pH=6.40. The data show the incorporation of the probe into the bilayer by the appearance of two bands, that correspond to the emission from neutral and anionic species.[37] This Figure shows that, on

increasing BHD-AOT concentration, the band that corresponds to the anionic species (λ=460 nm) begins to decrease, and the other one that belongs to the neutral species grows (λ=355 nm), with the presence of a neat isoemissive point at λ=427 nm.

This feature was explained by considering that the excited state deprotonation of NPh is significantly retarded in a confined environment such the vesicle bilayer. Thus, NPh species also emit from the NPh located in the BHD-AOT bilayer. In other words, in aqueous media at pH= 6.40, NPh in the ground state exists exclusively as neutral species but, after excitation, NPh rapidly dissociates to the anionic naphtholate (NPh^-) species and the emission comes exclusively from the anionic species (at λ =460 nm).

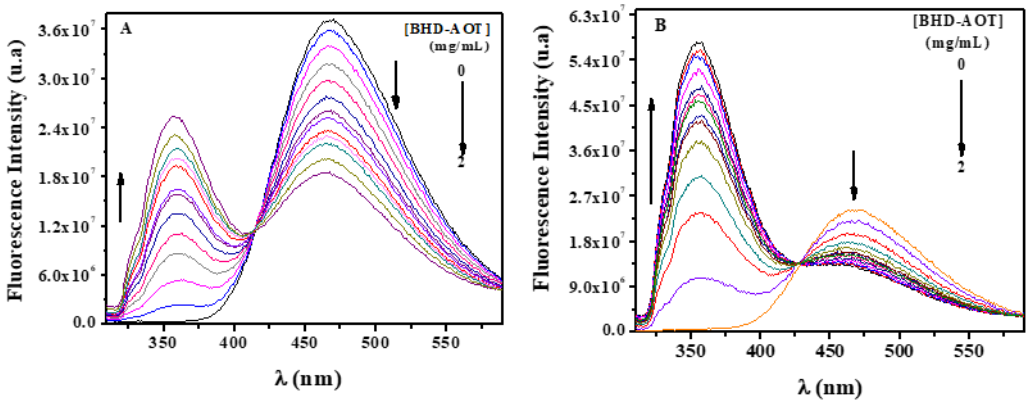

Figure 4. Emission spectra (λ_{exc} = 300 nm) of NPh^- at different BHD-AOT concentrations at pH=10.75 (A) and pH=6.40 (B). [NPh^-] = 1.00 x 10^{-4} M in [LiClO4] = 0.05 M. Data taken from reference 37.

In the vesicle media, for the species that exists in the bilayer, the deprotonation in the excited state is retarded and the emissions from both species are detected. The same is valid even at pH 10.75 where in the ground state only exist the anionic species. It seems that in BHD-AOT system, equilibrium is established in the excited state. Moreover, it seems that it is shifted to the NPh* neutral species formation by the presence of the BHD-AOT LUVs (See scheme 6). In other words, the proton transfer reaction from NPh to water is extremely slow when the molecule is embedded in the vesicle bilayer. Since it is known that the sulfonate group of Na-AOT in reverse micelles media are exceptional as hydrogen bond acceptor,[39] a question may arise here: is the AOT moiety of the BHD-AOT surfactant the responsible for this unusual behavior? Furthermore, is the sulfonate group of the free AOT the responsible? Or the surfactant has to be forming reverse micelles or being part of a bilayer for this unique behavior? In order to answer these questions, we performed experiments by using Na-AOT dissolved in water forming direct

micelles. It was observed a single emission band at λ=460 nm, which corresponds to the emission of the excited species ionized.[37] The conclusion that can be arrived is that in the excited state under this condition, only the ionized species is detected. Thus, it seems that AOT only shows the outstanding hydrogen bond acceptor capacity when forming part of the vesicle bilayer or reverse micelles. This behavior confirms once again that the properties of the original surfactant change when organized to form vesicles.

Therefore, the data show that only when AOT is part of the bilayer, the AOT polar head interacts strongly, through a hydrogen bond, with NPh favoring the formation of the neutral NPh* species resulting in the appearance of the band close to λ=355 nm. These results could have a tremendous impact on chemical reactions occurring in BHD-AOT vesicles, such as acid–base and/or enzyme-catalyzed reactions (Scheme 7).

3.3.2. The Permeability of the Vesicle BHD-AOT Bilayer.

As we have shown, the bilayer of these spontaneous unilamellar vesicles, seems to have unique properties. Thus, its permeability properties should also be special in comparison with "traditional" vesicles. In order to gain insights on this issue, we have calculated the permeability coefficient value (P) of 1-Naphthyl Phosphate (1-NP) through BHD-AOT vesicles bilayer.[40]

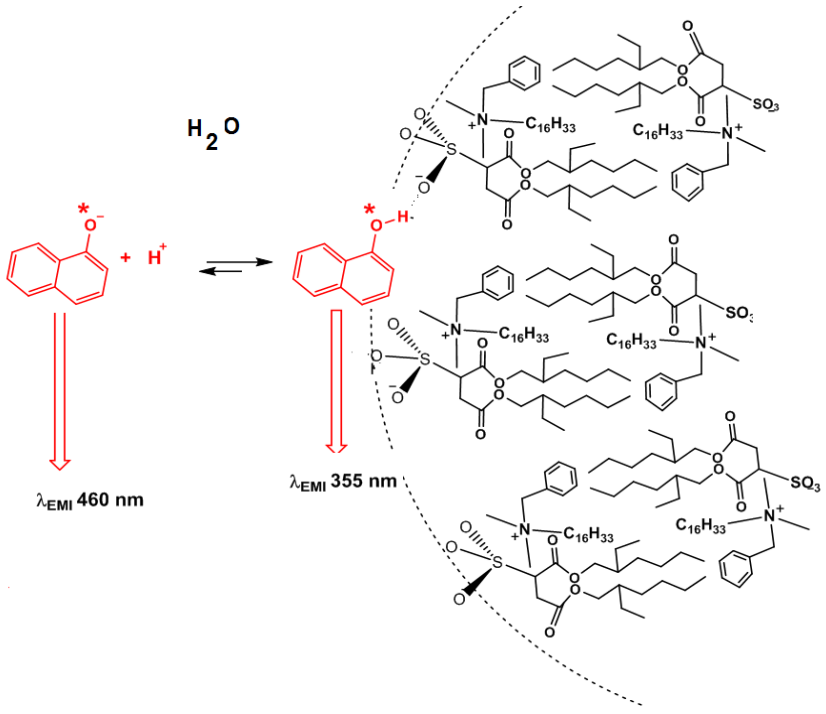

Scheme 7. Representation of the hydrogen bond interaction between NPh and the LUVs bilayer. Adapted from reference 37.

1-NP was added in the external phase, and must cross the bilayer of the vesicle to react with the encapsulated enzyme (alkaline phosphatase) to yield 1-Naphtholate (NPh^-), product of the enzymatic hydrolysis, as it is shown in Scheme 8. This product is electrochemically detected, at basic pH value, by Square Wave Voltammetry technique, which can be a good alternative over the spectroscopic one, to measure the vesicles solutions, since the scattering (due to its turbidity) does not make any influence in the electrochemical signal.[40] Thus, using a simple mathematical model, it is possible to determine the value of the permeability of 1-NP through the vesicle bilayer, which gives a value of $(1.00\pm0.15) \times 10^{-9}$ cm s^{-1}. Using other independent spectroscopic technique for comparison; the permeability value obtained was $(2.0\pm0.5) \times 10^{-9}$ cm s^{-1}, which shows a very good agreement. Also, it seems that the bilayer of the vesicle shows an exceptional low P value, in comparison with other substrates in DOPC vesicles, probably due to the unique characteristics shown in section 3.2. Thus, they can be a good media to encapsulate molecules without losing material because of the leakage through the bilayer. We highlight that, using an enzymatic hydrolysis reaction inside BHD-AOT vesicles and a simple mathematical model, it is possible to determine the permeability of the bilayer to the 1-NP.

3.3.3 The Use of BHD-AOT Vesicles as a Potential "Nano-Taxi" for Drug Delivery System.

Once the system was fully characterized, one of our main goals was to test the possibility of using the vesicles as drug delivery systems. We think that they are special systems since they form stable, spontaneous, with a size of around 100 nm unilamellar vesicles. The question to be answered is if they are *non*-toxic to living organisms.

We evaluate *in vitro* and *in vivo* toxicity and stability in acidic environment of the BHD-AOT vesicles, in order to investigate the potential application as drug delivery system via oral. Unilamellar vesicles were spontaneously formed by dissolving BHD-AOT in water and toxicity was evaluated throughout *in vitro* and *in vivo* assays. Cell membrane permeability assays (hemolytic activity, Trypan Blue assay) and cellular survival or proliferation (MTT assay) were performed.[41]

We observed that only the highest concentration of vesicles tested diminished the red blood cells resistance, showing a change in the cell membrane permeability. Interestingly, more dilute vesicles solutions showed similar hemolysis percentages to control, which would be indicative of little or no damage to cell membranes. Similar results were obtained from Trypan blue and MTT assays. Increasing BHD-AOT vesicles concentration from 0.05 mg/mL to 2 mg/mL results in an increase in the membrane and mitochondrial destabilization, but concentrations lower than 0.05 mg/mL showed the same values than control, which evidences the low toxicity of the system at these concentrations. Scheme 9 shows a possible explanation of what happens when different concentrations of vesicles interact with membranes (plasma or mitochondrial). We propose that

BHD-AOT vesicles are incorporated into cells by endocytosis at low concentrations. On the other hand, when the concentration is higher, the membrane cannot make this process and, consequently, the vesicles interacts strongly with the membrane resulting in the membrane deformation and permeability changes leading to cell death. *In vivo* toxicity evaluation was carried out on mice through the lethal dose 50 (LD 50) experiments. Lethal dose 50, LD 50, is the dose capable of causing the death of 50% of the animal population and it is frequently used to determine the dose capable of causing toxicity of a substance in a living organism reducing the number of required tests.[41] Our results show that the obtained value of LD 50 (118.03 % mg/kg) is higher than the one obtained for other systems such as polymeric nanoparticles of 110 nm (40 and 75 mg/kg).[42]

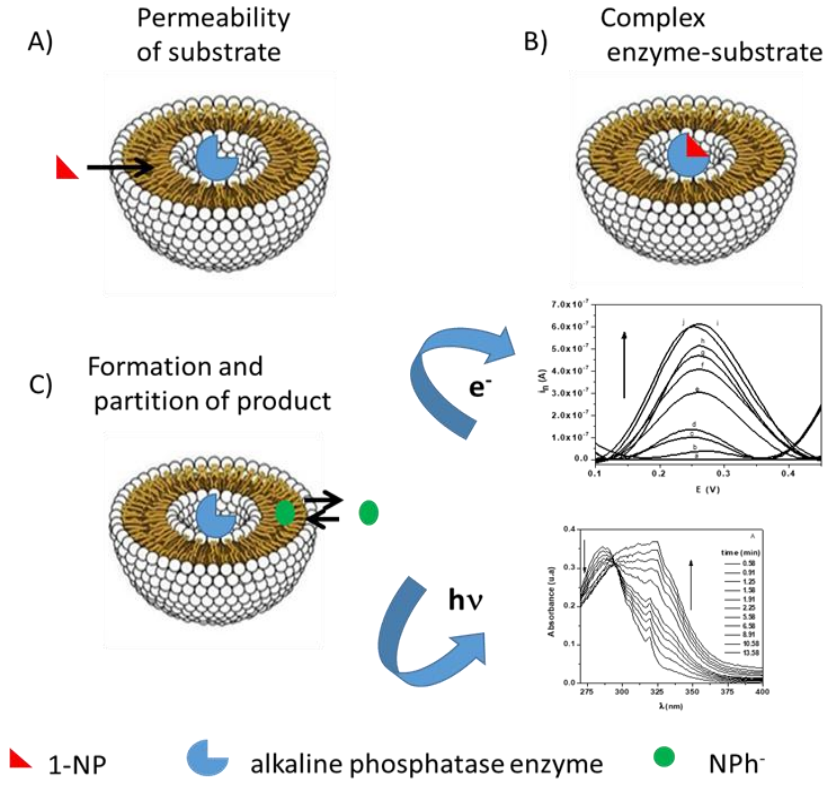

Scheme 8. Representation of the processes occurring in the enzymatic hydrolysis in the BHD-AOT LUVs. Adapted from reference 40.

Innocuousness observed in both *in vitro* (≤0.05 mg/ml) and *in vivo* (≤118.6 mg/Kg) studies could be associated with the fact that anionic systems are stable in biological media due to electrostatic repulsion with serum proteins, and also decreases its immunogenicity, increase its biological compatibility and its permanence in the cardiovascular system. In addition, the innocuousness of our system can also be explained because of its shape (spherical) and its size (around 100 nm).

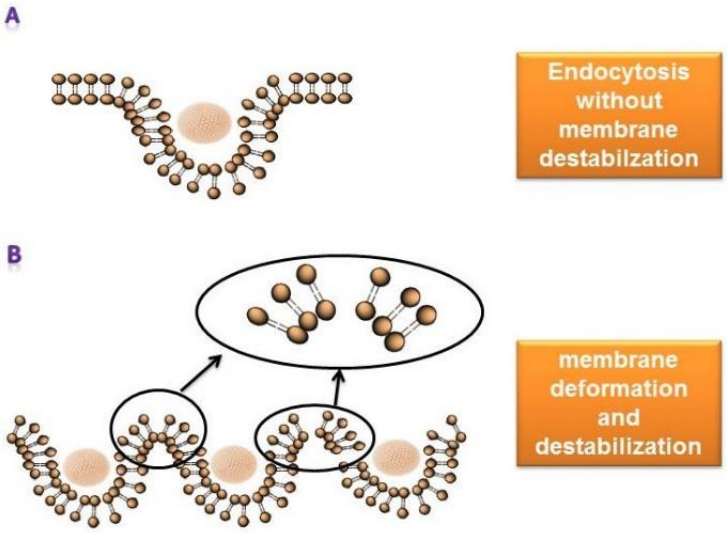

Scheme 9. Schematic representation of cell stability dependence with vesicles concentration. A- Low vesicles concentration. B- High vesicles concentration. Adapted from Reference 41.

It has previously been reported that the interaction of particles with cells is known to be strongly influenced by particle size and shape. Particles with a size smaller than 50 nm are internalized through mechanisms of direct penetration or passive density gradient diffusion causing the disruption of lipid membranes, leading to loss of cytoplasmic substance and culminating in cell death. On the other hand, the internalization of nanoparticles bigger than 50 nm depends on endocytosis of cell-surface receptors without damaging the cellular membrane ultrastructure.[41] This means that catanionic vesicles biocompatibility observed *in vitro* and *in vivo* may be closely associated with system properties (charge, size, and shape) as well as with the administered doses. Thus, they seem to be an excellent option for oral drug administration as proposed in Scheme 10.

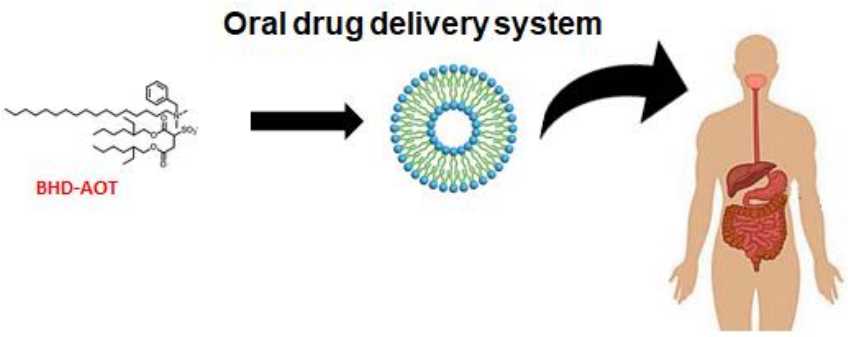

Scheme 10. Schematic representation of BHD-AOT vesicles as a potential nano-taxi for oral drug delivery. Adapted from Reference 41.

4. Conclusions

In this review, we have shown interesting properties of a new ionic liquid catanionic surfactant, BHD-AOT. This SAIL can form RMs or vesicles, depending on the surrounding media. Interesting, the vesicles formed are unilamellar and without needing any extra steps, contrary to the traditional vesicles formed with phospholipids.

One of the most important findings that we want to highlight is that the results of *in vitro* and *in vivo* and stomach like pH simulation studies have demonstrated the stability of our system to acid pH and safety to living systems due to the low toxicity observed in doses lower than 0.05 mg/mL *in vitro* or 118.6 mg/Kg *in vivo*. This characteristic makes our BHD-AOT vesicles highly biocompatible and very promising candidate for oral drug delivery, based on its unique bilayer properties.

Acknowledgments

Financial support from the Consejo Nacional de Investigaciones Científicas y Técnicas (PIP CONICET 112-201101-00204, PIP CONICET 112-2015-0100283), Universidad Nacional de Río Cuarto (PPI-UNRC 2016-2018), Agencia Nacional de Promoción Científica y Técnica (PICT 2012-0232, PICT 2012-0526, PICT 2015-0585 and PICT-2015-2151), and Ministerio de Ciencia y Tecnología, gobierno de la provincia de Córdoba (PID 2013) is gratefully acknowledged. C.C.V., A.K.C.S., S.S. and M.A.L. thank CONICET for a research fellowship. R.D.F., J.J.S., F.M., P.G.M. and, N.M.C. are staff members of CONICET, Argentina.

References

(1) Villa, C. C.; Moyano, F.; Ceolin, M.; Silber, J. J.; Falcone, R. D.; Correa, N. M. A Unique Ionic Liquid with Amphiphilic Properties That Can Form Reverse Micelles and Spontaneous Unilamellar Vesicles. *Chem. - A Eur. J.* **2012**, *18* (49), 15598–15601.

(2) Sagisaka, M.; Fujii, T.; Koike, D.; Yoda, S.; Takebayashi, Y.; Furuya, T.; Yoshizawa, A.; Sakai, H.; Abe, M.; Otake, K. Surfactant-Mixing Effects on the Interfacial Tension and the Microemulsion Formation in Water/supercritical CO2 System. *Langmuir* **2007**, *23* (5), 2369–2375.

(3) Villa, C. C.; Silber, J. J.; Falcone, R. D.; Correa, N. M. Subtleties of Catanionic Surfactant Reverse Micelle Assemblies Revealed by a Fluorescent Molecular Probe. *Methods Appl. Fluoresc.* **2017**, *5* (4), 44001.

(4) Silva, B. F. B.; Marques, E. F.; Olsson, U. Aqueous Phase Behavior of Salt-Free Catanionic Surfactants: The Influence of Solubility Mismatch on Spontaneous Curvature and Balance of Forces. *Soft Matter* **2011**, *7* (1), 225–236.

(5) Jokela, P.; Jönsson, B.; Khan, A. Phase Equilibria of Catanionic Surfactant-Water Systems. *J. Phys. Chem.* **1987**, *91* (12), 3291–3298.

(6) Silva, B. F. B.; Marques, E. F.; Olsson, U.; Pons, R. Headgroup Effects on the Unusual Lamellar-Lamellar Coexistence and Vesicle-to-Micelle Transition of Salt-Free Catanionic Amphiphiles. *Langmuir* **2010**, *26* (5), 3058–3066.

(7) Silva, B. F. B.; Marques, E. F.; Olsson, U. Unusual Vesicle-Micelle Transitions in a Salt-Free Catanionic Surfactant: Temperature and Concentration Effects. *Langmuir* **2008**, *24* (19), 10746–10754.

(8) Silva, B. F. B.; Marques, E. F.; Olsson, U. Lamellar Miscibility Gap in a Binary Catanionic Surfactant - Water System. *J. Phys. Chem. B* **2007**, *111* (48), 13520–13526.

(9) Hallett, J. P.; Welton, T. Room-Temperature Ionic Liquids: Solvents for Synthesis and Catalysis. 2. *Chem. Rev.* **2011**, *111* (5), 3508–3576.

(10) Brown, P.; Butts, C. P.; Eastoe, J.; Fermin, D.; Grillo, I.; Lee, H. C.; Parker, D.; Plana, D.; Richardson, R. M. Anionic Surfactant Ionic Liquids with 1-Butyl-3-Methyl-Imidazolium Cations: Characterization and Application. *Langmuir* **2012**, *28* (5), 2502–2509.

(11) Lépori, C. M. O.; Correa, N. M.; Silber, J. J.; Falcone, R. D. How the Cation 1-Butyl-3-Methylimidazolium Impacts the Interaction between the Entrapped Water and the Reverse Micelle Interface Created with an Ionic Liquid-like Surfactant. *Soft Matter* **2016**, *12* (3), 830–844.

(12) El Seoud, O. A.; Pires, P. A. R.; Abdel-Moghny, T.; Bastos, E. L. Synthesis and Micellar Properties of Surface-Active Ionic Liquids: 1-Alkyl-3-Methylimidazolium Chlorides. *J. Colloid Interface Sci.* **2007**, *313* (1), 296–304.

(13) Correa, N. M.; Silber, J. J.; Riter, R. E.; Levinger, N. E. Nonaqueous Polar Solvents in Reverse Micelle Systems. *Chem. Rev.* **2012**, *112* (8), 4569–4602.

(14) Moulik, S. P.; Paul, B. K. Structure, Dynamics and Transport Properties of Microemulsions. *Adv. Colloid Interface Sci.* **1998**, *78* (2), 99–195.

(15) Silber, J.; Biasutti, A.; Abuin, E.; Lissi, E. Interactions of Small Molecules with Reverse Micelles. *Adv. Colloid Interface Sci.* **1999**, *82*, 189–252.

(16) Correa, N. M.; Biasutti, M. A.; Silber, J. J. Micropolarity of Reversed Micelles: Comparison between Anionic, Cationic, and Nonionic Reversed Micelles. *J. Colloid Interface Sci.* **1996**, *184* (2), 570–578.

(17) Mcneil, R.; Thomas, J. K. Benzylhexadecyldimethylammonium Chloride in Microemulsions and Micelles. *J. Colloid Interface Sci.* **1981**, *83* (1), 57–65.

(18) Agazzi, F. M.; Correa, N. M.; Rodriguez, J. Molecular Dynamics Simulation of water/BHDC Cationic Reverse Micelles. Structural Characterization, Dynamical

Properties, and Influence of Solvent on Intermicellar Interactions. *Langmuir* **2014**, *30* (32), 9643–9653.

(19) Küchler, A.; Yoshimoto, M.; Luginbühl, S.; Mavelli, F.; Walde, P. Enzymatic Reactions in Confined Environments. *Nat. Nanotechnol.* **2016**, *11* (5), 409–420.

(20) Biasutti, M. A.; Abuin, E. B.; Silber, J. J.; Correa, N. M.; Lissi, E. A. Kinetics of Reactions Catalyzed by Enzymes in Solutions of Surfactants. *Adv. Colloid Interface Sci.* **2008**, *136* (1–2), 1–24.

(21) Durantini, A. M.; Falcone, R. D.; Silber, J. J.; Correa, N. M. Effect of Confinement on the Properties of Sequestered Mixed Polar Solvents: Enzymatic Catalysis in Nonaqueous 1,4-Bis-2-Ethylhexylsulfosuccinate Reverse Micelles. *ChemPhysChem* **2016**, *17* (11), 1678–1685.

(22) Blach, D.; Pessêgo, M.; Silber, J. J.; Correa, N. M.; García-Río, L.; Falcone, R. D. Ionic Liquids Entrapped in Reverse Micelles as Nanoreactors for Bimolecular Nucleophilic Substitution Reaction. Effect of the Confinement on the Chloride Ion Availability. *Langmuir* **2014**, *30* (41), 12130–12137.

(23) Kepczyński, M.; Nawalany, K.; Jachimska, B.; Romek, M.; Nowakowska, M. Pegylated Tetraarylporphyrin Entrapped in Liposomal Membranes. A Possible Novel Drug-Carrier System for Photodynamic Therapy. *Colloids Surfaces B Biointerfaces* **2006**, *49* (1), 22–30.

(24) Moyano, F.; Biasutti, M. A.; Silber, J. J.; Correa, N. M. New Insights on the Behavior of PRODAN in Homogeneous Media and in Large Unilamellar Vesicles. *J. Phys. Chem. B* **2006**, *110* (24), 11838–11846.

(25) Correa, N. M.; Zhang, H.; Schelly, Z. A. Preparation of AgBr Quantum Dots via Electroporation of Vesicles. *J. Am. Chem. Soc.* **2000**, *122* (1), 6432–6434.

(26) Luna, M. A.; Silber, J. J.; Sereno, L.; Correa, N. M.; Moyano, F. Determining the Substrate Permeability through the Bilayer of Large Unilamellar Vesicles of DOPC. A Kinetic Study. *RSC Adv.* **2016**, *6* (67), 62594–62601.

(27) Villa, C. C.; Correa, N. M.; Silber, J. J.; Moyano, F.; Falcone, R. D. Singularities in the Physicochemical Properties of Spontaneous AOT-BHD Unilamellar Vesicles in Comparison with DOPC Vesicles. *Phys. Chem. Chem. Phys.* **2015**, *17* (26), 17112–17121.

(28) Villa, C. C.; Silber, J. J.; Correa, N. M.; Falcone, R. D. Effect of the Cationic Surfactant Moiety on the Structure of Water Entrapped in Two Catanionic Reverse Micelles Created from Ionic Liquid-Like Surfactants. *ChemPhysChem* **2014**, *15* (14), 3097–3109.

(29) Falcone, R. D.; Silber, J. J.; Correa, N. M. What Are the Factors That Control Non-

aqueous/AOT/n-Heptane Reverse Micelle Sizes? A Dynamic Light Scattering Study. *Phys. Chem. Chem. Phys.* **2009**, *11* (47), 11096–11100.

(30) Luisi, P. L.; Giomini, M.; Pileni, M. P.; Robinson, B. H. Reverse Micelles as Hosts for Proteins and Small Molecules. *BBA - Rev. Biomembr.* **1988**, *947* (1), 209–246.

(31) *Liposomes. A Practical Approach*; New, R. R. C., Ed.; Oxford University Press inc.: New York, 1997.

(32) Lasic, D. D. *Liposomes: From Physics to Applications*; Elsevier Science B.V.: Amsterdam, 1995.

(33) Walde, P.; Ichikawa, S. Enzymes inside Lipid Vesicles: Preparation, Reactivity and Applications. *Biomol. Eng.* **2001**, *18* (4), 143–177.

(34) Brown, P.; Butts, C.; Dyer, R.; Eastoe, J.; Grillo, I.; Guittard, F.; Rogers, S.; Heenan, R. Anionic Surfactants and Surfactant Ionic Liquids with Quaternary Ammonium Counterions. *Langmuir* **2011**, *27* (8), 4563–4571.

(35) El Seoud, O. A.; Correa, N. M.; Novaki, L. P. Solubilization of Pure and Aqueous 1,2,3-Propanetriol by Reverse Aggregates of Aerosol-OT in Isooctane Probed by FTIR and 1H NMR Spectroscopy. *Langmuir* **2001**, *17* (6), 1847–1852.

(36) Falk, M. On the Satellite Bands Accompanying the OH and OD Stretching Fundamentals of Isotopically Dilute HDO in Ice Ih. *J. Chem. Phys.* **1987**, *87* (1), 28–30.

(37) Cobo Solis, A. K.; Correa, N. M.; Molina, P. G. Electrochemical and Photophysical Behavior of 1-Naphthol in Benzyl-N-Hexadecyldimethylammonium 1,4-bis(2-Ethylhexyl)sulfosuccinate Large Unilamellar Vesicles. *Phys. Chem. Chem. Phys.* **2016**, *18* (23), 15645–15653.

(38) Sujatha, J.; Mishra, A. K. Determination of the Partition Coefficient of 1-Naphthol, an Excited State Acid, in DMPC Membrane. *J. Photochem. Photobiol. A Chem.* **1996**, *101* (2–3), 215–219.

(39) Silva, O. F. F.; Fernández, M. A.; Silber, J. J. J.; De Rossi, R. H.; Correa, N. M.; Fernµndez, M. A.; Silber, J. J. J.; Rossi, R. H. De. Inhibited Phenol Ionization in Reverse Micelles : Confinement Effect at the Nanometer Scale. *ChemPhysChem* **2012**, *3* (1), 1–8.

(40) Cobo Solis, A. K.; Correa, N. M.; Molina, P. G. Determination of Benzyl-Hexadecyldimethylammonium 1,4-Bis(2-Ethylhexyl)sulfosuccinate Vesicle Permeability by Using Square Wave Voltammetry and an Enzymatic Reaction. *Langmuir* **2017**, *33* (43), 12080–12086.

(41) Stagnoli, S.; Luna, M. A.; Villa, C. C.; Alustiza, F.; Niebylski, A.; Moyano, F.; Correa, N. M.; Falcone, R. D. Unique Catanionic Vesicles as a Potential "Nano-Taxi" for Drug Delivery Systems. In Vitro and in Vivo Biocompatibility Evaluation. *RSC Adv.* **2017**, *7*

(9), 5372–5380.

(42) Plard, J-P. Bazile, D. Comparison of the Safety Profiles of PLA50 and\rMe.PEG-PLA50 Nanoparticles after Single Dose Intravenous\radministration to Rat. *Col. Surf. B Biointerf.* **1999**, *16*, 173–183.

Cristian Camilo Villa was born in Armenia, Quindío, Colombia. He received a Chemistry degree from Universidad del Quindío in Colombia. In 2015 he received his Ph. D degree from the National University of Río Cuarto (UNRC), through a CONICET (National Research Council of Argentina) scholarship and under guidance from Drs. Ruben Dario Falcone and Nestor Mariano Correa. In his thesis, Dr. Villa studied the supramolecular systems (reverse micelles and vesicles) formed by two new catanionic surfactants BHD-AOT and CTA-AOT, and their application as nanoreactors for chemical reactions and nanocarriers for oral delivery of drugs. Currently, Dr. Villa is an assistant professor at the chemistry department of Universidad del Quindío and a member of the Food science and technology research group (CYTA). At the moment, his research interests include the synthesis and characterization of starch-based nanocarriers and essential oils nanoemulsions that can be used for the encapsulation and controlled release of the bioactive molecules.

Airam Katiza Cobo Solís was born in Bugalagrande, Valle del Cauca, Colombia. She received her undergraduate degree in Chemistry from University of Quindío, Colombia in the Faculty of Basic Sciences and Technologies. Member of the research Group in Pesticides and Health, where she carried out her undergraduate research in the synthesis of Mercury (II) complexes with L-Cystein or L- Arginine at different pH. She is currently pursuing Doctoral studies in Chemical Sciences in the Faculty of Exact-Physical-Chemical and Natural Sciences of the National University of Río Cuarto in Argentina, in the research group in Organized Systems in the lines of Organic Physical-chemistry and Organic Electrochemistry under the guidance of Dr. Patricia Molina and Dr. N. Mariano Correa. The theme of her thesis is the use of electrochemical

techniques as a new tool in the study of organized systems, whose objective is to study the physicochemical properties of different solutes of known electrochemical behavior in different organized systems, deepening the study of their interactions, through the use of electrochemical techniques. In this way, it is intended to characterize new organized media by exploring, at the same time, different interfacial properties.

Antonela Soledad Stagnoli was born in Rivadavia, Mendoza, Argentina. She received her undergraduate degree as Biologist in the Universidad Nacional de Río Cuarto (UNRC).

Currently a 4rd-year PhD in Biological Sciences student at National University of Río Cuarto. "Development of supramolecular systems formed by catanionic surfactants. Evaluation of their use in nanomedicine". Advisor: Dr. Ana M. Niebylski, PhD (Department of Molecular Biology). Co-advisor: Dr. N. Mariano Correa (Department of Chemistry). Department of Molecular Biology, Animal Physiology Area and Department of Chemistry. Faculty of Exact, Physicochemical and Natural Sciences, UNRC. The main goal in her study is to evaluate the interaction of catanionic vesicles with biological systems both in vitro and in vivo, its stability in different medium and conditions. Besides, she evaluates the capacity of vesicles as nanocarrier that can work as specific release systems of drugs capable of overcoming the limitations that arise when using different routes of administration, for its potential application in nanomedicine. She has work in a doctoral position with support from CONICET (the National Research Council of Argentina) under the guidance of Dr. Mariano Correa. She is an Effective Senior Teaching Assistant at Department of Molecular Biology, Faculty of Exact, Physicochemical and Natural Sciences, UNRC.

M. Alejandra Luna was born in Río Cuarto, Argentina. She received her undergraduate degree as Microbiologist from Universidad Nacional de Río Cuarto (UNRC). Under the guidance of Dr. Fabiana D´Eramo, she earned the Ph.D. degree in Chemical Sciences from UNRC in 2013 where her research explored electrocatalysis with porphyrins. Following her graduate studies, Dr. Luna performed postdoctoral research at Universidad Nacional de Río Cuarto with Dr. N. Mariano Correa investigating different applications of organized systems, particularly vesicles. She has worked in a postdoctoral position with support from CONICET (the National Research Council of Argentina). Presently she applied for Assistant Researcher position on CONICET and she works with an effective position as teaching assistant at Universidad Nacional de Rio Cuarto. Her research interests include intermolecular interactions and chemical recognition in supramolecular structures and organized media and, using them as "smart" nanoreactors for different reactions such as nanoparticles synthesis and micellar enzymology, in the nanoscience field. The principal interest is to comprehend the interaction of organized systems with living organism, so they could be applicable in nanomedicine field for different uses, for example as nanocarriers. The supramolecular systems of interest are aqueous reverse micelles in organic solvents and vesicles.

.

Fernando Moyano was born on June 4, 1977 in Río Cuarto, Córdoba, Argentina. He received his university degree in Chemical Sciences in 2004 from the National University of Río Cuarto (UNRC). He obtained the Ph.D. Degree in Chemical Sciences in 2008, where he explored the physicochemical properties of unilamellar vesicles. He obtained a postdoctoral fellowship under

the direction of Prof. Leonides Sereno and acquired a postdoctoral internship at CNR, Bologna, Italy to investigate the radical damage of the vesicles formed by lecithin.

He currently holds the positions of professor and undersecretary of postgraduate studies at the School of Exact Physical-Chemical and Natural Sciences, UNRC and Scientific Research Assistant of CONICET (National Research Council of Argentina). His research focuses on different studies of physicochemical properties applied to new organized systems, such as micelles, reverse micelles and vesicles. These systems are modified to create "smarts nanotemplate" to perform the synthesis of nanoparticles and improve enzymatic reactions, catalysis or to use them as possible delivery vehicles for drugs.

Patricia G Molina obtained her Ph. D. in Chemistry (1999) from Río Cuarto National University (UNRC) (Río Cuarto, Argentina). She did the postdoctoral training (1999-2000) at University of Sevilla, Sevilla (Spain). Currently, she is Professor at UNRC and Researcher at Argentine Research Council (CONICET). Her research interest focus on several subjects, such as electrochemistry of mycotoxins, hormones, studies on characterization of organized systems employing electrochemistry techniques using ultramicroelectrodes and modified electrodes by self-assembled monolayers of thiols, carbon nanotubes, antibodies, etc and their use for electroanalytical applications. Development of electroanalytical techniques for the determination of mycotoxins and hormones in real matrixes (cereal, foods, animal serum, etc,) as well as design and characterization of chemical sensors, electrochemical immunoelectrodes based on nanostructured materials. Prof. Molina is an AAQA, AAIFQ and SIBAE fellow.

Juana J. Silber was born in Cordoba, Argentina. She graduated in 1967 with a degree in Biochemistry in the National University of La Plata and obtained her Ph.D. 1972 in Texas Tech University in Texas, USA under the supervision of Prof. Henry Shine. She is currently a Emeritus Professor in the Chemistry Department in the National University of Rio Cuarto. She is a Superior Scientist Researcher of CONICET (National Research Council of Argentina) and a member of the National Academy of Science of Argentine. Her current research interests include Intermolecular interactions-chemical recognition in supramolecular structures and organized media: microemulsions, dendrimers. Kinetics of reactions in environmentally friendly organized media. Micellar enzymology. Organic electrochemistry. Spectroelectrochemistry of biomimetic of dyes for solar energy conversion.

R. Dario Falcone was born in 1975 in Rio Cuarto (Cordoba), Argentina. He studied Chemistry at the Universidad Nacional de Río Cuarto (UNRC) where he graduated in 1998. He completed his Ph.D. degree with Professor Juana J. Silber on non-aqueous reverse micelles in 2004. He then performed postdoctoral research at Imperial College London under the supervision of Professor Tom Welton in Nucleophilic substitution processes in room-temperature ionic liquids. He currently is a Professor and Scientific Researcher of CONICET (the National Research Council of Argentina). His research centers on ionic liquids (synthesis and characterization) and especially on development of environmentally friendly organized media.

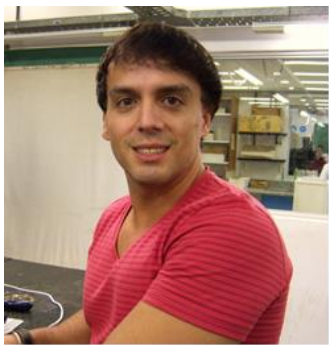

N. Mariano Correa was born in Mendoza, Argentina. He received his undergraduate degree with first class honors from Universidad Nacional de Río Cuarto (UNRC). Under the guidance of Prof. Juana J. Silber, he earned the Ph.D. degree in Chemical Sciences from UNRC in 1997 where his research explored reverse micelles. Following his graduate studies, Dr. Correa performed postdoctoral research at University of Texas at Arlington, USA with Prof. Zoltan A. Schelly investigating the mechanism of liposomes electroporation. He has worked with Prof. Omar El Seoud at Universidad de Paulo, Brazil and later with Prof. Nancy E. Levinger at Colorado State University, USA with support from a Fulbright award. Presently he holds the positions of Professor at Universidad Nacional de Rio Cuarto, Principal Scientific Researcher of CONICET (the National Research Council of Argentina) and, Associate Editor for the journal RSC-Advances (Royal Society of Chemistry). His research interests include intermolecular interactions and chemical recognition in supramolecular structures and organized media and, using them as "smart" nanoreactors for different reactions such as nanoparticles synthesis and micellar enzymology, in the nanoscience field. The studies are pointed to comprehend the factors that determine the interaction of a solute with a particular media, and apply them to several processes. The supramolecular systems of interest are aqueous and non aqueous reverse micelles in organic solvents and vesicles.

Group home page: http://gso-unrc.blogspot.com/.

Scholar profile: https://scholar.google.com/citations?user=IjqzVvgAAAAJ&hl=es&oi=ao